# EVALUATION OF MECHANICAL PROPERTIES OF STRUCTURAL MATERIALS USING MINIATURE TENSILE AND SMALL PUNCH TEST TECHNIQUES

*By*

**KUNDAN KUMAR**

**ENGG01200804004**

**Bhabha Atomic Research Centre, Mumbai**

***A thesis submitted to the***

***Board of Studies in Engineering Sciences***

***In partial fulfillment of the requirements***

***for the Degree of***

**DOCTOR OF PHILOSOPHY**

***of***

**HOMI BHABHA NATIONAL INSTITUTE**

**September, 2017**

# Homi Bhabha National Institute

## Recommendations of the Viva Voce Committee

As members of the Viva Voce Committee, we certify that we have read the dissertation prepared by Kundan Kumar entitled "Evaluation of Mechanical Properties of Structural Materials Using Miniature Tensile and Small Punch Test Techniques" and recommend that it may be accepted as fulfilling the thesis requirement for the award of Degree of Doctor of Philosophy.

Srikumar Banerjee
--------------------------------------------- Date:
(Chairman: Prof. S. Banerjee)

JK Chakravartty
--------------------------------------------- Date: 29/8/17
(Guide: Prof. J. K. Chakravartty)

BK Dutta
--------------------------------------------- Date: 29.8.17
(Co-Guide: Prof. B. K. Dutta)

Satyam Suwas
--------------------------------------------- Date: 29/8/17
(Examiner: Prof. Satyam Suwas)

Gautam Kumar Dey
--------------------------------------------- Date: 29/8/17
(Member-I: Prof. G. K. Dey)

--------------------------------------------- Date: 29.8.17
(Member-II: Dr. S.B. Roy)

--------------------------------------------- Date: 29/8/17
(Member-III: Dr. N.K. Maheswari)

Final approval and acceptance of this thesis is contingent upon the candidate's submission of the final copies of the thesis to HBNI. I/We hereby certify that I/we have read this thesis prepared under my/our direction and recommend that it may be accepted as fulfilling the thesis requirement.

**Date: 13.09.2017**

**Place: Mumbai**

BK Dutta
**Signature**
**Co-guide: Prof. B. K. Dutta**

JK Chakravartty
**Signature**
**Guide: Prof. J. K. Chakravartty**

## STATEMENT BY AUTHOR

This dissertation has been submitted in partial fulfilment of requirements for an advanced degree at Homi Bhabha National Institute (HBNI) and is deposited in the Library to be made available to borrowers under rules of the HBNI.

Brief quotations from this dissertation are allowable without special permission, provided that accurate acknowledgement of source is made. Requests for permission for extended quotation from or reproduction of this manuscript in whole or in part may be granted by the Competent Authority of HBNI when in his or her judgment the proposed use of the material is in the interests of scholarship. In all other instances, however, permission must be obtained from the author.

Kundan Kumar

# DECLARATION

I, hereby declare that the investigation presented in the thesis has been carried out by me. The work is original and has not been submitted earlier as a whole or in part for a degree / diploma at this or any other Institution / University.

Kundan Kumar

# List of Publications arising from the thesis

**International Journals: 03**

1. "Use of Miniature Tensile Specimen for Measurement of Mechanical Properties", Kundan Kumar, Arun Pooleery, K Madhusoodanan, R.N. Singh, J.K. Chakravartty, B.K. Dutta and R.K. Sinha, **Procedia Engineering**, 86 (2014) 899-909
2. "Evaluation of Ultimate Tensile Strength using Miniature Disk Bend Test" Kundan Kumar, Arun Pooleery, K. Madhusoodanan, R.N. Singh, J.K. Chakravartty, R S Shriwastaw, B.K. Dutta and R.K. Sinha, **Journal of Nuclear Materials**, 461 (2015) 100-111
3. "Optimisation of thickness of miniature tensile specimens for evaluation of mechanical properties", Kundan Kumar, Arun Pooleery, K. Madhusoodanan, R. N. Singh, Arnomitra Chatterjee, B. K. Dutta and R. K. Sinha, **Materials Science & Engineering A**, 675 (2016), pp. 32-43

**International Conferences: 02**

1. "Use of Miniature Tensile Specimen for Measurement of Mechanical Properties", Kundan Kumar, Arun Pooleery, K Madhusoodanan, R. N. Singh, J. K. Chakravartty, B. K. Dutta and R. K. Sinha, In the proceedings of First International Conference on Structural Integrity (ICONS-2014), 1179-1190, February 4-7, 2014, Kalpakkam, India
2. "Miniature test techniques for life management of operating Equipment", Kundan Kumar, Arun Pooleery, K Madhusoodanan, R. N. Singh, J. K. Chakravartty, B. K.

Dutta, R. K. Sinha, In the Proceedings Inetrnational workshop on CANSAS–2015 (CANDU Safety Association for Sustainability), & NRTHS – 2015 (New Horizons in Nuclear Reactor Thermal-Hydraulics and Safety), Paper No. F09, December 8–11, 2015, Anushaktinagar, Mumbai, India

**<u>Others: 01</u>**

1. “Use of Miniature Tensile Specimen and Video Extensometer for Measurement of Mechanical Properties”, Kundan Kumar, Arun Pooleery and K. Madhusoodanan, **BARC External Report No. BARC/2014/E/009**

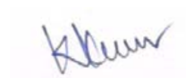

Kundan Kumar

# DEDICATIONS

I would dedicate this thesis to my grandfather, parents, family, colleagues and well-wishers.

My grandfather was a teacher and a peasant who worked very hard to manage both of these endeavours. I have learnt the value of time and untiring hard work from my grandfather. I have been very affectionate to my parents. My father has been a role model for me and from him I could learn kindness, sincerity and honesty. My mother is very simple, straightforward and sensitive person, which has made me blend of some of her qualities. My wife has played a role of a good companion always. She not only worked hard to manage her official and day-to-day domestic work at home, but also provided me moral support throughout my PhD work. My school going two sons had to manage themselves in their studies, as I could not give required time to them due to my office work and PhD work. I dedicate my work to all these family members.

I also dedicate my work to my senior colleagues Shri B B Rupani and Shri J N Kayal. I started my official carrier with Shri B B Rupani and I could learn from him many intricacies of design of life management tools for reactor components. Later I worked with Shri J N Kayal, from whom I learnt patience and practicality of things in official and personal lives. He not only guided me during my official work but also gave full freedom to work, which made me more responsible towards my work.

I also dedicate the work to all my friends and well-wishers.

# ACKNOWLEDGEMENTS

On completion of my PhD work, I take this opportunity to thank all persons in BARC, HBNI, BRNS and CSIR-NML, Jamshedpur whom I came across during my PhD work. To start with, I gratefully thank Dr. R. K. Sinha, ex-Chairman, AEC, who readily agreed to be my technical advisor for this work, despite his busy official work. I gratefully thank my guide, Dr. J. K. Chakravartty, ex-Director, Materials group, BARC who encouraged and provided all types of support and technical guidance throughout my work, which included his guidance for setting up a ‘Miniature Specimen Test Laboratory (MSTL)’ at Hall-7, BARC. I gratefully thank my co-guide, Dr. B. K. Dutta, Dean, HBNI, for providing me all the technical guidance and support during my PhD work. He also did the proofreading of this dissertation and gave useful guidance and feedback in completing it in effective manner. My special and grateful thank to Dr. S. Banerjee, ex-Chairman, AEC, for his continuous encouragement, support and guidance provided to me during my PhD work. He gave me lot of moral support and shared his technical expertise with me while perusing my PhD work. I have no words to thank to Dr. R. N. Singh and his team at MMD, who provided me a lot of time, technical help and guidance in every aspect of my PhD work during the whole tenure. He also provided me a lot of support in setting up the MSTL in Hall-7. My special thanks to him for all of his technical support & guidance and also for proofreading of this dissertation. Dr. P.K. Vijayan, ex-Director, RD&DG, was a big admirer of my idea of MSTL and supported me fully in setting up this facility in Hall-7, BARC. I gratefully thank him for his support and guidance in my PhD work. I gratefully thank BRNS, DAE for the approval provided for collaborative work on miniature specimens with CSIR-NML, Jamshedpur. I gratefully thank Dr. S. Tarafdar, Head, Material Science & Technology Division, CSIR-NML, Jamshedpur for his support and guidance during the BRNS project at CSIR-NML, Jamshedpur. I gratefully thank Dr. S. Sivaprasad, Dr. N. Narasaiah and Dr. Himadri N. Bar, for their help in experimental work, metallurgical and analytical analyses of the test specimens and results respectively. I also gratefully thank doctoral committee members Dr. G. K. Dey, Dr. S. B. Roy and Dr. N K Maheswari for their guidance and support towards completing my PhD work. I also thank Shri P. V. Durgaprasad, RSD, BARC and Shri Arun Pooleery, RCCS, RED who provided me technical support in my PhD work. I also thank my ex-colleagues Shri B. B. Rupani and Shri J. N. Kayal for their guidance and technical support provided to me during initial days of my PhD work. I also thank Shri B. S. V. G. Sharma, Shri Avaneesh Sharma, Shri I. V. Dulera, Shri K. Madhusoodanan, Shri S. K. Sinha, Shri A K Lal, Shri N. Das, Dr. A. K. Dureja, Shri S. Panwar and Shri D.K. Nathani for their guidance, encouragement and various feedbacks provided for my PhD work. I gratefully thank Shri S. P. Prabhakar, DRHR, Shri T V Shyam, RCCS and Shri R. S. Shriwastaw, PIED for their contributions in development and mock-up trials of the Boat Sampling Technique at Tarapur. I also thank Dr. Garima Sharma, MMD, Dr. Arnomitra Chatterjee, MMD, Shri Pyare Singh, MMD and A. C. Alawekar, RCCS, RED for their providing their technical support related to this work. I also thank Shri Narendra B Prabhulakar and Md. Ajaj from M/s Mahatech Engineers, Mumbai for their hard work in grinding and polishing of all the miniature test specimens to the required accuracy and finish.

I gratefully thank my wife Smt. Madhwi Kumari who provided me full co-operation and support during my PhD work and carried many of the domestic burdens alone. I thank my sons Master Shashwat Kumar and Master Saket Kumar who managed their own in their studies without bothering me.

Direct or indirect support received from other colleagues in BARC is gratefully acknowledged. I thank all persons who helped me directly or indirectly, whose contributions to this work have escaped my attention and thus have gone unnoticed.

Thanks are due to my parents, elders and friends for their best wishes and true blessings.

# CONTENTS

# SYNOPSIS

Evolution of methods for extraction of mechanical properties from a minimum volume of material has been ongoing process since more than three decades. Miniature test techniques have been an integral part of the development of new materials for fusion reactors as well, since it required testing a large number of candidate materials under varying test conditions; and using standard size specimens would have consumed huge amount of material for such activities. Similarly, in existing light water power reactor surveillance programs, adequate specimens can be prepared and tested from limited available material in order to obtain complete system information. Moreover, life management activities of in-service equipments are made possible by scooping out material from component to prepare miniature specimens for conducting tests and subsequently study the mechanical properties in service condition. In the process, many types of miniature test techniques have been developed, where various test specimens either have been scaled down, like in case of miniature tensile test, miniature charpy test and miniature fatigue test etc., or novel test techniques have been developed like automated ball indentation test, shear punch test, bulge test and small punch test etc.

In this process, a number of test techniques have evolved but still maturation of these is a phantasm. Many efforts are ongoing on the world foray to achieve the maturation; however, goal of standardization of the techniques seems to behave as an illusion. Even though miniature tests have emerged to be potential techniques in extracting mechanical properties of the materials for some specific cases, as mentioned above, over the conventional test procedures, its use has been somewhat restricted, as no standard procedure has evolved for such techniques. There are certain issues, which must be addressed for the successful application of these techniques. The areas, which are not very well defined in the miniature test techniques, need to be resolved first.

Although, there are lot many issues with a host of miniature test techniques, our attention is restricted to miniature tensile tests and small punch tests, in the present work. The reason for selection of the miniature tensile test is because it is the only test technique, which gives the full material data in form of stress-strain plots, like in the case of standard test and it has the potential to be futuristic and reliable test method. However, miniature tensile test has many generic issues related to gauge length, thickness and grain size dependence etc. in order to get data comparable to standard tensile test specimens. In this work attempt has been made to optimize these parameters based on the standard test specimen and its applicability for extraction of mechanical properties of components from any in-service plant.

The other technique undertaken for the study in present work is small punch test (SPT), reason being its capability to provide UTS and YS values from very small volume of material, as small as a TEM disk specimen, which makes it best suitable for in-service inspection for irradiated materials. SPT gives material data, like YS and UTS, through different correlations, developed by various researchers. It is known that there is more or less consensus on YS correlation of SPT, however, the UTS correlations have been open issue since the development of the technique and still no correlation is unanimously acceptable. In this work, a new correlation for UTS has been developed and proposed, which is based on the necking phenomenon of the SPT disks during experiments and has been developed using experimental and numerical analyses.

Towards the end, we would like to briefly address the application aspects of this work in core shrouds of TAPS 1 & 2 boiling water reactors. A technique of scooping of metal sample (boat sample) from the core shroud or any wall structure and fabrication of miniature specimens from the boat sample and validation of test data have been discussed in this thesis.

# List of Figures:

# List of Tables:

# Nomenclature:

| | |
|---|---|
| $A_0$ | initial cross-section area of tensile test specimen |
| b | width of gauge section of flat tensile specimen |
| d | average grain diameter |
| $D_0$ | initial diameter of tensile test specimen |
| $\Delta d$ | punch displacement in shear punch test |
| E | elastic modulus |
| $e_f$ | total elongation |
| $e_u$ | uniform elongation |
| F | punch friction in shear punch test |
| K | strength coefficient |
| $K_{cr}$ | failure parameter, a material constant |
| $k_y$ | material constant |
| l, L | gauge length of tensile specimen |
| $L_0$ | initial gauge length of tensile test specimen |
| $L_f$ | final gauge length |
| n | strain hardening exponent |
| P | load, kN |
| $P_{0.2}$ | load corresponding to 0.2mm punch displacement |
| $P_{0.4}$ | load corresponding to 0.4mm punch displacement |
| $P_{0.48}$ | load corresponding to 0.48mm punch displacement |
| $P_{max}$ | maximum load in the load-displacement plot of SPT |
| $P_y$ | load corresponding to deviation from the linearity in SPT plot |
| r | punch radius in shear punch test |
| $r_{ave}$ | the average radius between the punch and the die |

| | |
|---|---|
| R | radius of supporting specimen jig |
| s | total length of flat tensile specimen |
| t, T | specimen thickness |
| $t_c$ | critical thickness of miniature tensile specimen |
| $t_0$ | initial thickness of specimen |
| w | width of gauge section of flat tensile specimen |
| $w_0$ | initial width of specimen |
| α | local elongation at necking |
| β | constant |
| $\epsilon$ | strain in shear punch test |
| $\epsilon_y^{eff}$ | yield strain obtained in shear punch test |
| $\varepsilon$ | true strain |
| $\varepsilon_0^U$ | uniform elongation of standard specimen |
| $\varepsilon^U(t)$ | uniform elongation of thin miniature tensile specimen, |
| $\varepsilon_u$ | uniform strain |
| $\gamma$ | $\frac{\sigma_1}{\sigma_2}$ |
| δ | displacement, mm |
| $\delta_f$ | displacement at final drop in load in SPT plot |
| $\delta_{max}$ | displacement corresponding to maximum load in SPT plot |
| $\delta_u$ ` | displacement corresponding to maximum load in SPT plot |
| $\rho$ | contact radius |
| λ | grain dimension |
| $\nu$ | Poisson's ratio |
| σ | true stress |

| | |
|---|---|
| $\sigma_1, \sigma_2$ | principal stresses |
| $\sigma_{APP}$ | applied stress |
| $\sigma_{1B}$ | back stress in applied stress direction |
| $\sigma_{2B}$ | back stress in width direction |
| $\sigma_{3B}$ | back stress in thickness direction |
| $\sigma_u$ | ultimate tensile stress |
| $\sigma_y$ | yield stress |
| $\sigma_y^{eff}$ | yield stress obtained in shear punch test |
| $\sigma_y$(b) | yield stress of bulk material |
| $\sigma_y$(m) | yield stress of miniature tensile specimen |
| $\tau_{1\text{-}2}$ | maximum resolved shear stress on the 1-2 plane |
| $\tau_{1\text{-}3}$ | maximum resolved shear stress on the 1-3 plane |
| $\tau_{uts}$ | ultimate shear stress |
| $\tau_y$ | yield shear stress |
| $\tau_{sp}$ | shear stress obtained from shear punch test |
| $\theta$ | necking angle for tensile specimens |
| $\theta$(t) | necking angle for thin miniature tensile specimens |
| $\eta$ | ratio of the area of surface grains to the total area |
| $\psi$ | shape constant |

# Abbreviations:

| | |
|---|---|
| ABI | Automated Ball Indentation (Test) |
| ASTM | American Society for Testing and Materials |
| BST | Boat Sampling Technique |
| BWRs | Boiling Water Reactors |
| CBN | Cubic Boron Nitride |
| CT Specimen | Compact Tension Specimen |
| CW | Cold Worked |
| EBR-II | Experimental Breeder Reactor-II |
| EDM | Electro-Discharge Machining |
| FE | Finite Element |
| FEM | Finite Element Method |
| HAZ | Heat Affected Zone |
| HFIR | High Flux Isotope Reactor |
| IASCC | Irradiation Assisted Stress Corrosion Cracking |
| IGSCC | Intergranular Stress Corrosion Cracking |
| JFMS | Japanese ferritic /martensitic steel |
| JPCA | Japanese prime candidate alloys |
| LVDT | Linear Variable Displacement Transducer |
| MDBT | Miniature Disk Bend Test |
| MEMS | Micro Electro Mechanical Systems |
| MST | Miniature Specimen Testing |
| MSTTs | Miniaturised Specimen Test Techniques |
| NEMS | Nano Electro Mechanical Systems |
| ODS | Oxide Dispersion Strengthened |

| | |
|---|---|
| RIS | Radiation induced segregation |
| RPV | Reactor Pressure Vessel |
| SCC | Stress Corrosion Cracking |
| SPT | Small Punch Test |
| SSCs | Structure, System and Components |
| STP | Special Technical Publication |
| TAPS | Tarapur Atomic Power Station |
| TEM | Transmission Electron Microscopy |
| UTM | Universal Testing Machine |
| UTS | Ultimate Tensile Stress |
| VVER | Voda Voda Energo Reactor, meaning water-cooled, water moderated energy reactor |
| YS | Yield Stress |

# CHAPTER 1

# Introduction

## 1.1 The industrial needs

Material degradation is a life-limiting factor for operating structure, system and components (SSCs) and is a major safety concern in all the industries. Material degradation leads to deterioration in material properties of the component, which leads to reduction in safe operating margin in the material. In order to assess the available safe operating margin, the SSCs need to be periodically inspected and existing material properties evaluated.

Various inspection methods are used in the industry for estimating the existing material properties for ensuring continued operation of the SSC. In case of non-replaceable components, the inspection becomes vital and requires reliability of the inspection data, as erroneous data may lead to wrong assessment of safe operating life and may result in failure and subsequent major consequences. To evaluate the existing material properties of the in-service component precisely is a major area of thrust for long, which has resulted in development of many invasive and non-invasive techniques.

Hardness measurement based techniques, such as indentation, micro-hardness tests have been quite popular among other non-invasive techniques. Several researchers have used the indentation test and have suggested direct correlations of the measured hardness value with yield and tensile strengths [1-4] of the materials. The disadvantage of the suggested correlations is that they are valid only for specific classes of materials and this makes the use of the hardness properties a procedure lacking in accuracy and not generally appropriate for evaluating the main material strength parameters [5].

Alternatively, a physical representative sample from the SSCs is preferred, if margin is available in the material thickness. Sampling from service-exposed components is effectively non-invasive in the sense that material procurement does not require post-sampling repair or reduce operating functionality for subsequent service life. Here the key problem is how to remove samples from in-service components, in such a way that plant integrity is not compromised nor are the samples rendered unusable due to excessive residual stresses arising from the removal process. This matter is discussed more in detail in chapter-5 of this thesis.

The possibility to estimate the extent of properties degradation of the in-service SSCs and predict the residual service life becomes possible by testing of small-scale specimens, made out from the removed sample from the SSCs. The use of small-scale test specimens can overcome many of the material testing limitations of conventional test specimens. A standardized small-scale / miniature test technique can have a number of potential applications based on the needs, as mentioned below [5]:

- A need for minimally invasive assessment of structures, especially for thick components of plants
- A need for evaluation where the zone to be investigated is localised:
- A need for failure analysis of a wide range of components and products where the available material is restricted:
- A need for analysis of thin components:
- A need for weldment assessment including weld material and heat affected zones within the parent metal, coatings, claddings etc.

## 1.2 Miniature/localised material sampling

In the last three decades the needs for direct testing methods to determine the mechanical properties of structural materials in components has led to increased popularity for two basic test solutions [5]:

- **Reconstructed specimen technique**: Mechanical tests on specimens of conventional standard size (i.e. large, nonminiaturised), in which however only a small region of such specimens is made by the actual material under study, while the remaining non-important parts (out of gauge lengths, threaded connections etc.) are made of a completely different material; this is the so called "reconstructed specimen technique".
- **Miniaturised specimen test Techniques (MSTTs):** The retrieved material sample from SSCs is used for preparation of miniature test specimens for conducting various tests; however, the results from these miniature specimens have been found to be debatable.

The present work is inspired from the difficulties and challenges, faced by researchers' world over, in establishing these miniature specimens test techniques as useful and standard test techniques for evaluating mechanical properties of SSCs.

## 1.3 Miniature specimen test techniques

For the last few decades, MSTTs have found widespread applications in extracting mechanical properties from substantially smaller volume of material. Many reasons have been cited for the need for development of the techniques, such as limitations of hardness tensile property correlations, limited availability of material and extraction of statistically significant number of data from comparatively smaller volume of material, etc. However, a major thrust towards development of miniature test techniques came during development of new materials for fusion reactors [6-19], which started about more than three decades ago. The application of miniature test specimens, for development of fusion materials, was necessitated due to heavy reliance on fission-reactor-based irradiation data [6-16]; development of a correlation methodology based on a fundamental understanding of radiation damage and resulting property changes; extrapolation of the correlation methodology to fusion regime and verification of extrapolated predictions by comparison with neutron irradiation data [6-16]. To accomplish the verification of the extrapolated predictions required reliance on accelerator-based high-energy neutron sources, which were quite limited in irradiation volume. Therefore, there was a need to test irradiated materials using as little material as possible due to unavailability of larger irradiation facilities [6-20]. Due to this limitation, it became necessary to use of low-volume specimens and the development of corresponding techniques to extract useful properties from such specimens [6-20]. In case of nuclear applications, the efforts to develop and standardize miniature test specimens were driven by both intrinsic and extrinsic reasons [20]. The intrinsic ones arise from the limitations imposed by standard scale testing techniques; for example, the limited availability of space in the irradiation facilities. Another example is the technical impossibility of machining standard sized geometries out of commercially available structural components; such as tubes, pipes or grids that are irradiated in-service and from which post-irradiation evaluation might become mandatory. An example of extrinsic reason is the need to reduce the radiation dose to personnel as much as possible for post-irradiation testing.

Based on these logistics, work towards development of miniature test techniques were multi-pronged: (i) scaling down the size of conventional sample, (ii) development of new specimen geometries and (iii) development and application of new techniques to existing specimen geometries, such as TEM disk [7].

Consequently, a number of activities started in this direction and rapid progress was made in development of various techniques. These techniques helped in deriving a wide range of measured properties, and interest in these techniques became relatively widespread [6-95]. Simultaneously, concern had arisen that the new techniques might be developed and applied without adequate coordination among users, leading to unnecessary confusion, production of erroneous data, duplication of efforts among various researchers and misinterpretation of data. Therefore, a task group was formed under the auspices of ASTM subcommittee E10.02 on ‘behaviour and use of metallic materials in nuclear systems’ and to consider whether a set of recommended practices of individual small specimen test techniques might be useful and, if so, to prepare a document on such practices [21]. A number of international conferences, from 1986 till recently in 2014, on small-specimen testing were organized by this subcommittee; with an aim that this could serve as initial milestone in the development of these tests, and that the resulting publications could be used to help address questions concerning recommended practices [21-26]. As indicated above, these practices included works carried out towards scaled down versions of standard test specimens and some innovative or novel test techniques, such as indentation test, miniature disk bend test, bulge test and small punch test etc.

The application of miniature test techniques has been found in fusion material development [6-19, 21-27, 31, 37, 39, 40, 45, 46] and evaluation of material properties of operating components [19, 23, 29, 32, 34-36, 44, 47, 49, 52, 55, 57-59]. Due to miniaturization, radiation dose to the personnel is limited and adequate number of specimens could be prepared and tested from the surveillance material to obtain complete system information. Therefore, miniature specimens have been attempted to estimate the mechanical and fracture properties of reactor components, using surveillance coupons [19, 36, 66], in existing light water power reactors. In case of unavailability of surveillance coupons also, scooping method

[19, 29, 35, 49, 52, 54, 55, 57, 59] and trepanning method [58] have been used for obtaining component sample for estimation of existing mechanical properties using miniature specimens.

Application of MSTTs has also been attempted in non-nuclear areas, such as for determination of mechanical properties of weld region and heat affected zone (HAZ) [28, 32, 34, 45, 54, 56, 57], for considering point-to-point variation in welded structure. Only miniature test techniques are applicable for characterizing expensive advanced alloys that are typically available in small quantities [28], for study of mechanical behaviour of microstructure in micro components and for analysis of a failed component. Application of the miniature test technique has also been found in thin metal sheets [33, 60-64], composite material [45], ceramics [45], oxide dispersion strengthened (ODS) stainless steels [45] etc.

Thus, it is found that MSTTs are applicable for materials' investigations in nuclear as well as in non-nuclear structures and components. Going through the literature for worldwide practices, the application areas of MSTTs can be broadly categorized as mentioned below:

- **Mechanical property evaluation:** This area of MSTT application is meant for evaluation of mechanical properties, such as yield stress (YS), ultimate tensile stress (UTS), uniform elongation ($\varepsilon_u$), total elongation ($\varepsilon_f$), creep properties, fracture toughness and fatigue properties. Generally, these mechanical properties are evaluated using standard test specimens; however, either due to material limitation or due to some involved advantages in small-scale testing, it has enticed researchers for choosing and attempting miniature/small scale testing.
- **Development of new materials:** Application of MSTT is found in development of new exotic metal and alloys to cater the need for rapid measurement of properties

from small volume of material. Such test procedures allow sorting of design options for materials and selection of the most likely candidates.

- **Life assessment of in-service equipment:** MSTT has good application in remainder life assessment of operating components by scooping out a small volume from it, without affecting its integrity, for metallurgical analysis. In such cases, only small specimens are possible, as the taking out large specimens from the structure would put the component at immediate risk.
- **Weld characterisation:** Evaluation of actual material property of welds, HAZ and parent material can be done using MSTT. Welded components, like core shrouds of boiling water reactors (BWRs) have been characterised using MSTT for detailed analysis and their life assessment and continuity in service. This is a generic problem associated with all welds, where the local material structures are directly influenced by the heat flux from the welding process. Typical structural changes take place, due to which this has become a more important area of study with the development of larger and more comprehensive numerical analysis methods and the more general use of very fast and large computing systems.
- **Application in nanotechnology:** MSTT has been found to be suitable for characterisation of mechanical properties of nano-materials used for making very small components/ structures.
- **Nuclear Industries:** As discussed earlier in this chapter, there is a general need within the nuclear industry that encompasses many of the applications, discussed above, in one basic requirement to cover the specific areas of development of new material, irradiation related studies, material surveillance and life assessment of operating reactor components.

## 1.4 Classification of MSTTs

Various types of miniature test specimens have originated from the nuclear industry, for reasons already mentioned in section 1.1. Nuclear industry with its high construction costs, its need for identification of radiation effects on materials and stringent safety requirement has an overpowering requirement for small specimen testing, which can be readily justified economically. Going through the various designs of miniature specimens, used till date, the MSTT can be classified in two broad categories:

### *1.4.1 Scaled-down specimens similar in shape and form to standard specimens*

Various types of scaled down test specimens, which are similar in shape to the standard size test specimens were developed and tested. For example, scaled down specimens were developed for tensile test [6, 7, 9-14, 17, 18, 27, 29-37], fatigue test [13, 14, 17], bend test [8, 12], creep test [17] and Charpy V-notch test [8, 12-14, 17, 19]. A variety of scaled down composite specimens for different types of test have been reported in the literature [12, 13].

For scaled down tensile specimens, there have been large variations, like wire type test specimens, round specimen with threaded end, round specimens with collar end, flat specimens with pin holes, flat specimens with shoulder-supports etc. Typical designs of the smaller forms are generally from sheet and are flat rather than round specimens. Various combinations of specimen thickness, gauge lengths, and other dimensions have been found in literature.

Based on the published literature, it can be said that a large variation of sizes of miniature specimens have been used over the years. As the specimen sizes reduced, degree of difficulty in manufacturing, handling, testing and data interpretation increased. Indeed, researchers have overcome many of the expected handling and testing problems, however, it is pointed out that the test methods and handling are not trivial for such small samples.

### *1.4.2 Specimens of innovative designs*

As there was a need to test irradiated materials using as little material as possible due to unavailability of larger irradiation facilities, minimization of test specimen volume led to development of a number of novel test techniques. Such techniques are hardness test [1-5], micro-hardness test [8, 13-15, 19, 35], indentation test [12-14], indentation creep test [8, 14, 17], shear punch test [8, 13, 15, 17, 36], miniature disk bend test [11, 14, 39, 40, 43, 45], bulge test [8, 14], small punch test [16, 17, 19, 20, 29, 41, 42, 44, 46-56] and disk type tensile specimens [65-66], etc. This category of specimens can be further categorized as specimens, which give material data until they fail and the other types where specimen give data without leading to failure. For example, shear punch test, bulge test, miniature disk bend test and small punch test are of former types and micro-indentation tests and micro hardness test are the later types.

## 1.5 Worldwide evaluation and development programme

As mentioned earlier, a task group was formed under the auspices of ASTM subcommittee E10.02 on behaviour and use of metallic materials in nuclear systems, to avoid duplication of work and to make a set of recommended practices of individual small specimen techniques. The first symposium on MSTT was held at Albuquerque, in 1986, and resulted in publication of Special Technical Publication (STP) 888 [21]. The primary driving force behind that symposium was the need of the fusion reactor materials research community to assess effects of the very high levels of irradiation expected in the first wall of fusion reactor. The severely limited volume of materials, which could be irradiated in test reactors to high levels of fluence emphasized the need for small specimen technology. The major topics covered in the symposium were to evaluate strength & ductility and fatigue & fracture, using various methods, such as micro-hardness test, miniature disk bend test, small punch test, shear punch test, non-standard tensile test, sub-size fatigue test, sub-size bend test and sub-size charpy V-notch test.

Thereafter, the second symposium on small scale testing was held in New Orleans, Louisiana, on 29-31 Jan. 1992, which resulted in publication of STP-1204, entitled ‘Small Specimen Test Techniques Applied to Nuclear Reactor Vessel Thermal Annealing and Plant Life Extension’[22]. The topics covered in the symposiums were from small and miniature specimens, non-destructive, non-intrusive and in-situ test techniques for measuring mechanical and fracture properties, application of those techniques to assess irradiation-induced embrittlement, and actual examples of the use of these techniques to verify results of thermal annealing of vessels and to evaluate potential reactor-vessel life extension.

This symposium was held to bring together, in a single meeting, both the diverse interests and capabilities of the scientific testing community and the needs of the commercial light water cooled power reactor industry. Thus, in contrast with the earlier meetings, which focused exclusively on testing techniques, the symposium explicitly included the needs of MSTT and its applications to commercial nuclear power reactors. In addition, the program was strongly augmented by presentation of the continued development of testing technology within the fusion reactor research community. In the area of applications, an understanding of the usefulness of small specimen test techniques for commercial-nuclear power plant-life extension was discussed; work described the application of small specimen testing and sampling techniques to evaluate the potential for continued operation of various former eastern pressurized-water-reactor pressure vessels. In non-destructive and non-intrusive testing techniques, novel approaches were described for obtaining material information on thermal aging and embrittlement by electromagnetic and electrochemical techniques with little or no damage to the piece of material being sampled. A novel automated ball indentation techniques was reported to be successfully applied to measure yield strength and flow properties in a range of metallic materials including welds and heat-affected zones and was further applied to non-destructively examine a structural components in-situ, viz. a circumferential weld in a stainless steel structure.

In this symposium, numerous other novel and improved methods for obtaining and applying data from small specimens were discussed. Improvements in both the correlation methods with standard size specimens and test techniques with impact testing of sub-size charpy V-notch type specimens were discussed. Topic related to fracture toughness provided new insight into both the limitations and possible ways to correct and utilize measurements made using very small fracture toughness specimens. Innovative experimental approaches to obtaining fracture toughness data with small amount of test material included techniques for using very small-sized compact tension specimens as well as those describing radically new specimen designs. Improvements and innovations in some of the punch and disk testing, which had been described in the first symposium on the small-scale specimen testing at Albuquerque, were reported. New approaches for automatic and remote testing and evaluating the preparation of irradiated tension specimens were described as well as new means of obtaining their required elongation information by techniques as sophisticated as laser interferometer.

As a result of the keen interest in and obvious applications for the small specimens, non-destructive, non-intrusive, and in-situ testing techniques described at the meeting, it was agreed to initiate a follow up activity with the explicit purpose of evaluating the type of materials property data generated by these various methods. ASTM subcommittee E10.02 planned to coordinate such activities, which included the distribution of one or more common sets of material for examination by interested parties. The eventual goal was to compare results from numerous non-standard techniques with results from standardized tests and with each other.

The third symposium was held in New Orleans, Louisiana, on 13-14 January 1997 and resulted in publication of STP-1329; entitled 'Small Specimen Test Techniques'[23]. The publication covered a global review of state-of-the-art research in miniature specimen testing; which covered (a) International testing program evaluation to compare miniature specimen testing results and to investigate the impact of testing variables on component behavior predictions; (b) Innovative methods for obtaining and applying data from small specimens; (c) Improved correlation methods with standard-size specimens and test techniques; (d) The impact of numerous crucial parameters on the reconstitution process, including such areas as welding technique, insert size and specimen orientation; (e) Ways to correct and utilize measurements made using very small fracture toughness specimens; (f) The use of small fatigue-pre-cracked round bars to measure pressure vessel materials fracture toughness; and (g) Improvements and innovations in punch and disk testing techniques.

The fourth symposium was held in Reno, Nevada, during January 23-25, 2000, which resulted in publication STP-1418 in 2002 [24], which had a global review on various MSTTs, which included fracture toughness evaluation using Charpy V-notch specimen, mechanical properties evaluation using tensile, small punch test and disk bend test, etc.

The fifth symposium was held during January 31–February 1, 2007, in Anaheim, California, resulting in publication of STP 1502 [25], entitled 'Small Specimen Test Techniques: 5$^{th}$ Volume'. Most of the papers dealt with use of small size specimens for fracture toughness characterization of irradiated materials. The subject areas covered were (a) Specimen Size Limitations in J-R Curve Testing, (b) Fracture Toughness Evaluation, (c) Application of Sub-size Specimens for Re-Irradiation Embrittlement Monitoring of First Generation VVER-440 RPV Steels, (d) Use of KLST-type Miniature Charpy Specimens and (e) Small Punch Test

The sixth symposium was held during January 29-31, 2014, in Houston, Texas and resulted in publication of STP-1576 [26], which consisted of topics like (a) Small Scale Mechanical Tensile Testing on Structural Materials For Nuclear Applications, (b) In-Situ Micro Compression Testing, (c) Master Curve Reference Temperature Evaluation Utilizing Miniature CT Specimen, (d) J-R Curve Determination Based on Direct Current Potential Drop Technique, (e) Shear Punch and Small Punch Testing to determine Tensile and Fracture Properties, and (f) Evaluation of Fatigue Properties of Materials through Cyclic Small Punch Experiments [67], etc.

## 1.6 Present status

Mechanical characterization of materials at miniature scales is still increasingly gaining significant prominence and has become an intense area for research, in nuclear structures and components. Apart from nuclear area, the miniature specimen technology is also found to be applicable in many other engineering applications, where availability of material is so small that standard size specimens could not be tested. As such, application areas of miniature specimens are quite vast; ranging from several engineering applications such as thin films, miniaturized electronic devices and sensors used in Micro or Nano-Electro Mechanical Systems (MEMS/NEMS), thermal barrier coating systems for aerospace applications, etc.

The more and more research in the area of miniature specimens has also brought forward their own limitations and challenges also, which have been discussed by many researchers [6-67]. Many efforts have been put towards establishing the suitability of miniature test techniques [6-67] such that it could give the representative mechanical properties from a smaller volume of material. Despite a long list of research carried out at world level, which included a series of six international symposiums also, the task of standardization of MSTTs still seems to be incomplete.

## 1.7 Scope and objective of present work

With the large volume of work carried out towards development, small-scale test technique has the other aspect as well. The volume of work conveys in clear terms that the technique, even though it looks quite simple, poses many big challenges and has many dimensions. This gives scope and opportunity to researchers to explore more areas of the technique and to address many such unresolved issues towards maturity to such an extent that it is acceptable as standard test technique, worldwide.

The present works is an attempt towards maturation of miniature tensile and small punch test techniques by addressing some issues, related to: (i) geometric design of miniature tensile test specimen, and (ii) development of UTS correlation using small punch test technique.

The objectives of the thesis are as given below:

- Miniature tensile test technique
    - To design the geometry of miniature tensile specimens that can be made out from very small volume of material, such as scooped sample
    - To develop special grips for miniature tensile specimens
    - To optimise of the thickness of miniature specimens by conducting experiments, FEM analyses and fractography
    - To develop methodology for conducting tensile test experiments using video extensometer
    - To validate the results from miniature tensile specimens by comparing the test results from standard-size test specimens and FEM analysis
- Development of UTS correlation using Small punch test (SPT) technique

- To develop a test setup for conducting SPT experiments
- To establish procedure for fabrication and polishing of 3mm dia disk specimens
- To establish test procedure and conducting experiments of 3mm dia disk specimens
- To establish necking zone of SPT specimens, on load-displacement plot, using FEM
- To establish a correlations for evaluation of UTS using SPT load-displacement plot

➢ To establish applicability of MSTTs in life assessment of core shroud of Tarapur Atomic Power Station 1 & 2.

- To establish use of scooping device for core shroud of TAPS 1&2
- To establish fabrication of miniature test specimens from dummy scooped sample
- To validate the results of miniature tensile specimens fabricated from dummy scooped sample

## 1.8 Structure of thesis

The work carried out in this thesis is organised in six chapters. The structure of the remaining part of this thesis is as follows:

Chapter-2 of this thesis provides an exhaustive literature survey related to two of the selected miniature test techniques; i.e. (i) miniature tensile test and (ii) small punch test. The survey was conducted to understand the previous works done by various researchers in these two test techniques. Both analytical and experimental studies are covered. For the sake of completeness, a brief description of other types of miniature test techniques has also been covered. This chapter also explains the gap areas and unresolved issues in these test techniques, which should be addressed for tapping their vast potential in the areas of mechanical properties evaluation.

Chapter-3 describes development of boat sampling technique for scooping of metal sample from in-service equipment and fabrication of various types of miniature test specimens from the scooped sample. The chapter further describes design and development of special test fixtures for gripping the miniature tensile specimen, use of video extensometer for measuring strain values and standardisation of tensile test methodologies for miniature tensile specimens. This chapter also describes optimisation of thickness and other dimensions of the miniature tensile specimens, which could be fabricated from scooped volume of material. Determination of minimum thickness of miniature tensile specimens has been aided by metallographic analysis and FE analysis. Chapter-3 also establishes the acceptability of mechanical properties obtained by miniature tensile test results, which are within 7%, in comparison to sub-size tensile specimens.

SPT is a correlation based technique, and has been attempted by many researchers for the last three decades; however, the UTS correlation of the SPT is an open issue till date. Chapter-4 discusses this issue and suggests a new UTS correlation, based on the necking criteria of the test specimen. The new correlation has been developed based on SPT experimental results over a range of test temperatures 25°C-300°C and numerical analysis using FEM. The FEM was used to simulate the experimental load-deflection graphs of the tests and were analysed to establish the necking zone in the disk.

As a potential application of miniature test techniques in life management activity for in-service equipment, like core shroud of TAPS 1 & 2 boiling water reactor, applicability of boat sampling technique has been discussed in Chapter-5. In this chapter, problems of core shroud cracking world over, technique for scooping out sample from core shroud, fabrication of miniature specimen from scooped out dummy boat sample, testing of miniature tensile specimens and validation of the test results have been discussed.

Finally, the conclusion of the present work and suggestions for future work has been essayed in Chapter 6.

# CHAPTER-2

# Literature Review

## 2.1 Introduction

Chapter 1 described history of development of miniature test techniques, which were classified in two major groups:

i) techniques based on scaled down designs of specimens, and

ii) techniques based on innovative designs of specimens

In the present work, one technique from each of the above groups have been selected for further evaluation; they are miniature tensile test technique from first the group and small punch test technique from the second group. This literature review is limited to these two types of test techniques only and has objectives to find out unresolved issues related to them. The review covers various aspects of these two types of test techniques, which includes different designs of specimen geometries, types of specimen fabrication techniques, test apparatus, experimental procedures and the effects of all these factors on test results. The literature review is presented in two major sub-heads; one for miniature tensile test technique and the other for small punch test technique, as described below:

## 2.2 Miniature tensile test technique

Initially, when material limitation was felt, efforts were put towards estimation of mechanical properties from hardness test using conversion correlations [1-4], however, as increase of awareness, emphasis was given for extracting tensile property data from actual tensile type specimens [5-10, 21]. This was more imperative in light of information that the reported mechanical properties, predicted by the conversion correlations, were not universal and the values were different from the mechanical properties obtained by tensile testing [32, 35]. In addition, other techniques which used correlations for estimation of mechanical properties, like micro-hardness test, ABI, etc. could not provide information regarding deformation behaviour or plasticity of the metal, i.e. percentage elongation and reduction in area which are very important parameters in estimation of ductility [32, 35]. The complete material behaviour could be adequately and reliably depicted only by the entire stress-strain curve, which could not be provided by these indirect techniques. In case of an-isotropic materials, the mechanical properties in various orientations, like longitudinal, transverse or radial directions could not be given by these techniques [35]. Further, indirect methods give properties of the surface and not of the bulk material, so in view of surface effects such as oxidation or decarburisation, either during manufacturing or in service, mechanical properties of the surface layer are significantly different from properties of the bulk material [35]. Thus, tensile testing is the only reliable technique for determination of mechanical properties of materials and this cannot be dispensed with any alternative test method. Therefore, the 'limited material available' criteria has forced researchers to develop miniature tensile specimens of miniature or small scale sizes, as discussed further below. Apart from miniaturisation of the tensile specimens, other aspects of specimen fabrication, metrology and other related technologies involved in the miniature test techniques are also discussed in the succeeding paragraphs.

### *2.2.1 Types of miniature tensile specimens used till date*

Many designs of miniature tensile test specimens have originated from the nuclear industry, particularly during high energy neutron irradiated material testing programme for fusion reactors. Going through the various published literature, it is found that a wide variety of miniature tensile test specimens, varying from wire type specimen [6] to thin metal films type flat specimens [7], have been developed for evaluation of mechanical properties of materials for a range of applications.

Panayotou [6] reported design and fabrication of wire type specimens, having total length of 12.7mm, and grip section diameters as 0.75mm, as shown in Fig. 2.1. The gauge cross-section of the specimen had diameter of 0.25mm and gauge length as 3.5mm. These specimens were fabricated from 20% and 60% cold worked (CW), by area reduction of 0.76mm diameter wire stock of 316 stainless steel. Specimen blanks were cut from stock and were carefully coated with protective lacquer. A portion of the lacquer was then removed so that a chemical milling technique could produce a section with a reduced diameter. Once a reduced section diameter of approximately 0.28mm was obtained, the specimen was electro-polished at 20°C and using a solution of 10% perchloric acid and 90% acetic acid by volume. A laser measuring system was used to measure the diameter of the reduced section. The diameter was found to vary along the length of the reduced section from 0.21mm to 0.30mm. The minimum reduced section diameter was located near the center of the reduced section. Specimen gauge lengths also could not be precisely controlled and they varied from 2.0mm to 4.0mm, due to chemical milling process. The specimens were carefully cut to a nominal length of 13mm.

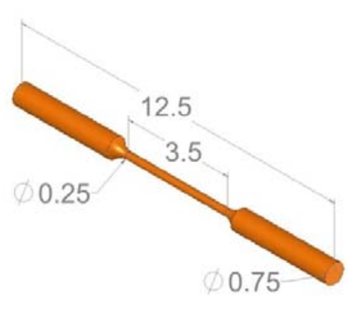


*Fig. 2.1: Wire type tensile test specimen made by chemical milling operation, (overall length 12.7mm, grip diameter as 0.75mm, and gauge cross-section as 0.25 mm dia. x 3.5mm) [6]*

Tensile test results of wire type specimens with 20% CW showed YS values in good agreement with the literature data; however, UTS value were 12.7% smaller and total elongation values whopping 50% larger in comparison to the literature data [6]. The large deviation in total elongation data was attributed to the variation in the gauge lengths of the specimens, whereas the UTS deviations were attributed to the uncertainties in determination of minimum cross-section area of the specimens. [6]

At Oak Ridge National Laboratory, United States, three types of miniature sheet type specimens, designated as SS-1 (Fig. 2.2a), one miniature rod type specimen (Fig. 2.2b), SS-2 (Fig. 2.2c) and SS-3 (Fig. 2.2d) were developed for use in irradiation-damage studies for fusion reactor materials [7]. These specimens also aimed for determination of design properties of irradiated materials. Comparison of tensile properties, determined, using these miniature specimens, was made by testing cold-worked and solution-annealed type 316 stainless steel sheet and rod, at room temperature, 300°C and 600°C. Miniature specimen of type SS-1 was developed in the Fast Breeder Reactor Program for irradiations in the Experimental Breeder Reactor-II (EBR-II). SS-1 had an overall length 0f 44.5mm and reduced gauge section 20.3mm long x1.52mm wide x0.76mm thick, as shown in Fig. 2.2a. The miniature rod type specimen, Fig. 2.2b, was developed for elevated temperature irradiations in the High Flux Isotope Reactor (HFIR). This specimen had gauge length of 18.3 mm and 2.03 mm diameter. At the ends of the specimens, spurs were provided for securing the specimen in the irradiation capsule.

To further reduce the space occupied by individual specimen and thus allowing for simultaneous irradiation of a larger number of specimens or to use for irradiation in an accelerator, SS-2 specimens, Fig. 2.2c, were developed. SS-2 type specimen was precision punched from 0.25mm thick sheet and had an overall length of 31.8mm with a gauge section 12.7mm long by 1.02mm wide. It was conveyed that because of space limitations for test specimens in most nuclear reactors used for irradiating materials for mechanical properties testing, further miniaturization of specimens was necessary. Therefore, SS-3 type specimens, Fig. 2.2c, were developed which had overall length of 25.4mm with gauge section as 7.62mm long by 1.52mm width by 0.76mm thickness [7].

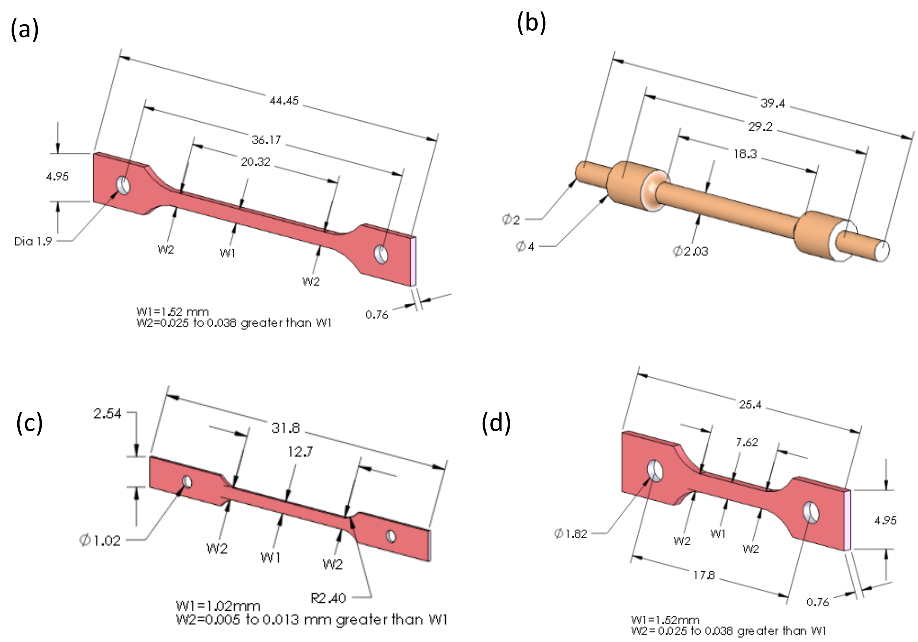


*Fig. 2.2: Miniature tensile test specimens designated as (a) SS-1, (b) rod type, (c) SS-2 and (d) SS-3, used in irradiation-damage studies for fusion reactor materials at Oak Ridge National Laboratory [7]*

Behind the miniaturization of the specimens, the objective of the study was to compare the tensile properties obtained from four different types of tensile specimens machined from same heat of material, as previously no comprehensive experimental comparison using the different specimens on a single heat of material was made [7]. Test specimens were fabricated from 316 stainless steel in the 20% CW condition and the solution-annealed condition. The SS-1 and SS-3 specimens were machined from 0.76mm thick sheet; the SS-2 specimens were punched from 0.25mm thick sheet. Prior to final 20% reduction by rolling, the sheet was annealed for 1h at 1050°C. Miniature rod type specimen were machined from 4.2mm diameter rod, which was also annealed for one hour at 1050°C prior to final reduction in area by swaging; the rod used for these tests contained ~23%CW. The solution annealed specimens were obtained by annealing the cold-worked rod or sheet specimens for 1h at 1050°C [7].

All four types of specimens were tensile tested in the solution-annealed and cold worked condition. Three of each type of specimen in each condition were tensile tested at room temperature, 300°C, and 600°C [7]. Tensile tests were conducted in a vacuum chamber on a 120kN capacity Instron closed loop, servo-hydraulic material test machine with a crosshead speed of 0.0085mm/s, which resulted in a different nominal strain rates for different types of specimens because of different gauge lengths.

The author has reported that the four types of specimens gave rise to several differences in measured mechanical properties [7]. The experimental results showed that one variant that was not directly attributable to the specimen type was the relatively higher YS and UTS of the cold worked rod-tensile specimens. In addition, the UTS of the rod specimen was also somewhat greater than solution annealed. The SS-3 specimens generally had the highest YS and UTS of the sheet specimens in both the solution-annealed and cold worked condition. There was relatively little difference between strength values of SS-1 and SS-2 specimens. For all the test conditions used, the greatest difference between the mean values for SS-1 and SS-3 was ~17% for YS at 300°C and 600°C for solution –annealed material. For the solution-annealed material, the uniform and total elongation values of the SS-3 specimens were considerably higher than for the SS-1, SS-2 and rod-tensile specimens, which had similar values. On examination of SS-3 specimen, it was observed that the deformation in the solution-annealed specimens was not confined to the reduced section but it extended up into the shoulder section, which is in contrast to what occurred for cold-worked SS-3 specimens, where all deformations were confined in the reduced section only. In effect, therefore the solution-annealed specimen had higher gauge length than used to calculate the uniform total elongation for SS-3 specimens. Many such observations have been described in the paper [7].

In summary, it is stated that the results showed consistently higher strength values determined from SS-3 specimens compared with the SS-1 specimens, especially the YS for cold worked material and the UTS for the cold-worked and annealed material, for which no explanation could be provided for similar test conditions. In addition, the concern was the differences noted for uniform elongation values, which were reported to be caused by the deformation outside the gauge length, which meant the gauge length over which the elongation values are to be determined was not defined. Differences in total elongation for the different specimens were expected, however part of that difference involved undefined gauge length, which introduced further uncertainty. Therefore, it was suggested by the researcher to exercise caution while comparing the properties. It was also suggested that discrepancies between various types of miniature specimens, especially SS-1 and SS-3, should be resolved prior to application of these specimens for determination of design-type data and for irradiation related studies. [7].

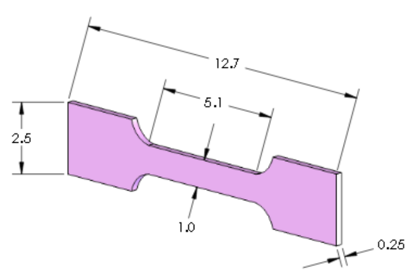


*Fig. 2.3: Sheet type specimen made by punching operation [9]*

Panayotou et al. [9] reviewed the various designs of miniature specimens, which were of wire type, Fig. 2.1; rod type, Fig. 2.2b; and sheet types, Fig. 2.2a, 2.2c and 2.2d; in light of their applications in the fusion reactor materials program, where radiation effects experiments were being performed at high energy neutron source, such as RTNS-II. The wire type specimen, as discussed above, was not found to be suitable due to various reasons, as discussed below:

i. large variation in specimen-to-specimen dimensions, mostly due to chemical milling process
ii. concerns of applicability of chemical milling process for fabrication of specimen from all fusion reactor materials,
iii. the chemical milling process needed to be optimised for all types of materials
iv. large hydrogen generated during the process could diffuse into the specimen and could alter the mechanical properties, and
v. specimens introduced unnecessary complications in analysis of radiation effect

In order to resolve these problems, miniature sheet type specimen was developed, which had overall length of 12.7mm having gauge section as 5.1mm length by 1mm width by 0.25mm thickness, Fig. 2.3 [9]. Specimens were fabricated using punching of 0.25mm thick sheet stock. Punching was selected over other available techniques because it allowed specimens with exceedingly good dimensional control to be produced rapidly and inexpensively. The variation in specimen-to-specimen dimensions for specimens punched with sharp die set was reported to be less than 1%. Before testing, the punched specimens needed careful polishing by hand on 600 grit size paper to remove the burrs produced during the punching operation. Data obtained using as-punched specimens (i.e. specimens with burrs) differed significantly from and show more scatter than data obtained using specimens which were deburred by hand. Automated deburring was found to be unsatisfactory. Commercially available automatic polishers, used for preparation of metallographic specimens were found to taper what were originally having uniform specimen cross-sections. These tapered specimens were found to give more data scatter in comparison to hand-polished specimens. Therefore, it was essential requirement to carry out manual polishing of punched specimens before testing.

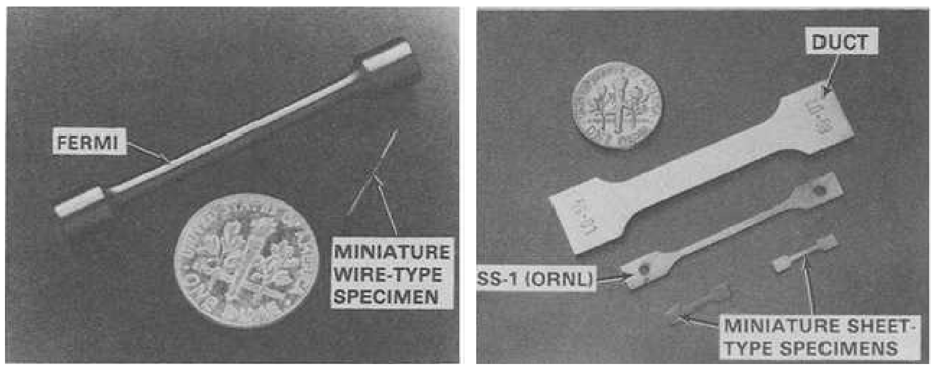


*Fig. 2.4 Comparison of a miniature wire-type specimen and miniature sheet-type specimens with larger tensile specimens [9]*

Tensile testing of miniature sheet type specimens were carried out using precision, horizontal test frame. The specimens were gripped between a stationary and a moveable crosshead. Load cell of capacity of 890N was used in the test frame. A linear variable displacement transducer (LVDT) was positioned to measure the crosshead displacement. Typically, both load and displacement data were recorded autographically. The specimens were gripped using serrated inserts placed inside parallel clamp [9].

Three different materials, namely SS316 stainless steel, HT-9 and Alloy 3, a Brush Wellman copper-nickel-beryllium alloy were used in the study [9]. Miniature wire type specimens were fabricated from SS316 stainless steel, using chemical milling process, discussed above [6]. Miniature sheet-type specimens from HT-9 were punched from cold-worked 0.25mm thick sheet stock and then were heat-treated. Specimen from Alloy-3 were punched from

0.28mm thick sheet. All the specimens were manually deburred. Miniature wire type specimens were tested at free-running cross-head speed of $1.2x10^{-3}$ mm/s, whereas miniature sheet type specimens were tested at a free-running speed of $2.5x10^{-3}$mm/s. For comparison purpose, larger Fermi specimens were also fabricated from the same materials and tested, Fig. 2.4. For 316 stainless steel, the volume of one Fermi specimen was approximately 175 times larger than the miniature wire-type specimen. Fermi specimens from SS316 stainless steel were tested using screw-driven Instron test frame at 25°C and free-running crosshead speed of $3.2x10^{-3}$ mm/s. For HT-9 the volume of the duct, the Fermi, the SS-1, and the miniature sheet-type specimens were in the approximate proportion 220:110:16:1. Flat type tensile specimen of large size, i.e. the duct specimen (from similar but not the same heat of material as used for the miniature tensile specimens) was also tested at 22°C at a free running crosshead speed of $8.5x10^{-3}$ mm/s. For Alloy 3, the volume of the larger specimen, which was 12.7-mm wide ASTM specimen, was approximately 140 times larger than the miniature sheet-type specimen. Tests on Alloy-3 were performed on standard 12.7mm wide ASTM sheet–type specimens (from identical heat of material as used for the miniature tensile specimens) at 25°C and free running crosshead speed of $2x10^{-2}$ mm/s up to yield point and $2x10^{-1}$mm/s from yield point till point of fracture.

The test results, reported by Panayotou et al. [9], for the three kinds of materials for larger and miniature size specimens are summarized in Table-2.1. It is seen that the total elongation data for miniature wire-type specimens of 20% cold-worked 316 differ significantly from data for larger specimens of the same alloy. This is not the case for miniature sheet-type specimens of HT-9 and Alloy 3. The author has reported that these differences were probably due to the lack of good control of the gauge length of the miniature wire-type specimens of 316 stainless steel, since the total elongation is a sensitive function of gauge length. The gauge length of the wire-type specimens ranged from 2.00 to 5.25 mm with a mean gauge length standard deviation of 33% [9]. On the other hand, the mean gauge lengths of punched sheet-type specimens had a standard deviation of less than 1% [9].

As an attempt to justify the use of miniature tensile specimens, despite the YS values differing most, it was argued by Panayotou et al. [9], that while UTS was the most commonly used parameter for ranking metals, and it was generally of little fundamental significance to use of YS. Further, the uniform elongation data was not available in the paper. For total elongation data, Barba's law was used for comparison of data from miniature specimens to larger specimens. It was also reported that limits of specimen size was not explored to have comparable results between miniature and larger size specimens. One interesting aspect was reported that the scatter of strength data in miniature specimens was much less than those from large specimens and it was attributed to the smaller volume of miniature specimens that might have smaller number of randomly distributed defects.

***Table 2.1: Test results of wire type, Fermi and miniature sheet type specimens [9]***

| Material | Specimen type | Mean values | | | Standard Deviation | | |
|---|---|---|---|---|---|---|---|
| | | YS, MPa | UTS, MPa | $e_f$, % | YS, MPa, (% of mean) | UTS, MPa, (% of mean) | $e_f$, (% of mean) |
| SS316 | Fermi Specimens | 669 | 832 | 25 | 59 (9%) | 22 (3%) | 4 (16%) |
| | Wire Specimens | 633 | 713 | 33 | 19 (3%) | 12 (2%) | 8 (24%) |
| | Range of data of wire specimens | 597-667 | 697-743 | 21-51 | | | |
| HT-9 | Larger Specimens | 607 | 778 | 14 | 45 (7%) | 36 (5%) | 3 (21%) |
| | Mini Specimens | 641 | 887 | 14 | 19 (3%) | 31 (3%) | 1 (7%) |
| | Range of data of mini specimens | 607-666 | 828-932 | 11-15 | | | |
| Alloy-3 | Larger Specimens | 739 | 814 | 11 | | | |
| | Mini Specimens | 721 | 829 | 10.7 | 13 (2%) | 3 (0.4%) | 0.7 (9%) |
| | Range of data of mini specimens | 703-738 | 826-833 | 10-12 | | | |

Kohyama et al. [10] studied size effects on tensile properties of SS316 and Cr-Mo dual phase steel using miniature tensile test specimens. Neutron irradiations of post-irradiation deformation response, microstructure prior to and after deformation were examined using transmission electron microscopy. The effects of specimen thickness and aspect ratio (thickness/width) on tensile properties were studied. Two types of tensile specimens, T1 and T2, were used, where the sizes of the gauge sections were 1.2 (w) x 5.0 (l) x 0.25 (t) mm for former and 2.4 (w) x 10.0 (l) x 0.5 (t) mm for the latter. Blank forms were machined from thick plate with the tensile specimens' profile, and individual specimens were saw cut to the desired thickness from the blank form. The surface was polished by wet emery paper. Specimen thickness to the specimen width ratio were varied from 0.01 to 1.0. [10, 27]

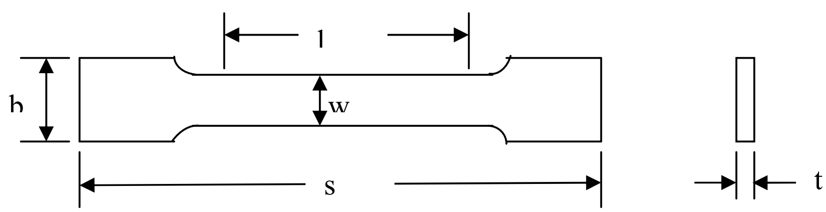


| Type of Specimens | b Width, mm | s Length, mm | w gauge width, mm | l gauge length, mm | t Thickness, mm |
|---|---|---|---|---|---|
| T-1 | 2.3 | 12.5 | 1.2 | 5.0 | 0.15 |
| T-2 | 4.6 | 25.0 | 2.4 | 10.0 | 0.30 |
| T-3 | 6.9 | 37.5 | 3.6 | 15.0 | 0.45 |

*Fig. 2.5: Type of tensile specimens, T-1, T-2 and T-3 [10, 27]*

To obtain basic knowledge of specimen size dependences of mechanical properties, investigations were carried out on un-irradiated specimens. In this work, specimen width was varied with specimen thickness, Fig. 2.5 [10]. The results suggested that specimen width did not affect the YS and that only specimen thickness, t, affected the results for thicknesses smaller than critical thickness, $t_c$. It was reported that critical thickness for ferrous materials was about 6 to 10 times the average grain size. A correlation between test results of yield stress, $\sigma_y$(m), with yield stress of bulk, $\sigma_y$(b), was proposed, for specimen with thickness, t<$t_c$, which was given as follows [10, 27]:

$$\sigma_y(m)=\sigma_y(\text{b})-\psi\left(\frac{1}{t}-\frac{1}{t_c}\right)k_y d^{\frac{1}{2}}, \tag{2.1}$$

where, 'd' is average grain diameter $k_y$ and ψ are material and shape constants, respectively.

The critical thickness for UTS was found to be affected by specimen width, as shown in Fig. 2.6a [10]. A similar dependence of ultimate strain on aspect ratio is shown in Fig. 2.6b. The work hardening coefficient was found to be quite independent of specimens' thickness and width.

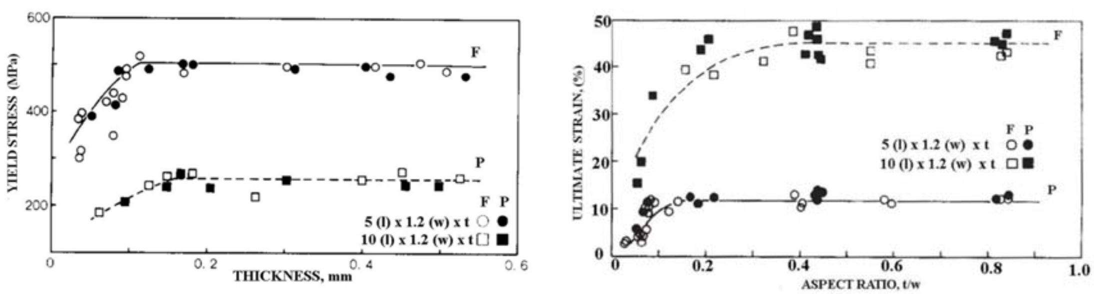


(a) (b)

*Fig. 2.6: (a) Specimen thickness dependence of YS with variation of specimen width, and (b) Aspect ratio dependence on ultimate strain[10]*

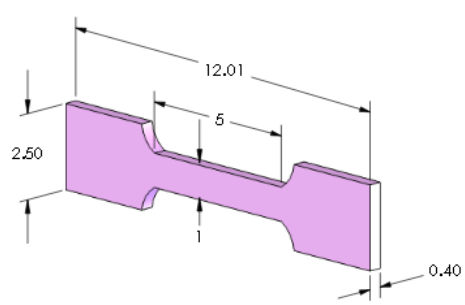


*Fig. 2.7: Miniature specimen dimensions recommended by Jung et al.[17]*

Jung et al. [17] overviewed the various miniature test techniques, that were being used world over in various fields of application. Based on the review, he recommended specimens' dimensions for various types of miniature test techniques, which included tensile test as well, which is shown in Fig. 2.7.

Konho et al. [18] studied the effect of specimen size on the tensile properties of modified SS316, designated as JPCA and ferritic/martensitic dual phase steel, designated as JFMS and have reported that effect of specimen size on YS and UTS was small, however the ductility showed significant dependence on specimen aspect ratio.

Konho et al. [18] used two types of specimens, S type and W type. S type specimen had gauge dimensions as 1.2mm wide x 5.0 mm long x 0.25mm thick, whereas the W type specimen had gauge dimensions as 2.4 mm wide x 10.0 mm long x 0.5mm thick. The blanks were cut from the thick plate with profiles of S and W type specimens, and they were sliced with wire saw to obtain specimens. The aspect ratio of the specimens was varied from 0.01 to 1 and the experiments were conducted at RT with strain rate $6.7 \times 10^{-4}$ per sec. They showed that specimen width did not affect the YS values, but the thickness smaller than the critical thickness affected them. They estimated the critical thickness of the JPCA material as 0.12mm and for JFMS material to be 0.19mm.

Byun et al. [30] studied the thickness dependence of the tensile properties of miniature specimen, with a focus on deformation and failure characteristics for SA508 steel and gave a correlation with the properties of standard test specimens. Experiments were conducted on tensile specimens of varying thickness from 0.1mm-2mm. The overall size of the tensile test specimen was 8mm x 30 mm long and gauge section as 3 mm wide x 10mm long. The specimens were provided with 3mm diameter holes at both ends for loading. Specimens were prepared using electro-discharge machining (EDM) and multistep polishing. The tests were conducted on room temperature with a cross-head speed of 1mm/min, which resulted in the strain-rate of 0.1 per min, i.e. $1.67 \times 10^{-3}$ per sec.

Byun et al. [30] reported that reduction in the YS and UTS appear when the specimen thickness was less than about 0.2mm. Fig. 2.9 shows the thickness dependence of the strength and ductility data from tensile specimens. They also gave a correlation to predict the uniform elongation of miniature specimen, $\varepsilon^U(t)$:

$$\varepsilon^U(t) = \frac{1}{2}\left[1 - \frac{2cos2\theta(t)}{3+2cos2\theta(t)}\right]\varepsilon_0^U \qquad (2.2)$$

where, $\varepsilon_0^U$ is the uniform elongation of standard specimen and θ(t) is the necking angle of thin miniature tensile specimen.

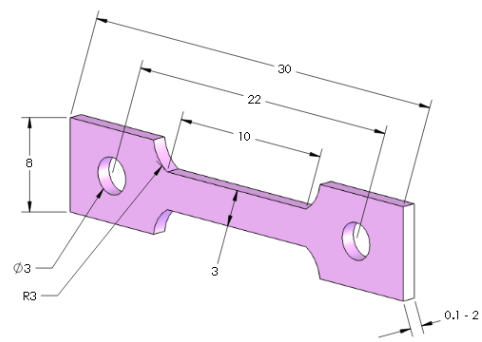


*Fig. 2.8: Geometry and dimensions of miniature sheet type tensile specimen used by Byun. Thickness of the specimen was varied from 0.1mm to 2mm [30].*

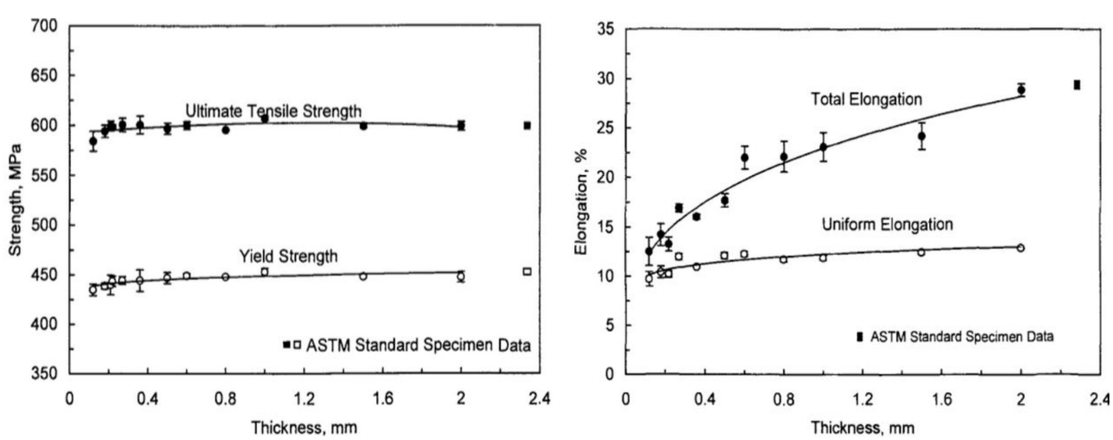


*Fig. 2.9: Thickness effect on strength and ductility data from tensile test [30]*

Dai et al. [31] studied SS316LN steel for un-irradiated and irradiated conditions. They used two types of tensile specimens; first specimen had overall size 2.5mm wide and 12mm long with gauge section as 5mm long x 1mm wide x 0.40mm thickness, while the second specimen had overall size of 4mm wide x 16mm long with gauge section as 5mm long x 1.5mm wide x 0.75mm thickness, Fig. 2.10. Experiments were conducted over a range of temperature from ambient temperature to 400°C. For un-irradiated specimens, it was found that strength and ductility decreased with increasing testing temperature. Results of irradiated specimens have not been discussed here.

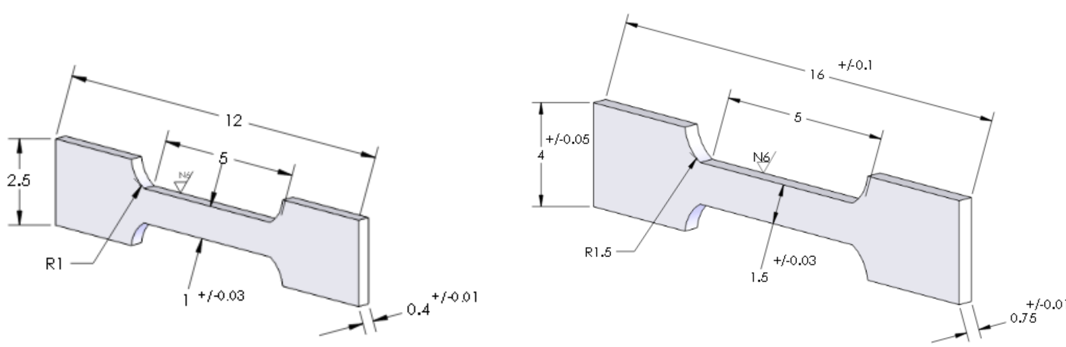


(a) (b)

*Fig. 2.10: (a) S-tensile specimen and (b) L-tensile specimen used by Dai et al. [31]*

Dobi and Junghans [32] strongly recommended conducting tensile test in lieu of general and easy hardness test for getting the tensile properties of the material. They debated that the entire stress-strain curve depicts the tensile behaviour of material, and determining YS, UTS and Young's modulus only are not the aim of tensile testing. Further, they argued that comparison of tensile data, obtained from hardness tests, within the same testing method iss generally accepted and makes sense, e.g. the comparison of hardness HB with HV and HRC. However, conversion of hardness values into tensile strength, or even worse into yield strength, is incorrect and not allowed because within these two testing methods physically different damage processes occur.

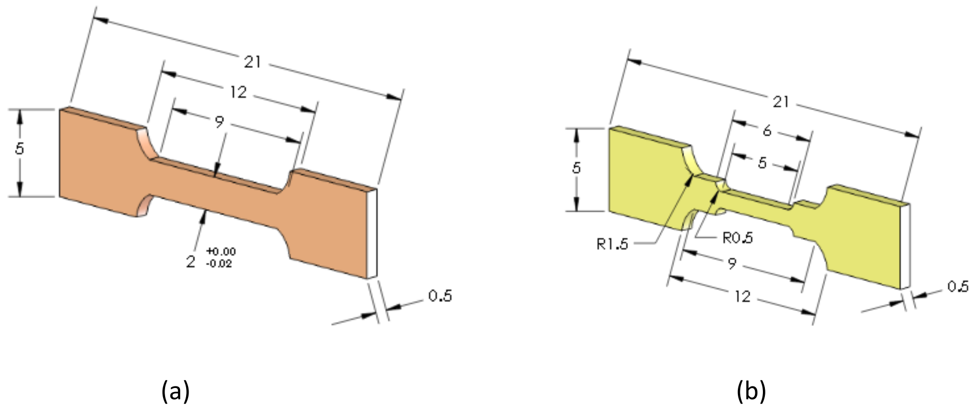


*Fig. 2.11: Mini flat specimens used by Dobi and Junghans [32]*

Dobi and Junghans [32] used two types of flat miniature tensile specimen with overall size as 21mm long and 5 mm wide, having gauge section as 2mm wide and 9mm gauge length, Fig. 2.11a; and the other had overall size same as earlier but the gauge section as 1 mm wide and 5mm long, Fig.2.10b. They used these test specimens for characterisation of explosive cladded joint, exhibiting a strong gradient in the mechanical properties.

Sergueeva et al. [33] studied gauge length and specimen size effect on measured tensile properties on 0.115mm thin sheet of Ti-6Al-4V alloy and 0.05mm thin melt-spun ribbons of Fe based metallic glass. Dog-bone tensile specimens with gauge width of 1mm and gauge lengths of 2, 5, 10, 22, 30 and 40mm were cut from the titanium sheet using wire cutting in water at low speed to prevent damage due to cutting process, Fig. 2.12. Ribbons cut from Ti sheet with corresponding width and length were tested at a strain rate of ~$10^{-3}$ per sec and at RT with a specially developed horizontal tensile testing machine. No difference in mechanical behaviour of ribbons and dog-bone shaped specimens were detected. The same gauge lengths were used during tensile testing of amorphous melt-spun ribbons. Ribbon width varied from 1.0 to 1.4mm. It has been reported that measured ductility and Young's modulus have demonstrated a strong dependence on initial gauge length. Factors affecting the tensile properties, like system compliance correction due to use on a non-standard specimens, has been discussed in this paper. It has been conveyed that tensile testing results are dependent not only on the property of material itself and testing conditions (i.e. strain rate, temp etc.), but also on specimen size and geometry. Significant drop in uniform elongation for thin sheet material was observed with increasing gauge length/width ratio. Both materials did not show any noticeable effect of the gauge length on the YS and UTS values. It was advocated to use uniform elongation values as a measure of ductility data for all materials. Young's modulus values gradually increased with increasing the gauge length and they approached their actual values at longer gauge lengths.

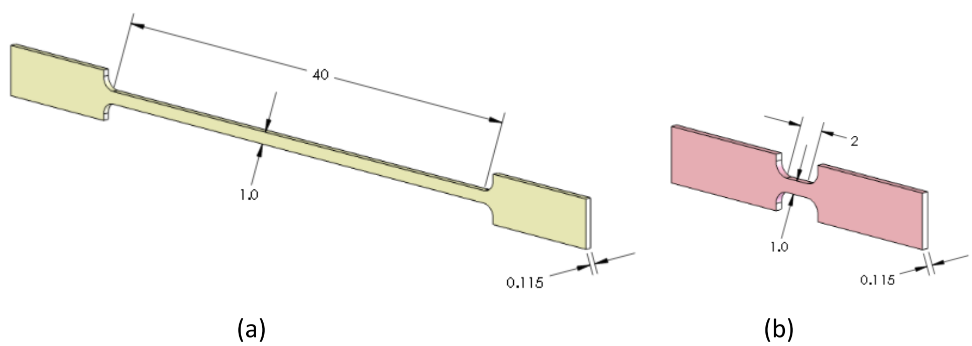


*Fig. 2.12: Specimens with varying gauge lengths of 2, 5, 10, 22, 30 and 40mm were tested. The figure shows the specimens of largest gauge length of 40mm and smallest gauge length of 2mm [33]*

Kim et al. [34] investigated the distribution of mechanical and micro-structural properties at two test temperatures, RT and 320°C, for the dissimilar metal weld joints between SA508 Gr. 1a ferritic steel and F316 austenitic stainless steel with alloy 82/182 filler metal using small-size flat tensile specimen of gauge section 2mm x 14mm x 0.5mm, Fig. 2.13a. This specimen was used for measuring local tensile properties, while standard tensile round, Fig. 2.13b, specimens of size 4mm gauge dia x 30 mm gauge length, were used to confirm the reliability of the data obtained from small-size flat specimens. The dimensions of small-size specimen were determined from the width of HAZs and buttering layers measured macroscopically.

The welded plates, Fig. 2.13c, were first cut into six blocks: four blocks for small-size flat specimens and two blocks for standard cylindrical specimens. Specimens were extracted from each block using electro-discharge machining, along the direction of the weldment, i.e. parallel to fusion line. Small-size specimens were taken from different material zones across the weld joint, including the weld metal, buttering layer, ferritic and austenitic HAZs, and both base metals at three different thickness locations: at the bottom, mid-point, and top of the weld. The standard round specimens were taken from three typical materials zones covering both base metals and the alloy 82/182 fusion area.

Tests were conducted using motor-driven UTM at RT and 320°C in air at a nominal strain rate of $5x10^{-4}$ per second. Displacements were measured using extensometers with gauge lengths of either 10mm or 25mm, depending upon the specimen type.

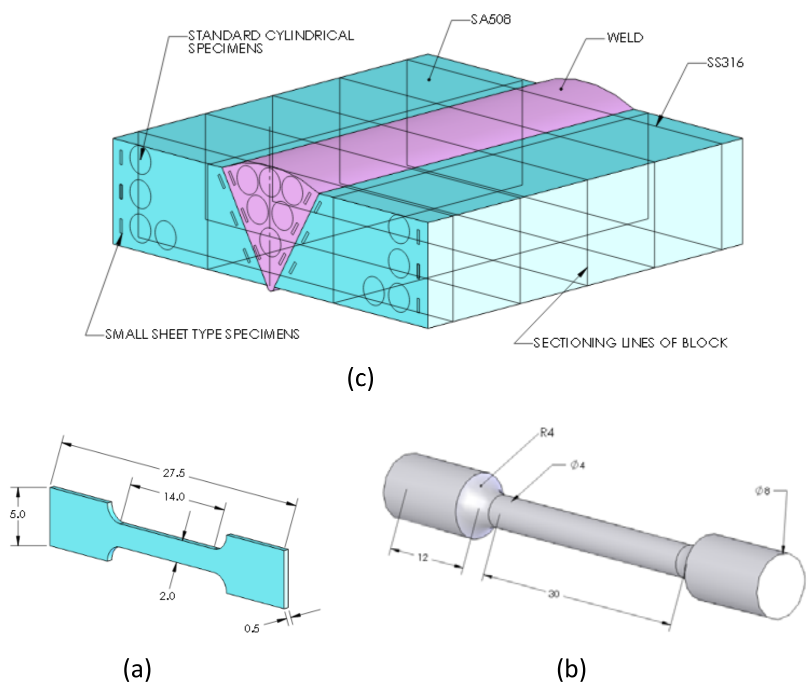


*Fig. 2.13: (a) Small sheet type specimen and (b) standard cylindrical specimen machined out from the welded block as shown in (c) with specimen layout and orientation [34]*

Validation of tensile data from small–size flat specimens was done by comparing the tensile data from standard round specimens for the base metal region. No significant differences were observed except for significantly lower elongations of alloy 82/182 weld metal from small-size flat specimens; the differences were less than 20% for other cases.

By the virtue of use of small specimens, significant gradient of mechanical properties were observed near both the HAZ of F316 SS and SA508 Gr. 1a and it could be found that YS under-matched with respect to both HAZs, although the YS of weld metal was over matched with respect to the both base metals. The minimum ductility occurred in the HAZ of SA508 Gr. 1a at both test temperatures.

Dedov and Klevstov [35] compared direct and indirect methods of determining tensile properties for post-exposed power plant steels, which saw degradation after long term operation. The results from the indirect techniques, which were based on the correlations between tensile properties and hardness and from direct tensile test, were compared. The tensile specimens of overall size of 10.65mm x 3mm wide with gauge section dimensions as 2mm x 5.65mm x 0.5mm thickness, Fig. 2.14 were fabricated from the scooped out material from the ageing component. It was shown that the values predicted by the correlations were significantly higher than the values of mechanical properties, obtained from tensile testing. It was further conveyed that automated ball indentation (ABI) technique could also be applied to evaluate the tensile properties, like YS, UTS, however plasticity of the metal (% elongation and reduction of area) could neither be measured by the technique nor by conversion of hardness value. Further, the YS or UTS values obtained from ABI or tensile correlations did not provide any information whether obtained properties were from transverse or from longitudinal direction. Additionally, hardness and ABI values were obtained from surface, so they could not give the property of the bulk material. In view of surface effects such as oxidation or carbon depletion, either during manufacturing or in service, mechanical properties of the surface layer are significantly different from properties of the bulk metal. Thus, it was emphasized in the paper that the tensile properties of the actual material could be obtained only by means of direct tensile testing. It stated further that the complete material behaviour could be adequately and reliably depicted only by the entire stress-strain curve, which could not be provided by indirect techniques.

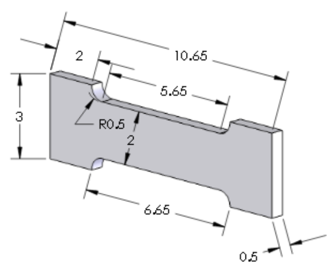


*Fig. 2.14: Miniature tensile specimen fabricated from material extracted from the in-service equipment [35]*

Rabenberg et al. [36] studied mechanical behaviour of SS304 material using miniature tensile test. They conducted tensile tests on miniature, sub-size and standard size flat specimens at RT. Miniature tensile tests were conducted using wedge-grips and through crosshead displacement measurement, at a strain rate of $3.3 \times 10^{-3}$ per sec. They suggested for an alignment fixture for mounting the miniature tensile test specimens into the wedge grips for proper alignment with machine axis. They suggested a linear correlation between shear punch and tensile data for UTS and YS as given below:

$$\sigma_u = 1.4\tau_{uts} \tag{2.3}$$

$$\sigma_{y(0.2\%\ offset)} = 1.5\tau_{y(2.2\%\ offset)} \tag{2.4}$$

Lord et al. [28] described various application areas of miniature testing, viz. assessment of remnant life of operating plants, new material development, characterising of expensive alloys, characterisation of welds & HAZ, and testing of small size components. The paper discusses issues related to measurement of strength and strain data due to size limitation of miniature specimens. The paper also discusses various types of test specimens, like simple parallel sided rectangular specimen of size 40mm x 2mm x 1mm, waisted test specimens (width at centre 1.2mm) and bowtie shaped specimens, as shown in Fig. 2.15. The usual specimen fabrication method has been described as EDM, which may have cast layer up to 50μm, which needs to be removed by polishing. It has been reported that unpolished specimen gave lesser value of ductility data in comparison to polished specimen, in case of miniature test specimens, however these differences were not found when used for macroscopic (factor of 3) test specimens.

This paper has identified a number of generic issues related to miniature tests, which include:

i. the requirement to have sufficient representative volume elements within the gauge volume
ii. the necessity to ensure the effects of constraint features (such as notches, edges, and corners) are addressed
iii. the increased likelihood of probabilistic events from small heterogeneities impinging on gross mechanical properties
iv. the lack of standardisation supported by international round robins to validate micro scale test procedures
v. the importance of specimen geometry, preparation and surface finish
vi. the possibility of surface residual stresses influencing measured gross mechanical behaviour
vii. the challenge of accurate strain measurement at these length scales, and

viii. the need to assess the statistical variation in data.

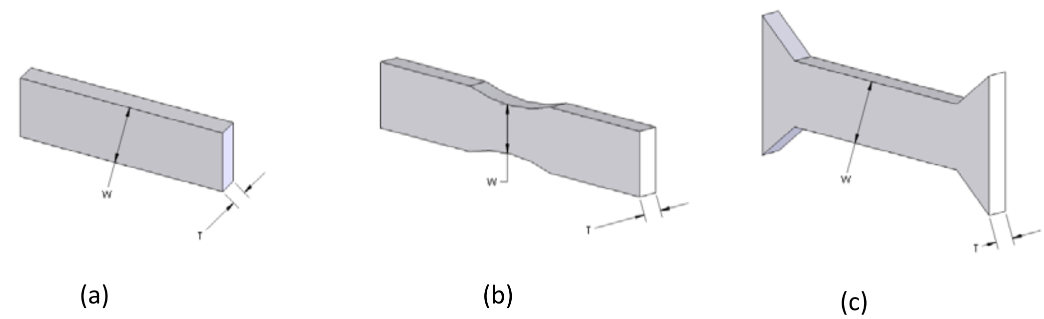


*Fig. 2.15: Miniature tensile specimens of (a) rectangular shape, (b) waisted shape and (c) bowtie shaped [28]*

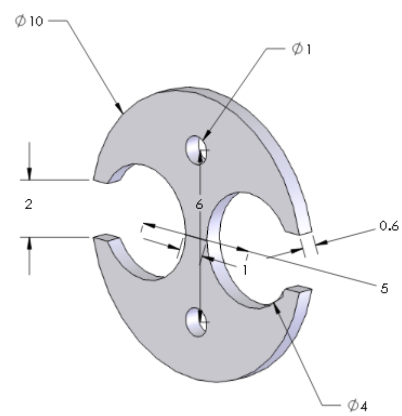


*Fig. 2.16: Non-conventional shape of tensile test specimen, as used by Partheepan et al. [65]*

Partheepan et al. [65] used a non-conventional shape of specimen to conduct tensile test. A circular disc of 10 mm diameter and 0.6mm thickness was converted into tensile specimen by cutting out two circular discs across the gauge section, as shown in Fig. 2.16. The shape of specimen was selected, as conveyed by the author, due to the convenience in analytical modelling. Specimen was also provided with two holes of 1mm diameter for loading. Final thickness of 0.5mm was obtained by polishing using grit 600 size emery paper. The gauge section of the specimen was not having any parallel length and the minimum width was 1.0 mm. The total elongation of the specimen was of the order of $10^{-1}$ mm and was measured using a mechanical extensometer, with 1 μm least count. The extensometer was attached to the fixture holding the specimen due to limitation of space (4mm) on the specimen. The testing speed was 0.05mm/min. Analytical modelling using FEM was done to generate load-elongation graph, which was found in good agreement with the experimental data [66].

Sharpe and Fowler [68] developed a dog-bone shaped specimen, Fig. 2.17a, of overall length of 3mm and both width and thicknesses are 0.2mm. The specimen was made by EDM and special grips Fig. 2.17b, were developed for conducting the tensile test. The frame had wedge-shaped grips into which the ends of the specimen were fit.

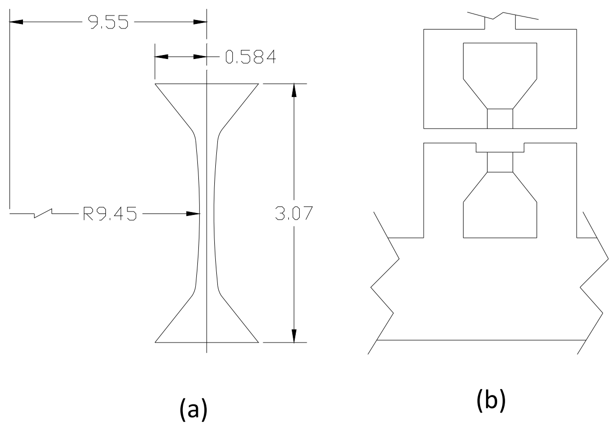


*Fig. 2.17: (a) Dog-bone shaped of tensile test specimen and (b) Special grips for tensile testing of the specimens, used by Sharpe and Fowler [68]*

### *2.2.2 Grain size effect on mechanical properties*

The experiments were conducted by Klueh [7] on cold-worked and solution-annealed type 316 stainless steel sheet and rod, at room temperature, 300°C and 600°C, using type SS-1, SS-2, SS-3 and rod type tensile specimens, as shown in Fig. 2.2, in earlier section. Comparison of tensile properties with standard size specimen found no grain-size effect on UTS values for the solution-annealed and cold-worked specimens; however, the YS values found to depend on the Hall-Petch relationship, with strength proportional to $d^{-1/2}$.

Panayutou et al. [9] has mentioned that the materials, SS316, HT-9 and Alloy-3, which were used for experiments using sheet type tensile specimens, as shown in Fig. 2.3, were having grain sizes as 32µm, 45-64µm and 15-22µm respectively. Accordingly, there were on the average 8, 4-5, and 11-17 grains across the smallest cross-sectional dimensions of the miniature sheet type specimens, made from SS316, HT-9 and Alloy-3 materials, respectively. Panayutou et al. [9] suspected the tensile test data obtained from miniature test specimens from SS316 and HT-9 materials, as the requirements of minimum 10 grains across the cross-section, as per ASTM were not fulfilled. However, it was argued that due to fine-scale structure some deviation in the 10 grains requirement was reasonable.

Byun et al. [30] studied the thickness dependence of the tensile properties of miniature specimen for SA508 steel with the grain size of 40 microns. It was reported that reduction in the YS and UTS appear when the specimen thickness was less than about 0.2mm, as shown in Fig. 2.9.

Miyahara et al. [60] studied the effect of grain size and specimen thickness on mechanical properties of type 316 stainless steel, at room temperature. The researcher used SS316, from three different sources, designated as SS316-A, A' and B; and the Japanese Primary Candidate Alloy (second heat, JPCA-2) for first wall material, designated as SS316-C. SS316-A and A' were commercial foils of 30-350µm thickness, and thin sheets of SS316-B and C were obtained by cold rolling. Tensile specimens of gauge length of 15mm and width of 4mm were cut from foils and thin sheets. Solution treatment of the specimens was done at various temperatures in the range 1320K to 1570K for 30 to 60 minutes in an air, in order to vary the average grain size. The tensile tests were conducted at room temperature at a strain rate of $4.5 \times 10^{-4}$ per sec. They have concluded that the YS value depends upon the specimen thickness, when the value of t/d is larger than the critical value, which was five in this case, the YS of this specimen becomes equal to the bulk specimens. The UTS also showed dependence on the specimen thickness, and it was reported that for t/d values larger than 3-5, the UTS values of thin specimens become equal to that of bulk material. The total elongation was considerably affected by the specimen thickness at a constant grain size. The researcher conveyed that it was difficult to deduce the total elongation of bulk material from the results using the thin specimen, when the grain size dependence of the total elongation was small. It was further reported that the effect of grain size and specimen thickness on the work hardening exponent of SS316 material was not large. However, the work hardening exponent, n, gradually decreased with decreasing specimen thickness.

Klein et al. [61] investigated stress-strain behaviour of thin metallic foils of Cu and Al with varying thickness ranging from 10 μm to 250 μm using a micro tensile machine in combination with a non-contacting laser-optical speckle correlation sensor to determine strain with high resolution. The foil specimens of rectangular shape (10mm x 40mm) were glued in to specially designed grips and were aligned in the testing machine using specially developed die. The strain measurement was determined by tracking of the speckles by digital image correlation technique. The grain size of the specimens varied between 2 μm and upto 250μm. The stress strain plot for varying grain sizes is shown in Fig. 2.18.

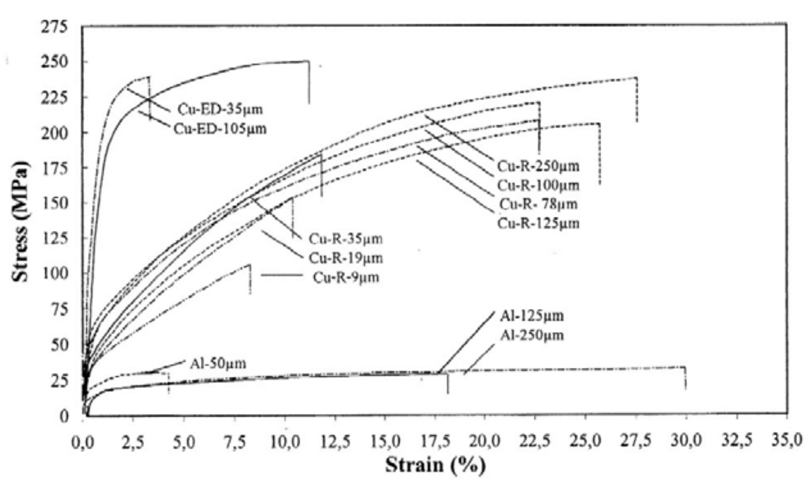


*Fig. 2.18: Stress-strain plot for Cu and Al foils with varying grain sizes[61]*

The plots can divided into three groups: (i) curves of low stress-high strain values (Al foils), (ii) intermediate values of both stress and strain belong to the rolled Cu foils and (iii) higher stress values correspond to the electro-deposited Cu foils. For all investigated materials, a similar hardening behaviour, almost independent of thickness was observed. In contrast, the fracture strain was found to be strongly dependent on the foil thickness.

Raulea et al. [62] investigated the influence of the grain sizes on the mechanical properties of soft aluminium sheets. They used miniature tensile specimen of size 15 mm width x 65mm length and 0.17-2.0 mm thickness, with gauge length and width as 65mm and 20mm, respectively, Fig. 2.18a. They conducted uniaxial tensile tests in order to investigate the influence of thickness reduction, while keeping the grain size constant.

The experimental results showed a decrease of the YS with the decreasing specimen thickness, Fig. 2.19b. This effect attributed mainly to the influence of the free specimen surface. To study the influence of specimen free surface, a parameter, η, representing ratio of the area of surface grains to the total area of the specimen cross-section was given as

$$\eta = 1 - \frac{(w_0 - 2\lambda)(t_0 - 2\lambda)}{w_0 t_0} \qquad (2.5)$$

where $w_0$ is the initial specimen width, $t_0$ is initial specimen thickness and λ is the grain dimension.

The effect of β on the tensile strength of the specimen is shown in Fig. 2.19c, which shows a relative increase of the area of surface grains leads to a decrease in the YS and UTS. In other words, the behaviour of the grains located near the free surface becomes more and more dominant.

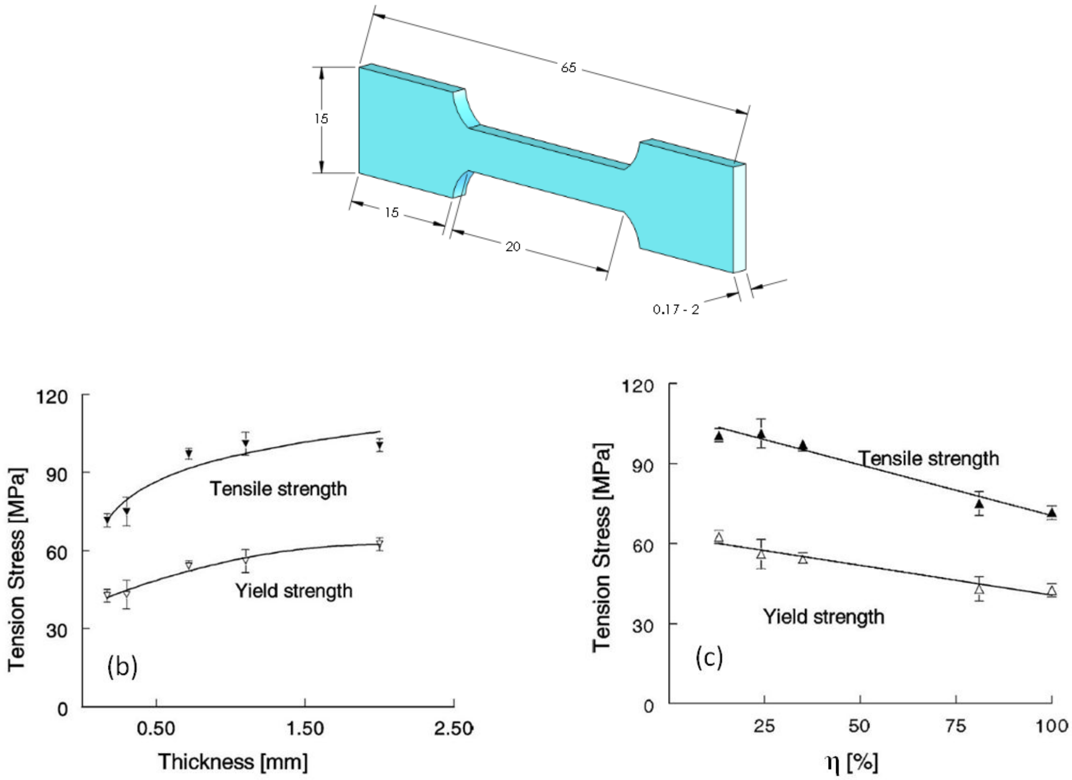


*Fig. 2.19: (a) Tensile Test specimen used by Raulea [62] and Variation of ultimate tensile strength and yield strength with (b) specimen thickness and (c) η (ratio of total area of surface grains to the total area of specimen cross-section)*

Fülöp et al. [63] carried out uniaxial tensile test on thin metal sheets of thicknesses 0.1mm, 0.25mm and 0.5mm with uniform grain size of 100µm, in all cases, thus varying the number of grains across the thickness of test specimens from 1 to 5. The miniature tensile specimen gauge sections were 2 x 0.8 x 0.1mm, 5x2x0.25mm and 10 x 4 x0.5mm. It was observed that development of flow stress deformation depended on the number of grains in the thickness direction and both initial yield limit and hardening decreased with decreasing specimen thickness. It was further reported that due to different orientations of the grains located in specimen, deformation was not uniform in tensile tests.

Li and Cui [64] studied dependence of yield strength, elongation and toughness on grain size in low carbon steel and commercial pure aluminium. They have conveyed that YS and toughness decreased and uniform elongation increased with increase in grain size, for the study carried out on grain sizes more than 100µm. They have optimised the grain size of 3-5µ for best results of YS, uniform elongation and toughness values of low alloy steels. They have correlated grain size with yield stress and uniform elongation for low carbon steel and Aluminium, as given below:

For low carbon steel,

$$\sigma_y = 0.15 + 0.51 d^{-1/2} \tag{2.6}$$

$$\varepsilon_u = 0.164 - \frac{1}{6.1 + 4d} \tag{2.7}$$

For aluminium

$$\sigma_y = 0.004 + 0.113 d^{-1/2} \tag{2.8}$$

$$\varepsilon_u = 0.385 - \frac{1}{2.4 + 0.56d} \tag{2.9}$$

where d, grain size, is in micrometres and $\sigma_y$ in GPa.

### *2.2.3 Fabrication methods for miniature test specimens*

A reliable and reproducible test results from miniature tensile test require very good control over their fabrication. In the literature, it is found that three fabrication processes have been used by most of the researchers [6, 7, 9-11, 18, 27, 30-37, 59-65]. These processes are chemical milling, punching and electro discharge machining (EDM).

#### (a) Chemical milling

Chemical milling is a photo-chemical etching technique frequently used to make high precision components for a number of industries and was attractive due to its low cost and relatively rapid operation for the production of large number of specimens. It requires masking the surface, stripping the mask from the areas to be etched away, chemically etching away the undesired regions, and removing the mask. While part outlines can be achieved with a large accuracy, the edges eaten away are known to be somewhat uneven and undercut depending on material, shape, size and thickness [6, 7, 9, 69].

A wire type specimen, of gauge diameter 0.25mm and 3.5mm gauge length, was used in liquid metal fast breeder reactor radiation program [6, 9]. This specimen had initial dimension as 0.75mm diameter and 12.7mm length and gauge section was fabricated using chemical milling operation. Several problems with this type of specimen were identified, as mentioned in section 2.2.1. Concerns rose over whether or not the chemical milling technique could be applied to all metals of interest to the fusion material program [9]. Hydrogen, generated during the milling process may diffuse into some metals altering their mechanical properties [9].

**(b) Punching method**

To resolve the issues related with chemical milling, punching method was developed to fabricate sheet-type miniature tensile specimens. Klueh [7] used punching method for the first time for making sheet type specimens, designated as SS-1, SS-2 and SS-3, as shown in Fig. 2.2. Later Panayotou et al. [9] and Hamilton et al. [69] used punching method for making miniature tensile specimens.

Punching method has benefits like good dimensional control of the specimen geometry, rapidity and inexpensive. The variation in specimen-to-specimen dimensions for specimens, punched with a sharp die set, found to be less than 1%; whereas these variations were upto

33% in case of chemically milled SS316 specimens [9]. However, the major disadvantage of the punched specimen was found to be unavoidable deformation of the specimen. Even under optimum conditions, the best specimens were likely to exhibit some cupping [69]. It was found that if the punch clearance and sharpness were not optimum, the cupping could be more severe and a burr would be present that must be polished away. Although such problems were found to be worst in very soft and very tough materials, their effects could frequently be improved by performing the required heat treatments after the punching operation. It is reported that despite some difficulties with the punched specimens, it was possible to generate reproducible results for the changes in tensile behaviour caused by irradiation [69], particularly when punching was coupled with a polishing operation to deburr the specimens. It was suggested that to produce good specimens consistently, the punch and die must be kept sharp. In addition, the clearance between punch and die must be appropriate for material being punched. The major limitation with the process is that the punches could be sharpened only a limited number of times and there are chances of being damaged during handling [69].

Before testing, the as-punched specimens needed polishing with 600 grit size aluminium oxide grinding papers to remove burr [69]. Data obtained using as-punched specimens (i.e. specimens with burr) differ significantly from, and show more scatter than data obtained using specimens which were deburred by hand. Therefore, it was suggested that the burrs must be removed before testing. Automated deburring was found to be unsatisfactory. Commercial available automatic polishers, used for the preparation of metallographic specimens, were found to taper what were originally having quite uniform specimen cross sections. These tapered specimens were found to have significantly more data scatter than hand polished specimens. Therefore, despite being tedious process, careful deburring by hand was essential if data scatter was to be minimized [9].

### (c) Electro discharge machining (EDM)

EDM is the most expensive of the three techniques, i.e. chemical milling, punching and EDM, on a per-specimen basis, but is best suitable for distortion-free and reproducible specimens. EDM is a means of shaping conductive materials by arc erosion. In this process, a tool held at a small distance from the work piece, while an electrical input builds up a charge and raises the voltage across the gap between the two, which is filled with a dielectric fluid. When the potential reaches a certain level, a discharge occurs between the closest points of the two surfaces. The discharge causes melting of minute amount of metal, which is expelled in a globular form, leaving a small crater. This process is repeated 20000 to 30000 times per second with the spark positioned by a servo-control device [69].

### (d) Comparison of chemical milling, punching and EDM methods

A detailed study regarding the effect of fabrication processes on the test specimens and on their results were carried out by Manahan et al. [11] and Hamilton et al. [68]. Work by Manahan et al. [11] was on the TEM size disk specimen to determine the extent of disturbed layer produced by various cutting processes [11]. It was mentioned that a standard fine-blade cut-off wheel could produce as much as 0.6mm thick layer of damage near surface. Precision lapping was recommended procedure to eliminate this layer. However, this can be slow and costly process when a great deal of material must be lapped off or when the specimens in the lap batch are of widely differing thicknesses. In EDM, the recast layer is typically of the order of 0.005 to 0.008mm thick [11], depending on the material and cutting conditions, which is much less than the 0.6mm of disturbed layer produce by cut-off wheels. In addition to recast layer created during the EDM cutting, there is also a heat-affected zone adjacent to the recast layer. The HAZ thickness is approximately the same as the recast layer of steels. Both layers must be removed by lapping.

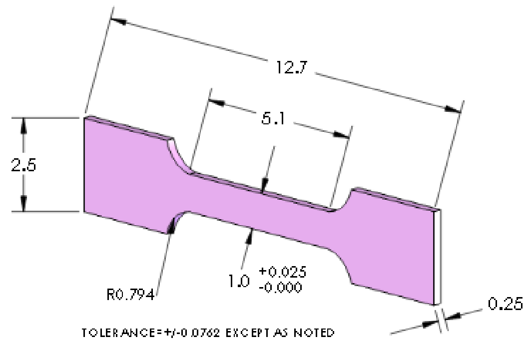


*Fig. 2.20: Miniature tensile specimen used by Hamilton et al. [69]*

The work by Hamilton et al. [69] was on sheet type tensile specimen, as shown in Fig. 2.20. In order to compare the three techniques, i.e. chemical milling, punching and EDM, three types of examinations were performed on each specimen type to determine the effect of production process on the quality of the specimens. The fabrication techniques were compared and evaluated based on various parameters, such as dimensional accuracy of specimens, optical metallography of specimens for determining change in microstructure due to fabrication procedure, hardness measurement of specimens, variability in cross sectional area of the specimens and tensile data obtained by conducting uni-axial tensile experiments. The results of the comparative studies of the specimens, as discussed above [69], are summarised in Table 2.2.

The gauge dimensions of the specimens, fabricated by the three methods, were measured to determine the cross section, which are given in Table-2.2. Optical microscopy was performed on transverse specimen sections to determine 1) whether there was evidence of micro structural change at the specimen edges, and 2) the variability in specimen cross section associated with each technique. Quantitative evidence for material distortion was obtained by comparing Knoop hardness measurement taken on the transverse specimen sections at both the cut edge and in the body of the specimen, as mentioned Table-2.2. With the dimensional measurement, given in Table-2.2, it was found that while punching produced most uniform measurements of specimen width, it also gave rise to the largest variability in measured gauge thickness, presumably due to the cupping of the specimen during the punching operation. Conversely, chemical milling produced the least distortion in the measured specimen thickness but the largest variability in gauge width. The variation in gauge width originated because chemical milling was accompanied by photographically etching the sheet stock from both sides, producing a slight bevel from each surface to the centre of the sheet thickness. It was conveyed that the variability in width produced by chemical milling was more significant for hardened steel than for solution annealed steel, most likely because the larger stored energy of the hardened steel increased non-uniformity of the etching process [69].

Knoop hardness was measured using a 200-g load on the transverse metallographic sections both at the specimen edge and at the specimen centre [69], and is given in Table-2.2. The average hardness values were almost identical at the edges and the centers of the annealed specimens, produced by chemical milling and by EDM. It was evident that punching operation severely deformed the microstructure at the edges of the specimens, even of those that were produced with new punch and die. The punching operation also caused the hardness in the centre of the annealed specimens to increase slightly relative to the hardness increase by other two methods. It was also found that both EDM and chemical milling caused a small difference in hardness between the centre and the edges. The reason for this appeared to be related to the relaxation of the microstructure allowed by the melting or etching that occurred at the specimen edges [69].

Strength calculation requires an accurate determination of the cross-sectional area of the specimens. Some error is typically associated with standard measurement techniques applied to punched specimens, given the tendency of such specimens to become cupped during punching and the potential non-uniformity of the deburring operation that usually follows punching. Several types of area calculations were performed to assess both the variability in the actual cross sectional area and the validity of the standard area calculation for each fabrication technique. The largest error in area calculation was obtained with punched specimens, while the least was obtained with EDM specimens [69], as given in Table-2.3. The UTS of the punched specimen was almost identical to that of the EDM and chemically milled specimens, the yield strength was about 15% higher and the ductility was significantly lower [69].

The metallographic analysis carried out on the specimens fabricated by three methods, by sectioning, mounting and polishing of the transverse section through the gauge section [69]. The edges of the punched specimen were reportedly somewhat deformed, although they might not need deburring, indicating that the clearance between the punch and die was reasonable for SS304 steel. The chemically etched specimen exhibited a wavy, non-uniform surface that appeared to be more variable in solution-annealed specimens than in hardened specimens. The EDM specimen showed relatively good squared-off edge with a minimal amount of probably non-adherent debris in the vicinity of the edge. Neither the chemically milled nor the EDM specimens showed evidence of micro structural change at the machined edges [69].

The metallographic, hardness and tensile data obtained, as given in Table-2.3, demonstrated that punching was likely to alter the structure of the edges of the specimens. Punching could therefore, only be considered acceptable if the specimens produced were heat treated following the fabrication to remove the deformation remaining at the specimen edges after punching.

***Table 2.2: Average dimensions, hardness and cross-sectional area of Miniature tensile specimens from SS304, fabricated by different methods [69]***

| Fabrication Process | Dimension | | Hardness, Knoop | | Deviation in Cross sectional area |
|---|---|---|---|---|---|
| | Thickness, micron | Width, micron | At Edge | At Centre | |
| Punching | 259±3 | 1027±1 | 357±18 | 173±5 | 3.8±1.6 |
| Chemical Milling | 260±1 | 1025±5 | 151±5 | 161±4 | 1.4±0.9 |
| EDM | 265±1 | 1035±3 | 157±8 | 163±2 | 0.8±0.4 |

***Table 2.3: Average tensile data obtained by tensile test on miniature specimens from SS304, fabricated by different methods [69]***

| Fabrication Process | Yield Strength, MPa | Ultimate Strength, MPa | Uniform Elongation, % | Total Elongation, % | Equivalent cold work level, % |
|---|---|---|---|---|---|
| Punching | 306±17 | 637±6 | 46.6±1.4 | 49.9±1.4 | 3 |
| Chemical Milling | 261±3 | 630±4 | 66.5±3.3 | 73.2±2.8 | 1 |
| EDM | 263±9 | 626±2 | 59.6±1.7 | 68.0±2.5 | 1 |
| Previously punched | 383±17 | 700±8 | 35.5±2.9 | 38.5±3.0 | 5 |

### *2.2.4 Test frame and extensometer*

Due to very minute sizes of the miniature test specimens of all the three types; i.e. wire type, rod type and sheet type, needed special handling not only for fabrication & polishing but also for conducting experiments. Special testing machines of lower load-capacity, lower travel, higher displacement resolution and special grips were required. Due to very small thicknesses, the specimens are very delicate in nature and alignment has been a bigger issue for all these testing machine. Panayotou et al. [6] used a horizontal load train to conduct tensile test of wire type specimens. The load train consisted of a precision motor-driven roller slide in series with a load cell and specimen. Displacements were measured with two position transducers mounted on each side of the specimen and co-planar with the specimen and screw drive axis. Specimen were gripped between a pair of serrated, hardened–steel collets. Load and deflection data were recorded on x-y chart recorder. All tests were performed at room temperature and at a free cross-head speed of $1.2x10^{-4}$ mm/s, which resulted in different strain rate for specimens, as gauge lengths varied from 2.0mm to 5.25mm [6]. This large variation in gauge lengths in the tests conducted by Klueh [7] using SS-1, SS-2, SS-3 and rod tensile specimens in a vacuum chamber on a 120kN capacity Instron closed loop, servo-hydraulic material testing machine using a cross-head speed of 0.0085 mm/s, resulted in different nominal strain rates for different specimens because of different gauge lengths.

Miniature sheet-type specimens were also tested by Panayotou et al. [9] using the same test horizontal test frame which was originally designed to test miniature wire type specimens. Wire type specimens were gripped between a pair of serrated, tool steel collets. The grips of wire type specimens were designed so that the specimen would not be loaded during gripping. This was not the case for the grips used for miniature sheet-type test specimens. With the moveable cross head fixed, a miniature sheet-type of specimen gripped between the two crossheads was subjected to small bending strain since the stationary cross head is rigidly fixed to the base of load train. Specimens were gripped between a stationary and a moveable crosshead. The moveable crosshead consisted of a jaw assembly attached to a precision slide table. A dc servomotor through a gear reduction system drove the slide table. Free running crosshead speed could be achieved from $1.0x10^{-4}$ to $5.1x10^{-3}$ mm/s and a speed of $2.5x10^{-3}$ mm/s was used for the miniature sheet type specimens. The crosshead motion was monitored by a LVDT. A load cell of 890N was positioned in the load train between the slide table and the moveable crosshead. The moveable and stationary crosshead alignment towards longitudinal axis was within 0.1°.

Lord et al. [28] described various issues related to measurement of strength and strain data from miniature tensile specimens. Due to size limitations, conventional extensometer and strain gauges cannot be used and a number of options for strain and displacement measurements, such as LVDT, electrical resistance based gauges, capacitance gauges, line scan cameras, Moiré interferometry, laser interferometry, digital speckle pattern interferometry, digital image correlation, photo-elastic stress analysis and thermo-elastic stress analysis, etc. have been discussed by them, along with advantages and disadvantages.

Dobi and Junghans [32] developed miniature flat specimens having width 2mm and thickness 0.5mm and gauge length $L= 5.65\sqrt{A}$. Due to practical difficulty of mounting standard extensometer on the miniature specimen, they attempted various modes of strain measurement, as shown in Fig. 2.21a, like cross-head travel away from the specimen, marked as ‘A’, near to the specimen, marked as ‘B’ and on the specimen, marked as ‘C’. It was reported that method ‘C’ was very close to the strain data from standard round tensile specimen, as shown in Fig. 2.21b. It was concluded that for correct stress-strain curve the elongation has to be measured directly on the specimen.

Sergueeva et al. [33] used a micro-scale tensile testing apparatus for conducting tensile tests on thin sheets of Ti6Al4V alloy of 0.115mm thickness and melt-spun ribbons of 0.05mm Fe based metallic glass. The displacement was applied by a stepping motor through the gripping system while the load was measured by a load cell that was connected to the end of one gripping jaw. Displacement was obtained through LVDT which was attached to the two gripping jaws to measure the change of gauge length. Alignment of the specimen was performed in accordance with ASTM E1012-05 and all tests were performed under displacement control with a strain rate of $1 \times 10^{-3}$ per second.

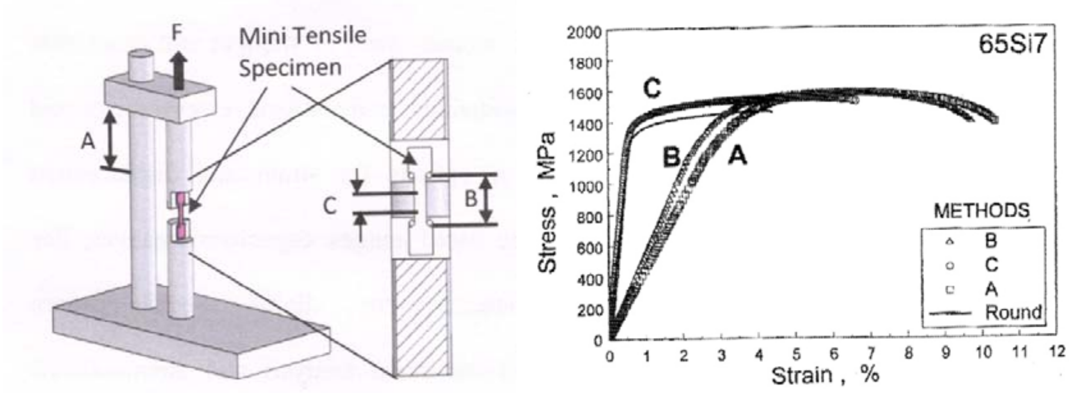


(a) (b)

*Fig. 2.21: Different methods of elongation measurement attempted is shown in figure (a) 'A' represents elongation measurement by cross-head movement, 'B' represents elongation measurement by specimen shoulder movement and 'C' represents elongation measurement directly on specimen and (b) the stress-strain plots for respective test methods [32].*

Sharpe and Fowler [68] have discussed a different design of tension test machine, Fig. 2.22, which was suitable for a dog-bone type test specimen, having overall length of 3 mm and thickness of 0.2mm. The load frame was of overall size of 20mm wide, 12mm high and 3mm thick. The frame had wedge-shaped grips into which the ends of the specimen could fit. A thin wire was fastened through the hole, in the upper grip, and pulled to displace it and load in wire was measured. The upper grip was held in place laterally by the thin cross member. Strain was measured directly on the specimen with laser-based interferometry from two tiny indentations placed on the specimens.

Okada [71] has discussed development of a robot-based tensile testing system for mechanical testing of radioactive specimens. The system was designed to accommodate a miniature tensile test specimen with a gauge section of 5.5mm x 1.2mm x0.2 mm with a total length and width of 12.5 and 2.3mm, respectively. The system consisted of a manipulator, a vibration-type specimen feeder, a rotating type specimen tray, a specimen observation system, a simulated tension test fixture, and a microcomputer for controlling the system. The system could accomplish specimen arrangement in specimen tray, specimen transportation, loading of specimen to the test fixture, conducting test and removing broken specimen from test fixture. As all these processes could be done remotely and at fast pace resulting a very less radiation dose to operator.

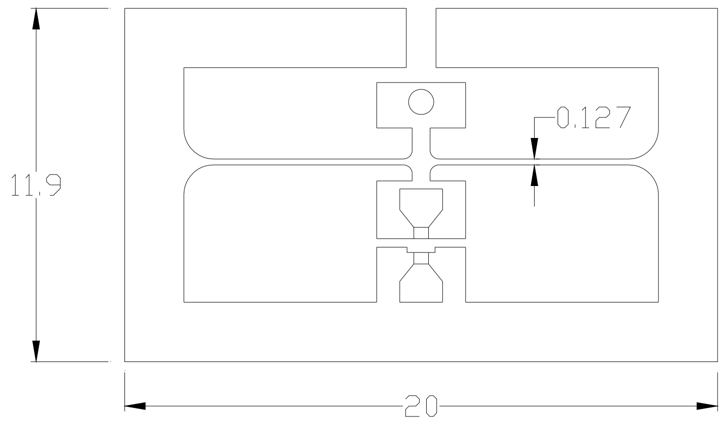


*Fig. 2.22: Special load frame developed for 3mm long dog-bone shaped specimen [68]*

Kohyama et al. [72] also developed a fully automatic tensile testing machine for irradiated specimens. The system had capability that specimen could be tested in a vacuum of $6x10^{-5}$ Pa at room temperature and in a $5x10^{-4}$ Pa at 873K or in an inert gas environment.

### *2.2.5 Issues with miniature tensile test technique*

(a**) Specimen geometry and fabrication**

As could be seen through the above discussions, in absence of any available standard for miniature tensile specimens, a wide variety of miniature specimens have been developed world over. These designs of the miniature tensile specimens have been mostly driven by need-based; such as development of new alloy & irradiation studies [6,7,9,10,17, 18, 27, 28] and life assessment of operating equipment [13, 19, 28-30, 34-36, 43, 44, 49, 52, 54, 55, 57-59] etc. Miniature tensile test has also been used in a range of other applications, varying from thin metal foils [61], thin metal sheets [62] and thin metal films for metal forming application for MEMS [63]. The miniaturization of specimen causes the so-called 'size effect' or 'scaling effect', which leads to different material behaviour in the micro-scale compared to the meso-scale and macro-scale [33]. In mechanics, this effect is limited to the strength dependence on cross-sectional area, however in general it is much wider and may relate not only to specimen size and geometry, but also, to other factors, such as micro-structural constraints, viz. thickness, grain size, anisotropy due to microstructure & crystallographic texture, micro-structural and chemical inhomogeneity etc., surface effect and residual stresses. This has led to a number of parametric studies in terms of gauge length, cross-section, thickness, grain-size, number of grains in cross-section, fabrication method, load frame, test parameters etc. [7, 9, 10, 17, 18, 27, 30, 32, 33, 60-64].

In the early eighties, Panayotou at el [6] had reported that UTS and YS data from miniature specimen were comparable; however, ductilility data needed some improvements. Klueh [7] used three types of miniature sheet type specimen of thicknesses 0.76mm & 0.25mm and found that UTS and YS properties were within 10% of the bulk properties. The total elongations of 0.25 mm specimen were found to be lower in comparison of standard specimen. Panayotou et al. [9] developed a specimen of total length 12.7mm with gauge length as 5.1mm with cross-section dimensions, as 0.25mm thickness and 1mm width, for radiation effects experiments for austenitic, ferritic and precipitation hardened alloy. Fulop et al. [63] studied size effects from grain statistics in ultra-thin metal sheets and had reported that the development of flow stress during deformation depends on the number of grains in the thickness direction and both the initial yield limit and the hardening decrease with decreasing thickness. Miyahara et al. [60] reported that UTS, YS from thin specimen of SS316 material found to be same as bulk material however, the thickness effect on the total elongation was found to be large.

An study carried out by Sergueeva et al. [33] concluded that the tensile testing results are dependent not only on the property of the material itself and testing conditions (strain rate, temperature etc.) but also on specimen size and geometry. It was conveyed again that there was no noticeable effect of gauge length on UTS and YS, however there was significant drop in uniform and total elongation for thin sheets with increasing gauge length/width ratio. Also for constant cross sectional area of the specimens, there was strong dependence of the ductility and Young's modulus on the gauge length.

As found in literature, results from miniature tensile specimen are not always correct and require validation. Therefore, for a new design of geometry of miniature tensile specimen, it is always required to validate the design by way of validating their tensile test results experimentally as well as numerically, in order to use the specimen any further. Also, it was reported that miniature specimen data could be in excellent agreement with large specimen data if specimens of controlled dimensions are prepared using proper fabrication techniques.

Based on above discussions, the following are the guiding criteria for the design and fabrication of miniature tensile test specimens:

- Specimen geometry should be suitable to be fit in available volume of material
- Number of specimen (to be fabricated from the available material) should be more to have more results
- Fabrication methods should not affect the property of the specimen, i.e. specimen should not be spoiled/damaged
- Design of gauge section of the specimen based on the available reliable method for strain/displacement measurement

- Design of grip section and special grips for positive and distortion-free gripping of the test specimen, and
- Method for validation of tensile data from miniature specimen

**(b) Minimum thickness of material in gauge section**

Apart from deciding gauge section (length and width), grip section and overall size of the miniature specimen, specimen thickness determination is a very important aspect in geometrical design of miniature tensile specimens and it requires special consideration. It has been reported [63] that due to different orientations of the grains, the deformation is no longer uniform even under homogeneous loading conditions. Klein et al. [61] studied size effect on the stress-strain properties of thin Cu and Al metallic foils of thickness 10µm to 250 µm with grain sizes 2 µm to 250 µm. It was reported that size effect was detected mainly on the fracture strain, which was explained as an effect of reduced number of activated slip systems due to the ratio of grain size to foil thickness, approaching unity. Raulea et al. [62] studied grain size effect on processing of thin Al sheets of thickness ranging from 0.17 to 2mm and grain sizes 0.016 to 600 mm$^2$. It has been reported that yield strength as well as the maximum load decrease with decreasing number of grains over thickness. For grain sizes larger than the specimen thickness, the value of yield strength appears to increase with grain size. Behaviour of each grain differs strongly due to variations in orientation.

Thus, in order to get comparable stress-strain curve from miniature tensile specimens, it is required to determine the minimum thickness of the specimen, or minimum value of thickness/grain-size ratio.

**(c) Strain measurement**

During the initial period of development of miniature specimen testing, strain data was obtained by measurement of the displacement of the crosshead of the machine [6, 7, 9], however, it is known fact that such data have compliance issues. Dobi and Junghans [32] have quantified the difference between various methods of strain measurement and concluded that correct stress-strain data are obtained when strain is directly measured on the test specimen.

Generally, miniature specimens have very small gauge length (≤5 mm), on which any conventional extensometer or strain gauges cannot be mounted and it is always a major challenge to obtain reliable strain directly on the specimen.

## 2.3 Small punch test

During the development of miniature test technique, apart from scaled down versions of standard test specimens, some innovative novel test techniques such as indentation test, miniature disk bend test, bulge test, shear punch test and small punch test etc. have been developed. In the series of development of these innovative novel test techniques, first comes instrumented micro-hardness test, which is based on the indentation of a sample surface by a spherical indenter. The test has the advantages of the standard micro-hardness test as it is relatively simple and inexpensive to perform and only a small region of test-specimen surface is damaged for each indentation. Therefore, the sample can be reused in subsequent studies. The test has the additional advantage over the conventional micro-hardness test of providing more extensive flow property information. But this technique has limitation, such as it does not provide ductility data, directly.

Consequently, to complement the micro-hardness test, several test techniques were investigated to directly measure ductility, and primarily the failure ductility. These techniques were largely based on tests used in the sheet forming industry [8, 39]. The idea involved in development such techniques was to use bending in place of tension (which is used in UTM) to extract mechanical properties of a material. This method, to extract stress-strain behaviour from a pure bending, was first attempted by Herbert [39] for cast iron bars. Sometime later, Crocker [39] obtained stress-strain information for large deflections and plastic strains using a three point rotary bend test. Stelson et al. [39] used an adaptive controller to measure force and displacement during brake forming to estimate work piece parameters with a micrometer, which were then used in analytical elastic-plastic material model to predict correct final punch position. Although these developments at that time were useful for metal forming industries, they were not readily adaptable to post-irradiation mechanical behaviour testing because of large size and awkward loading configuration [8, 11, 39]. Later, these developments were extended to miniaturized disks, which required modifications due to very small specimen size and precisely controlled loading conditions; the technique latter called as "**miniature disk bend test**" [8, 11, 39, 40]. One of the initial attempts for MDBT was done by Manahan et al. in early eighties [11, 39] when a hemispherical punch of 1mm diameter was forced through a TEM sized disk, which was simply supported over a 2.46mm hole with a rounded shoulder; the load displacement curve obtained was used to identify various deformation regions. Though any correlations were not suggested, however it was shown that the technique had the capability to determine biaxial stress/strain response, biaxial ductility, stress relaxation behaviour and biaxial creep response. The technique used by Manahan et al. [11, 39] required a test setup, Fig. 2.23, to provide simply-supported loading condition to a miniaturized disk of the size of TEM specimens. The development of the test setup further required optimisation of various design parameters through bench-testing. This test set-up was made of high density Alumina, because of high compressive strength, good wear resistance, and low thermal conductivity in comparison to the steel specimens. An alignment fixture was used for accurate alignment of specimens, within 0.0254mm. The maximum error in deflection measurement over the entire calibrated range was reported as 0.00254mm. The specimens were stamped out from rolled sheet to a diameter of 3.0 ±0.0076mm and subsequently precision lapped to a thickness of 0.254±0.00254mm. Punch velocity effects at RT were found to be unresolved for punch speeds ranging from $8.47 \times 10^{-4}$ mm/s to $8.4 \times 10^{-2}$ mm/s, therefore a convenient velocity of $4.23 \times 10^{-3}$ mm/s (0.254mm/min) was chosen for subsequent experiments. Experiments carried out on Be, Cu, SS302 and SS316 stamped out specimens and each material had unique and distinguishable load-deflection graph. Based on the experiments, it has been reported that higher yield strength corresponded to larger elastic central loads and higher elastic modulus indicated larger slope in the elastic region. Effect of temperature was also indicated in qualitative terms as rise in temperature resulted in reduction in YS and UTS values [11, 39].

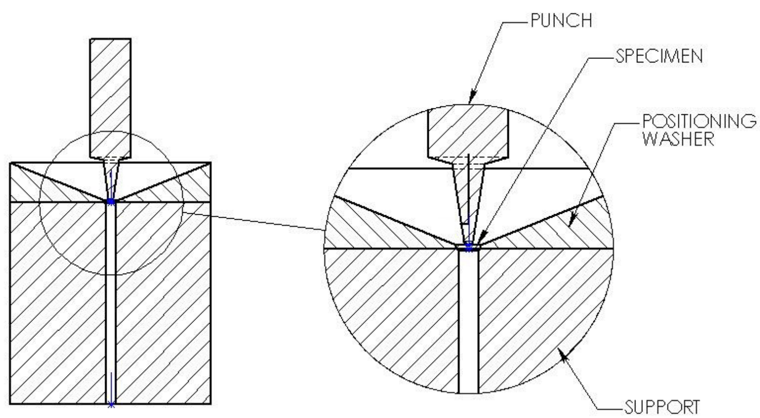


*Fig. 2.23: Schematic of miniature disk bend test setup [39]*

Vorlick et al. [43] used 3mm x 0.25mm thick disk to conduct miniature disk bend test for derivation of Young's modulus, YS and UTS of $2\frac{1}{4}$ Cr1Mo steel over a temperature range of -196°C to 25°C. The specimen were prepared from a rod machined to 3mm diameter, which was sliced into disks of ~0.4mm thickness. Each specimen was then precision ground to the final dimension of 0.25mm using 800 and 1200 grit silicon carbide paper. The surface finish was ensured to be 4 micron. The thickness of specimen was measured using optical projection system and was accurate to 0.005mm.

The upper and lower dies were joined by four screws in such a way that the geometry constrained the specimen from cupping upwards at the periphery during testing. The clearance between the specimen and upper die was kept 0.01mm. Tests were conducted at RT and at a speed of 0.2mm per second. The correlation for YS and UTS were given as:

$$\sigma_y = 3\frac{P_y}{2\pi t_0^2} \tag{2.10}$$

$$\sigma_u = \frac{P_{max}}{22\pi r t_0} \tag{2.11}$$

Correlation for elastic modulus was given as

$$E = \left(\frac{P}{\pi\delta t_0}\right)[1.2(1+\nu)\ln\left(\frac{R}{\rho}\right) + \frac{0.75R^2(1-\nu^2)}{t_0^2} \tag{2.12}$$

where, $t_0$=specimen initial thickness, $\delta$ =displacement, R=radius of supporting specimen jig, $\rho$ =contact radius, $\nu$=Poisson's ratio, $P_y$ = Load corresponding to elastic to plastic transition in P- $\delta$ plot and $P_{max}$= maximum load in P- $\delta$ plot

Equation for E, assumes that the contact radius is constant throughout elastic deformation of the disk and there is no friction at the contact surface. However, because contact radius increases as the load is increased, this would lead to the evaluated value of E being an underestimate of the true value.

Xu et al. [19] and Chen et al. [45] carried out MDBT experiment on 3mm diameter and 0.3mm thick specimen at RT and used elastic-plastic bulge deformation principle of medium–thick plate. With the assumption that fringe of the plate was fixed and maximum central deflection is less than four times the plate thickness, and the plate thickness was about one-tenth of the diameter of the plate, the yield strength of the material could be given as

$$\sigma_y = 0.477\frac{P_y}{t_0^2} \tag{2.13}$$

The UTS could be given as

$$\sigma_u = \sigma_t e^{-\varepsilon_t} \tag{2.14}$$

and the uniform elongation could be give as

$$\epsilon_u = e^{-\varepsilon_t} - 1 \tag{2.15}$$

where $\sigma_t$ and $\varepsilon_t$ are true stress and true strain, which could be calculated by load-deflection curve by and ASTM method [45]. About the accuracy of results, it was reported that standard deviation was less than 3% for strength data, however it was much larger for uniform elongation data.

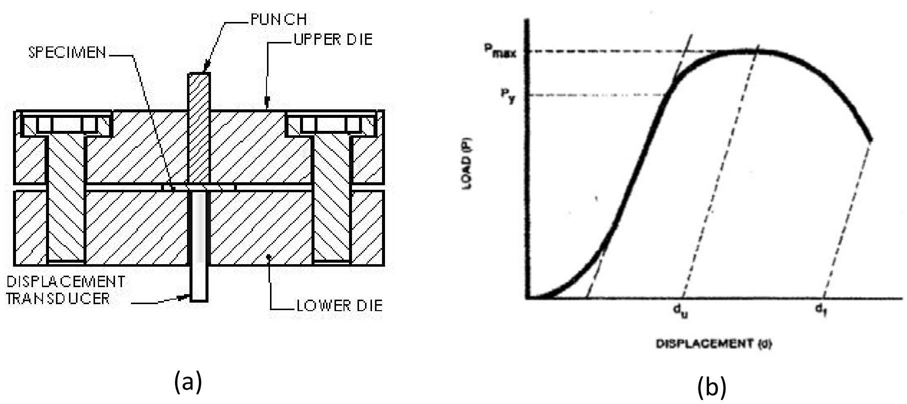


*Fig. 2.24: (a) Schematic of shear punch test and (b) Typical load displacement curve of the shear punch test [8]*

The other technique in this category, which was developed, was '**shear punch test'** [8], which had the potential to provide strength and work hardening information. The schematic arrangement of the test setup was as shown in Fig. 2.24a. It consisted of a lower and upper die and a cylindrical punch. The upper and lower dies had concentric, hardened steel bushings. The upper bushing served as a guide for the punch and the lower bushing and punch acted as the two blades in shearing the disk from the sample. In testing, a thin specimen was held between the two dies and a hole was punched by pressing the punch through the specimens. Both the load and displacement of the punch were continuously monitored, during the test by means of a load cell in series with the load train and a displacement transducer. A typical load displacement curve of the shear punch test is shown in Fig. 2.24b. It exhibits an initial, nearly linear portion, a subsequent deviation from the linearity (at load $P_y$) and non-linear increase of load with displacement; a maximum load ($P_{max}$) and a decrease in load with displacement ($\delta_u$) until a final drop in load ($\delta_f$) signals completion of the punching process. Various points of the load-displacement graph, as shown in Fig. 2.23b, have been correlated with various mechanical properties of the material, viz. the $P_y$ value was found to be successfully correlated with YS, $P_{max}$ with UTS, $\delta_u$ with uniform elongation and $\delta_f$ with total elongation. These correlations were found to be valid for different punch diameters, viz. 6.35mm, 3mm and 1mm. The uniaxial yield stress, $\sigma_y$, obtained in test on sample of aluminium, copper, yellow brass, SAE 1015 steel, SS304 and four pressure vessel steels were compared to the values of $\sigma_y^{eff}$ obtained in shear punch tests on the same material. Thus $\sigma_y^{eff}$ is defined as

$$\sigma_y^{eff} = \frac{P_y - F}{2\pi r t_0} \qquad (2.16)$$

where, F= punch friction, r=punch radius, and $t_0$= sample thickness

The total uniaxial ductility for materials listed above was plotted against $\epsilon_f^{eff}$, where $\epsilon_f^{eff}$ is defined by

$$\epsilon_f^{eff} = \frac{\delta_f}{t} \qquad (2.17)$$

where $\delta_f$ is the total plastic displacement till failure, as shown in Fig. 2.24b

While there is reasonable correlation between the two quantities $\delta_f$ and $\epsilon_f^{eff}$ for each type of punch, it is clearly not a linear relation as it was for YS and $\sigma_f^{eff}$. While shear punch test have advantages over indentation tests as it provides ductility apart from strength values, it is less sensitive to microstructure and sample preparation as sample size is larger than in case of micro-hardness test. The major disadvantages are that the test is destructive and the stress and deformation states in the process zone are highly complex, thus making physically based correlations of the data rather than simple empirical correlations most difficult.

Rabenberg et al. [36] studied mechanical behaviour of SS304 material using shear punch test and derived correlations for YS and UTS. Shear punch tests were conducted at RT on an electromechanical test frame, using a displacement rate of $4x10^{-3}$ mm per sec. The punch displacement was measured using a LVDT attached to the crosshead of the test frame. The average shear yield stress was determined using a predetermined 2.2% strain offset. Shear stress, $\tau_{sp}$, obtained from shear punch test was given as

$$\tau_{sp} = \frac{P}{2\pi r_{ave} t} \qquad (2.18)$$

where P is applied load, $r_{ave}$ the average radius between punch and the die and t is the specimen thickness. The displacement is recorded and a normalised displacement is used for strain which is defined as :

$$\epsilon = \frac{\Delta d}{t} \qquad (2.19)$$

where $\Delta d$ is the punch displacement and t is the specimen thickness. The average UTS and YS obtained using miniature tensile tests were plotted against those obtained using shear punch tests to determine correlations. Linear correlations were observed as given below:

$$\sigma_u = 1.4\, \tau_{uts} \qquad (2.20)$$

$$\sigma_{y\,(0.2\%\, offset)} = 1.5 \tau_{y(2.2\%\, offset)} \qquad (2.21)$$

It was further stated that there was negligible dependence of surface finish on the shear strength of SS304.

Lucas et al. [8] attempted **'bulge test'**, in which the specimen was clamped between upper and lower dies and a spherical ball was used for creating displacement, however, he limited this as a test for getting ductility information and ductile fracture parameter, $K_{cr}$ for failure analysis of thin-walled structure. As bulge test was based on the approach used in metal sheet forming analyses, in an attempt to make smaller test specimen, this test was first conducted on 20mm x 20mm x 0.5mm thick test specimen [8]. Schematic arrangement of bulge test setup is shown in Fig. 2.25 [8]. The punch is forced into the specimen in controlled manner to bulge until its failure. The upper die features a hardened bushing guide for the punch and the lower guide has shouldered hole into which the sample is bulged.

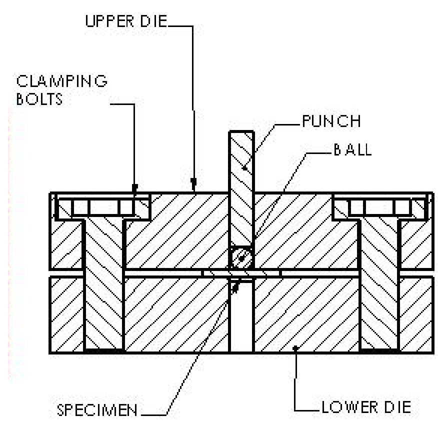


*Fig. 2.25: Schematic of bulge test setup [8]*

Unlike in shear punch test, in this case deformation is not localized in the small area of specimen and is spread over whole region of the sample that is not clamped. In addition, the stress and the deformation state change with radial position from the bulge center. The biaxial (in case of bulge test) and uniaxial (tensile test) data was best related by a model of Ghosh

[8], which is based on the assumption that ductile failure occurs by the growth and shear linkage of micro-voids; mathematically the criterion reduces to:

$$\sigma_1^2(\gamma + 1) = K_{cr} \tag{2.22}$$

where $\gamma$=$\sigma_1/\sigma_2$; $\sigma_1, \sigma_2$=principal stresses and $K_{cr}$= failure parameter, a material constant. In theory, once $K_{cr}$ is known, the principal strains at failure (ductility) can be determined for any planar stress state by tracking the deformation history of the specimen with an approximate constitutive equation and flow rule until the above equation is satisfied. Using value of $K_{cr}$, obtained by uniaxial tensile test, principal strains to failure were predicted for balanced biaxial tension, which were found to be in fairly good agreement with actual data obtained in the bulge test.

Lucas et al. [40] carried out parametric studies for bulge test to understand the behaviour of a load displacement graph due to change in ball size, receiver hole size, specimen thickness etc. It was reported that load displacement data was most sensitive to specimen thickness [16] and also that yield load, maximum load and maximum punch displacement all increase due to increase in specimen thickness. It was also reported that increase in ball size increased the yield load, maximum load and slightly decrease the displacement to failure [16], whereas increasing the receiver hole size does not have any effect other than to shift the transition from bending to stretching type deformation to higher displacements [16].

Lucas [8] concluded that Bulge test has the advantage over the shear punch test that the stress and deformation state are more amenable to analytical description; thus, it has more useful for fundamental studies of ductility. Further, he conveyed that bulge test was more difficult to conduct on small scale than the shear punch test. Scaling studies on relatively large coupon samples indicate that sample must have a width–to-thickness ratio greater than 30 and a width greater than 3 times the hole diameter for there to be sufficient material to keep the sample clamped in place during bulging.

Bulge test, with clamped specimen and spherical indenter, is now-a-days, exclusively referred as **'Small punch test'.** In this technique a TEM disk specimens of 3 mm diameter or 10mm square specimen is clamped in a die assembly and is centrally loaded by a spherical ball and a punch in a position controlled manner. This produces a bulge in the disk rather than a shear cut at the flat punch edge as in 'Shear punch testing'. The economics of production and evaluation of the newer exotic materials and the physics of radiation damage, of any form, coupled to the need to handle materials, which were active, led to the development of these very small specimen designs. The 3 mm disk design, which is a standard for TEM examination, has obvious attractions including the already developed handling methods, etc. and the ability to subsequently use the specimens for TEM and optical studies. This results in a complex deformation pattern during the full penetration of the disk by the punch.

In Small Punch Test (SPT) a small disk specimen is clamped within a die assembly, Fig. 2.26a, and is pressed by a punch in a controlled manner and a typical displacement- load record is obtained as shown in Fig. 2.26b. The general form of the plot suggests that the yield stress is associated with the change in linearity, marked as $P_y$, the UTS with the peak load and ductility with the maximum displacement. However, for full comparison, more accurate and verified values are required. Even at this level, there is a possibility of the use of the test for initially rating materials. The general form is directly influenced by geometry and loading parameters, and is illustrated by various correlations developed by researchers, discussed below.

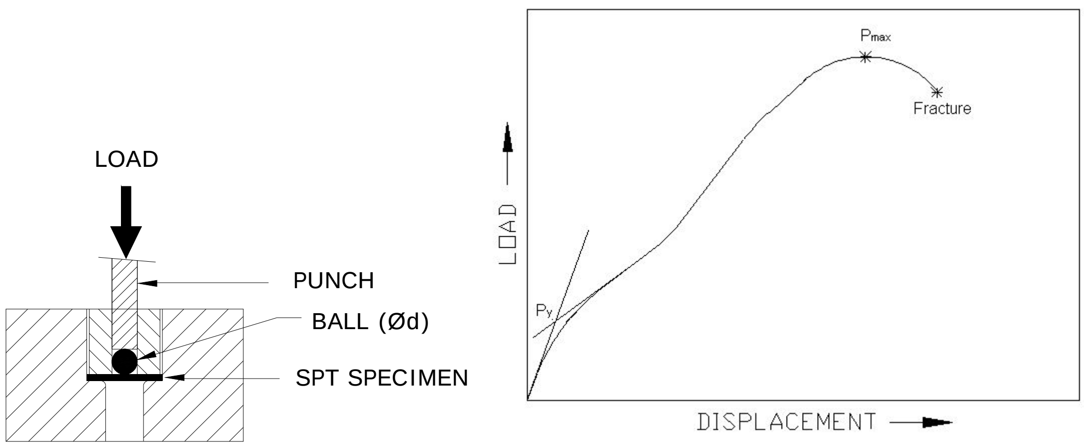


(a) (b)

*Fig. 2.26 (a) Small punch test (SPT) setup and (b) Typical SPT load vs. displacement plot*

### 2.3.1 Correlations of SPT

Mao and Takahashi [41] used 3mm diameter and 0.25mm thick TEM disk and 10mm square and 0.3-0.5 mm specimen for conducting the SPT. All the tests were conducted at RT and at a crosshead speed of 0.2mm/min. It was suggested that alignment of the punch and die as well as load-line centering were critical in SPT in order to eliminate or minimize anisotropy effects, which are caused by eccentricity. It was reported that there were three basic contributions to planar isotropic deformation in bulge testing that are of prime importance:

- a punch axis of a symmetry coincident with die axis of symmetry
- strict design tolerances for the punch and upper and lower dies, and
- a specimen with constant thickness at any point

The first requirement could be met by using a precision alignment fixture; the second and third, by careful experimentation and by accurate machining of the punch, the dies and the specimen. A check of the centering of the load line in each specimen could be made by applying a small load on the specimen, and subsequently measuring the location of the punch-plastic indentation center and the die-plastic indentation ring in an optical comparator.

Mao and Takahashi [36] gave the following correlations for evaluation of YS and UTS using SPT:

$$\sigma_y = 360\frac{P_y}{t_0^2} \tag{2.23}$$

$$\sigma_u = 130\frac{P_{max}}{t_0^2} - 320 \tag{2.24}$$

where, $t_0$=specimen initial thickness, mm, $\sigma_u$=ultimate tensile strength, MPa, $P_y$=yield load, kN and $P_{max}$=maximum load, kN

It was reported that YS correlation was similar for both types of specimen, i.e. 3mm TEM disk and 10mm square, however, the UTS correlation for 10mm square x 0.3mm specimen, the results showed larger scatter. The reason given was the differences in the onset of necking in the membrane stretching region, for 10mm square x0.3mm specimens.

Takahashi et al. [42] prepared a recommended practice for small punch testing of metallic material using TEM disk 3mm x 0.25mm thick, 10mm square x0.5mm thick and 10mm square x 0.25 mm thick specimens. In this practice, they have shown various regions of P-δ plot of SPT and deformation and fracture processes, Fig. 2.27 [42], as described below:

(1) Plastic membrane stretching after plastic deformation

(2) Micro-cracks yield in tension side of specimen at $P_{max}$

(3) Micro cracks grow to main crack

(4) Main crack penetrate through thickness and the sudden load drop occurs at $P_f$.

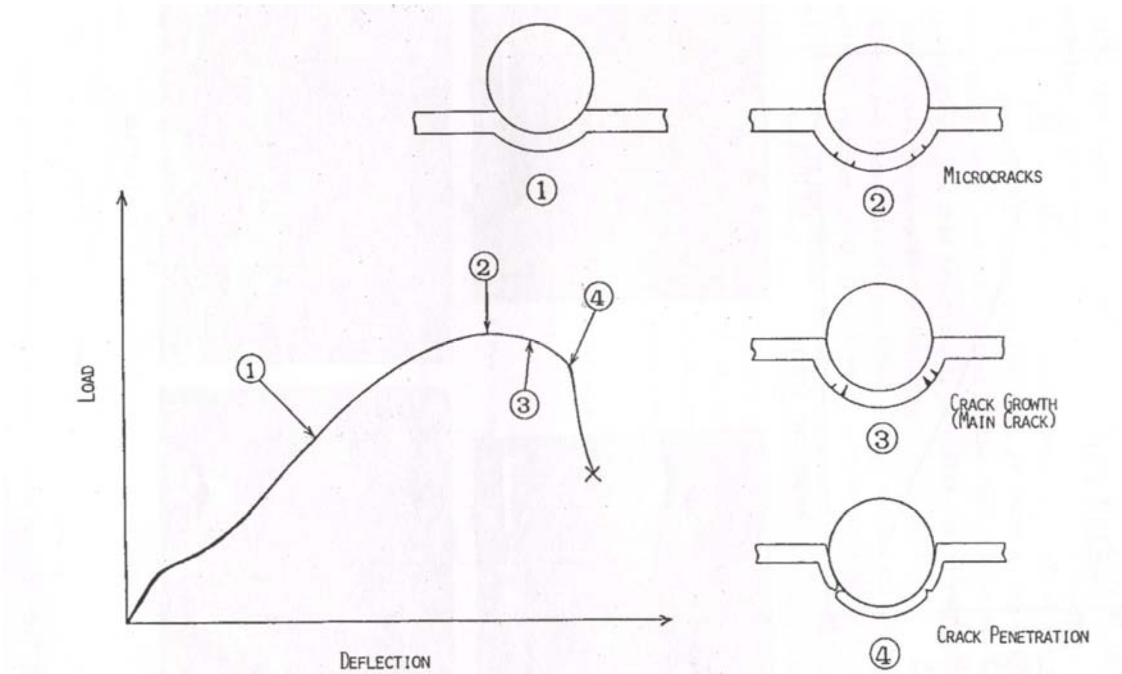


*Fig. 2.27: Schematic illustration of deformation and fracture process in SP Test [42]*

SPT has also been attempted by Campitelli [20], Fleury and Ha [44], Garcia [54] and others [46-56] with various objectives, which includes development of YS and UTS correlations.

Garcia et al. [54] has argued that rather than using $P_{max}/t_0^2$ , $Pmax/t_0*\delta_{max}$ should be used for calculation of ultimate tensile strength, based on the fact that necking initiates before the $P_{max}$ position and maximum load acts on the reduced thickness of specimen, however, $P_{max}/t_0^2$ does not consider this. In contrast, the displacement at maximum load ($\delta_{max}$) indirectly represents the reduction in thickness taking place during the test as larger the $\delta_{max}$ larger is the reduction in thickness. Garcia et al. have suggested the following correlation for UTS:

$$\sigma_u = 0.277 \frac{P_{max}}{\delta_{max} * t} \tag{2.25}$$

Apart from these, other correlations have also been developed or used by various authors [45, 48, 49, 52, 53], still there seems no consistency in UTS correlations. Most of the correlations, described above, are based on $P_{max}$, $t_0$ and $\delta_{max}$ values, however, there are too much deviations and a lot of scatter of data. But one thing is common in all these correlations, as they have used $P_{max}$ invariably, with an innocent assumption that $P_{max}$ in SPT curve is similar to UTS in stress-strain graph of uniaxial tensile test. But researchers have found that this assumption itself is not fully justifiable as in SPT micro-cracks have been observed at $P_{max}$[20], whereas in case of tensile test at UTS no such crack occurs. Even Takahashi et al. [42] in their schematic illustrations, Fig. 2.27, have shown micro-cracks appearing at $P_{max}$. Based on these findings by many, Campitelli [20] have objected the UTS correlations based on $P_{max}$ and has argued that as $P_{max}$ is not representative of UTS state of stress as in case of uniaxial tensile test. Also, Kameda and Mao [16] have reported that UTS correlations in their experimental results were not found to be unique.

### *2.3.2 Issues with SPT correlations*

While there is agreement among researchers about the correlation of YS using SPT, however the UTS correlations are an open issue since evolution of the SPT technique. The main reason appears the innocent assumption that $P_{max}$ value in the load-deflection plots of SPT and are equivalent to the $P_{max}$, i.e. UTS of uniaxial test. As a matter of fact, in uniaxial test, $P_{max}$ in stress-strain curve corresponds to start of necking during the tensile deformation of ductile material, whereas in SPT, deformation behaviour is different at $P_{max}$,. Further, at $P_{max}$, in SPT, micro-cracks have been reported by many, including the most popular correlation given by Mao and Takahashi, correlations of UTS cannot be based on $P_{max}$, which does not correspond to necking. By definition, necking or localised deformation begins at maximum load, where the increase in stress due to decrease in the cross-sectional area of the specimen becomes greater than the increase in load carrying ability of the metal due to strain hardening. However, in SPT it is a foregone conclusion that $P_{max}$ region does not represent necking zone and that necking starts earlier to $P_{max}$ zone. Based on the objections by various researchers, as discussed in para 2.3.1, the UTS correlation of SPT is an open issue till date.

## 2.4 Gap areas of miniature tensile & SPT techniques and problems formulation

Even though miniature tests have emerged to be a potential techniques in extracting mechanical properties of the materials for some specific cases, as mentioned earlier, over the conventional test procedures, its use has been somewhat restricted as no standard procedure was evolved for such techniques. There are certain issues, which must be addressed for the successful application of these techniques. The areas, which are not very well defined in the miniature test techniques, need to be resolved first.

In the present work, our attention is specially confined in miniature tensile test and small punch test. Miniature tensile tests, like the standard test, give the full material data in form of stress-strain graph and they have shown the potential to be a futuristic and reliable test methods. On the other hand, small punch test gives material data through correlations; however, the requirement of material volume is much small, which makes it best suitable for health monitoring of in-service equipment or radioactive materials. The important observations regarding development, applicability and limitations of these two miniature test techniques are outlined as follows:

I. **Gap areas in miniature tensile test techniques:** Design of geometry and determination of size of miniature tensile test specimen is a crucial aspect, as this has to emulate the results from standard tensile test specimens. The design requires, apart from determination of cross-section, several other factors, such as micro-structural requirements, viz. thickness/grain size ratio, number, shape, size and distribution of micro-constituents, anisotropy due to microstructure, crystallographic texture and chemical inhomogeneity etc., surface effect and residual stresses. A lot of work has been carried out earlier, however, some important issues in this field are listed below:

a. Geometry of test specimen: In case of miniature tensile tests, many efforts have been put towards development of various designs of test specimens [7, 10, 17, 27, 30]; however, no consensus has been arrived on standardised miniature test specimen geometries [5, 28] and still there is an ambiguity in this regard.

b. Minimum representative volume elements in gauge section [10, 28, 30, 61-63]: Miniaturisation of specimen causes the so-called ‘size effect’ or ‘scaling effect’, which leads to different material behaviour in the micro-scale compared to the meso-scale and macro-scale [28]. No consensus has been arrived so far to define the minimum representative volume elements in the gauge section for such tests [10, 30].

c. Ductility Data: Non-conformity of ductility data from miniature tensile test have led to a number of parametric studies for size effect [7, 9, 10, 17, 18, 27, 30, 33] in terms of material, gauge length, cross-section, thickness, grain-size, number of grains in cross-section, fabrication method, load frame, test parameters etc. Even though some correlations [10, 30] have also been developed, it is still an unresolved issue.

II. **Gap areas in SPT technique:** SPT is a very good technique for evaluation of YS and UTS using correlations using minimum volume of material. It may be noted that the correlations for evaluation of YS [7, 15, 16, 20, 44, 54, 55] using $P_y$ (value of load), are more or less in agreement with YS obtainable from conventional tensile tests, but correlations for evaluation of UTS using $P_{max}$ (max. value of load) of SPT graph are in disagreement [7, 15, 54, 55]. In fact, correlations for evaluation of UTS [11, 15, 16, 20, 41, 44, 54, 55] based on $P_{max}$, have been an open issue since the development of this technique. The reason for disagreement is the point, corresponding to $P_{max}$ on

SPT curve, which is used for UTS correlation, does not represent a necking situation [16, 20, 54], as in case of UTS, in a uniaxial tensile test.

# CHAPTER-3

# Design and Development of Miniature Tensile Specimens and Validation of Test Technique

## 3.1 Introduction

As discussed in chapters-1 and 2, one of the application areas of the miniature test techniques has been found in evaluation of mechanical properties of in-service equipment. In order to preserve the integrity and predict the remaining service life of the equipment, the scooping operation should be done in a non-destructive manner. For the present work, a scooping device was developed, as shown in Fig. 3.1a [59, 72]. Details of the scooping device have been given in chapter-5 of this thesis. The device scoops metal sample (known as boat sample) working on the principle of internal grinding operation using abrasive coated cutter which grinds out the boat sample from the in-service equipment, Fig. 3.1b. Typical dimensions of the boat sample and the scooped region are shown in Fig. 3.2a and 3.2b respectively. The scooped sample is of elliptical in shape and has minor diameter of 25mm, major diameter of 40mm and maximum thickness of 3mm at centre. The boat sample can be used for extracting various types of miniature test specimens, such as tensile, Charpy, small punch test and hour-glass shaped fatigue specimens, etc. Fig. 3.3 shows the schematic of extraction of the various types of miniature test specimens from the boat sample and actual extraction of the specimens from boat sample has been discussed in chapter-5.

This chapter aims towards addressing the various issues related to miniature tensile test, as highlighted in chapter-2. This chapter is divided in two parts; the first part is from section 3.3 to 3.6 and the second part is section 3.7 onwards. The first part discusses design and optimization of geometry of the miniature tensile test specimen, based on its extractability from the boat sample while maintaining the necessary features of a tensile specimen. Second part of this chapter establishes the test results from miniature specimen with standard test specimens and through FEM analysis.

Other types of miniature specimens, as shown in Fig. 3.3, are SPT specimen, Charpy specimen and hour-glass-shaped fatigue specimens. SPT specimens have been discussed in next chapter, i.e. chapter-4, for derivation of a UTS correlation. The other two types of specimens, charpy specimen and hour-glass-shaped specimen, are not part of this thesis.

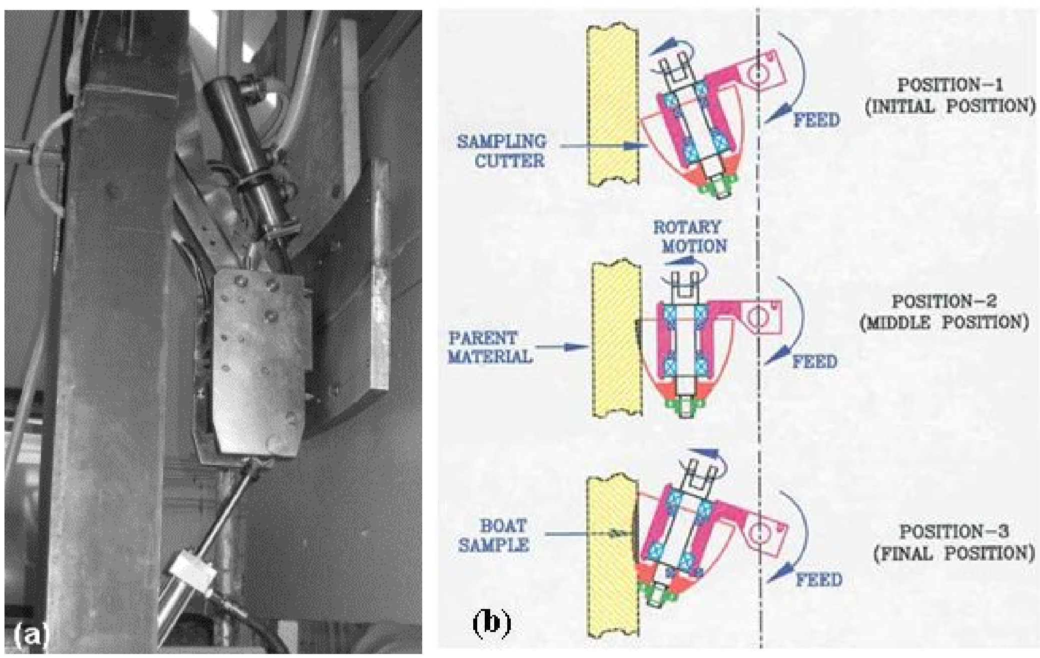


*Fig. 3.1: (a) Schematic of scooping of boat sample from in-service equipment (b)Various positions of the cutter during the scooping operation*

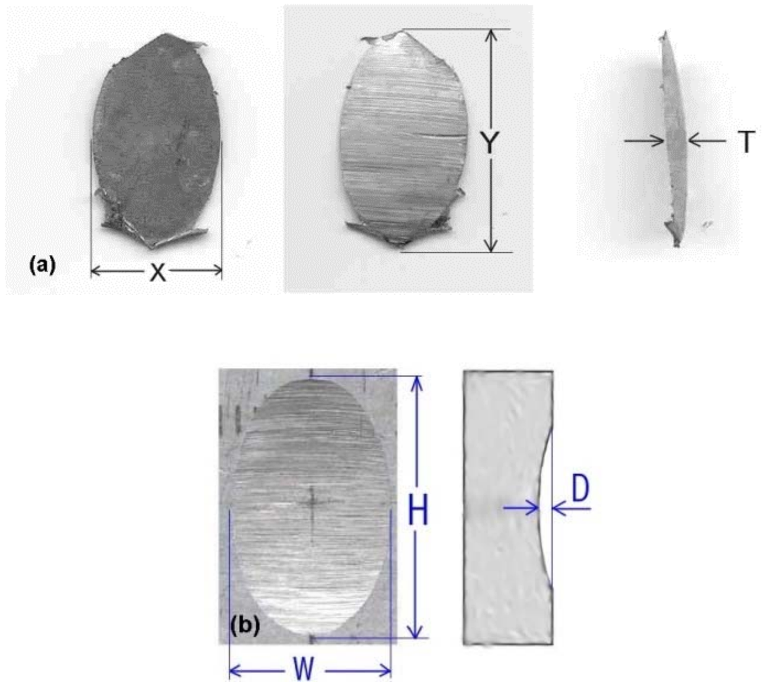


*Fig. 3.2: Typical geometry of (a) Boat sample (X=25mm, Y=40mm, T=3mm) and (b) Scooped region (H=45mm, W=30mm, D=4.5mm)*

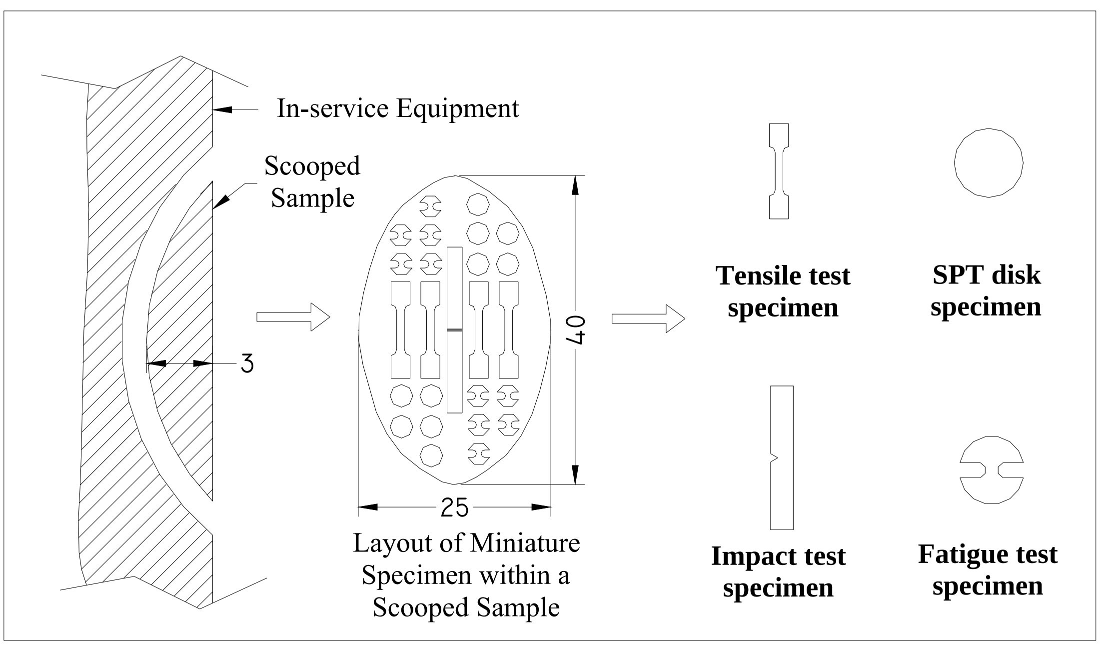


*Fig 3.3: Scheme of extraction of miniature tensile and other types of miniature test specimens from the scooped sample*

### 3.2 Issues with miniature tensile test technique

The major issues prohibiting wide acceptability of miniature tensile test techniques, as highlighted in chapter-2, are, unavailability of universally agreeable geometry of test specimen [6, 28], lack of clarity on minimum representative volume elements in gauge section [28, 30], and non-conformity of ductility data with standard tensile tests [28, 32]. This chapter aims at addressing these issues by geometric design of miniature tensile test specimen based on technical information available in published literature. The geometric design of the specimen would be verified by fabrication of test specimens, experimentation, metallurgical evaluation, numerical analysis and validation of tensile data.

The geometric design consists of dimensioning of the gauge section and grip section to make the miniature specimen geometrically similar to the standard test specimens. The overall dimension of the test specimen should be such that sufficient number of specimen can be prepared from a small coupon, viz. scooped sample, of material. The design of specimens also includes optimization of thickness of miniature specimen to get minimum representative volume in order to get mechanical data comparable to standard test results. Thickness optimization has been done by experimental, metallurgical and numerical analysis. The chapter also discusses development of special test fixtures, suitable to the geometry of the miniature tensile test specimens, and application of camera-based extensometer for conducting the tensile test experiments. At the end of the chapter, comparison of tensile tests data from standard and miniature specimens has been carried out to validate the design of miniature tensile specimens.

### 3.3 Materials for study

Two pressure vessel materials, 20MnMoNi55 and CrMoV low alloy steels and one piping material, austenitic stainless steel 304LN were selected for conducting the experiments.

20MnMoNi55 steel was cut from 130mm thick plate, whereas CrMoV was in 240mm x 170mm x60mm thick plate. SS304LN was a cut section of a pipe of inner diameter 275mm and outer diameter of 325mm. 20MnMoNi55 and SS304LN materials were used for making test specimens in as received condition, whereas CrMoV steel was subjected to quenching and tempering treatment. Quenching of CrMoV steel was carried out from 950°C followed by tempering at 650°C for 25 hours. Chemical compositions of these materials are given in Table-3.1 and the microstructures are shown in Fig. 3.4.

***Table-3.1 Chemical composition (wt %) of materials taken for study***

| **Material** | **C** | **Cr** | **Mo** | **Mn** | **Ni** | **S** | **P** | **Si** | **Cu** | **Co** | **N** | **V** |
|---|---|---|---|---|---|---|---|---|---|---|---|---|
| 20MnNiMo55 | 0.18 | 0.078 | 0.49 | 1.24 | 0.58 | 0.007 | 0.014 | 0.23 | 0.067 | 0.0069 | 0.0068 | -- |
| CrMoV | 0.17 | 2.51 | 0.63 | 0.38 | 0.8 | 0.009 | 0.015 | 0.28 | 0.054 | 0.013 | 0.065 | 0.17 |
| SS304 LN | 0.022 | 18.60 | 0.24 | 1.73 | 9.32 | 0.004 | 0.018 | 0.46 | 0.28 | 0.11 | 0.071 | -- |

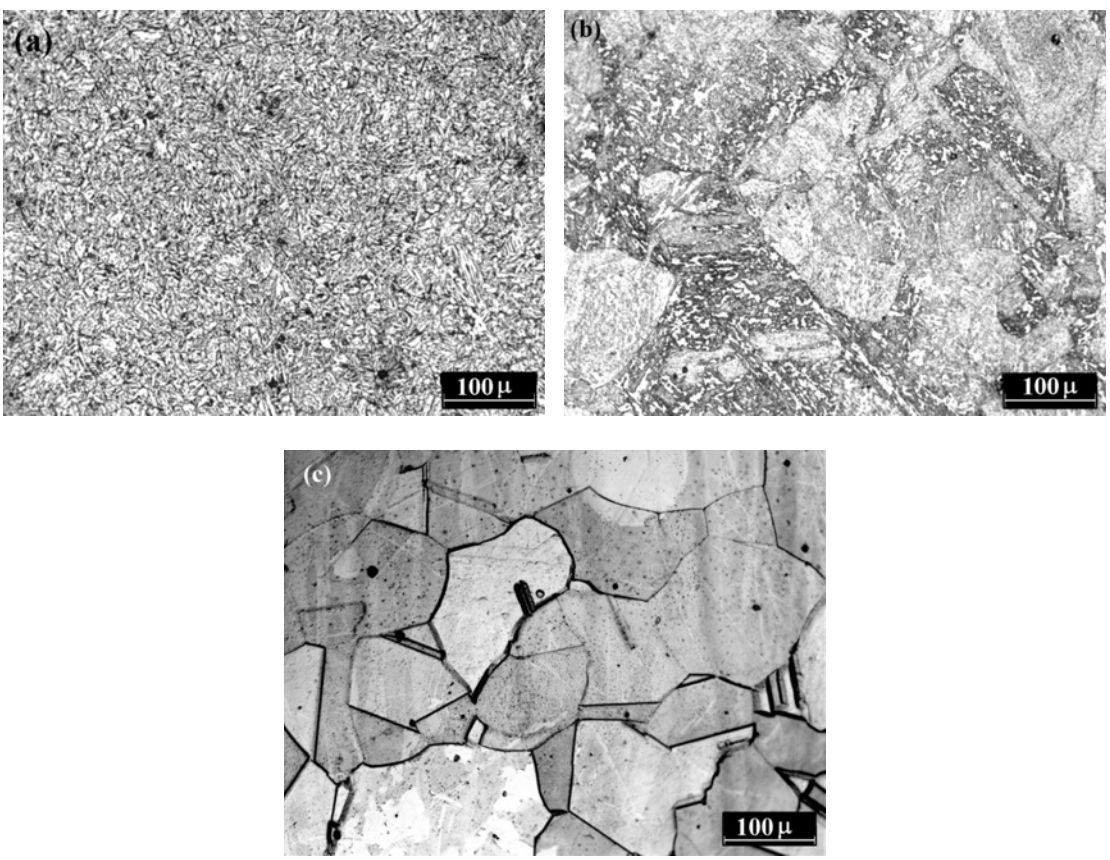


*Fig. 3.4: Microstructure of (a) 20MnMoNi55, (b) CrMoV Steel and (c) SS304LN*

The mechanical properties, given in Table 3.2, of these materials were determined by conducting tensile test on sub-size flat tensile test specimens, as shown in Fig. 3.5.

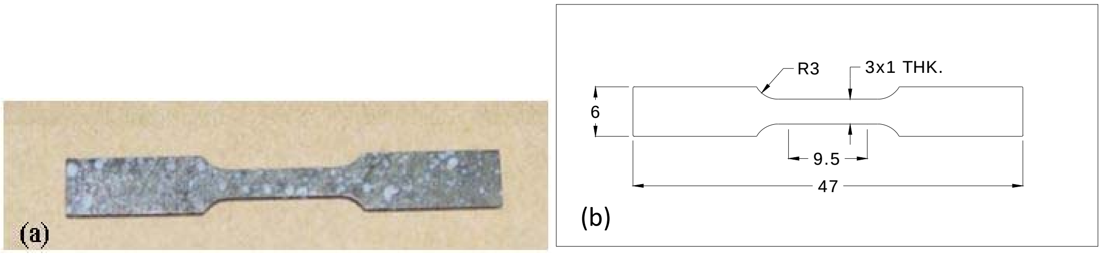


*Fig. 3.5: (a) Photograph and (b) dimensional details of sub-size flat specimen used to determine mechanical properties of the materials*

***Table 3.2: Mechanical properties of materials taken for experiment***

| Temp | 20MnMoNi55 | | | | CrMoV steel | | | | SS304LN | | | |
|---|---|---|---|---|---|---|---|---|---|---|---|---|
| °C | YS MPa | UTS MPa | $e_u$ % | $e_f$ % | YS MPa | UTS MPa | $e_u$ % | $e_f$ % | YS MPa | UTS MPa | $e_u$ % | $e_f$ % |
| 28 | 490 | 627 | 11.5 | 22.8 | 449 | 594 | 9.7 | 21.7 | 307 | 639 | 54.8 | 68.9 |
| Range of data | 485 - 494 | 627 - 629 | 11.4-11.5 | 22.3-23.4 | 439-455 | 591-599 | 8.7-10.9 | 21.3-22.4 | 289-318 | 636-641 | 53.9-56.2 | 68.3-69.7 |

### 3.4 Geometric design of miniature tensile specimen

Geometric design of miniature tensile specimen was mainly governed by following two factors:

i) size of the specimen should be smallest possible so that sufficient number of specimens could be derived from small volume of material, such as from boat sample, and
ii) specimen should be geometrically similar to standard test specimens to match the tensile test results

Literature review, presented in chapter-2, shows that sheet type miniature specimens [7, 9, 10, 17, 27, 28, 30-35, 69] were preferred over wire type [6, 9] or miniature rod type specimens [7] due to ease of fabrication, ability to maintain dimensional accuracy of the specimens and repeatability of test results, etc. Based on these factors, it was decided to use sheet type specimen for the present work also. Even in sheet type specimens, there were large varieties, as discussed in chapter-2, however, the design, used by most researchers [9, 17, 31, 69], had gauge section as 1mm width x 5mm length with different thicknesses; 0.25mm [9, 69], 0.4mm [17, 31]. This specimen, Fig. 3.6, had overall length of 12.7mm and grip width as 2.5mm and appeared to be attractive and relevant for the present study. Therefore, it was decided to examine this specimen geometry based on the above-mentioned two factors and modify, if required.

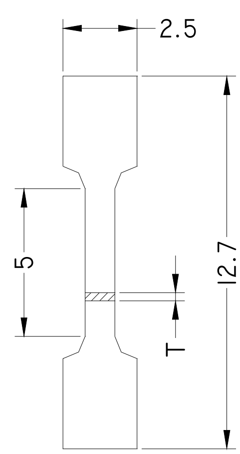


*Fig. 3.6: Sheet type tensile specimen used by most researchers [9, 17, 31, 69]*

The first criterion for the geometric design of the miniature tensile specimen was based on the feasibility of sufficient number of miniature tensile test specimens from a very small volume of material. It was found that 6-8 numbers of miniature tensile specimens of the given dimensions could be extracted from a scooped sample, as shown in Fig. 3.3, apart from other types of miniature specimens. This criterion was found to be fulfilled by this specimen geometry; therefore, it was decided to examine the second criterion.

The second criterion required that specimen should be geometrically similar to standard test specimens to match the tensile test results [70]. Keeping this in mind, various sections of the specimen, such as grip-section, gauge section and thickness, were examined and finalized, as discussed below.

**Design of grip section:** The grip-section width, in all these cases [9, 17, 31, 69], was 2.5mm, which seems to as per relevant ASTM guidelines for standard size specimens. Whether same guidelines could be followed for defining the grip-section width of miniature tensile specimens, is a matter of argument due to unavailability of any test standards for miniature specimens. The miniature specimens having very small thicknesses may need special guide and support to guard against buckling / warping failure of the grip section during experiments. As alternative to guard against likelihood of such failures, it seems that width of miniature specimens should be increased. Additionally, in present work, it was also planned to provide 1mm pinholes in both ends of the specimen, in the grip sections, for conducting the experiments. In such case, 2.5mm ligament across the pinholes was required for satisfying the criteria used by others [9, 17, 31, 69]. Based on these two arguments the width of grip-section of the specimen was selected as 3mm, instead of 2.5mm used by others [9, 17, 31, 69]. Thus, in present work, two alternative designs of test specimens were considered for fabrication and conducting the experiments; the first, specimens with pin-holes, Fig. 3.7a, and the second, the specimens without pin-holes, Fig. 3.7b. The specimens with pin holes could be loaded through pins whereas specimens without pin holes could be loaded through their shoulders. Both types of specimens required two different designs of special grips, which are discussed in section 3.5.2. Considering these loading conditions, length of the grip section of the specimen was kept at 3mm, in order to have uniform geometry for both types of specimens. Precaution was also taken, such that there should not be any undercut in the transition zone between gauge section and grip section, and therefore a smoothly merging radius of 1mm was provided as shown in Figs. 3.7a and 3.7b.

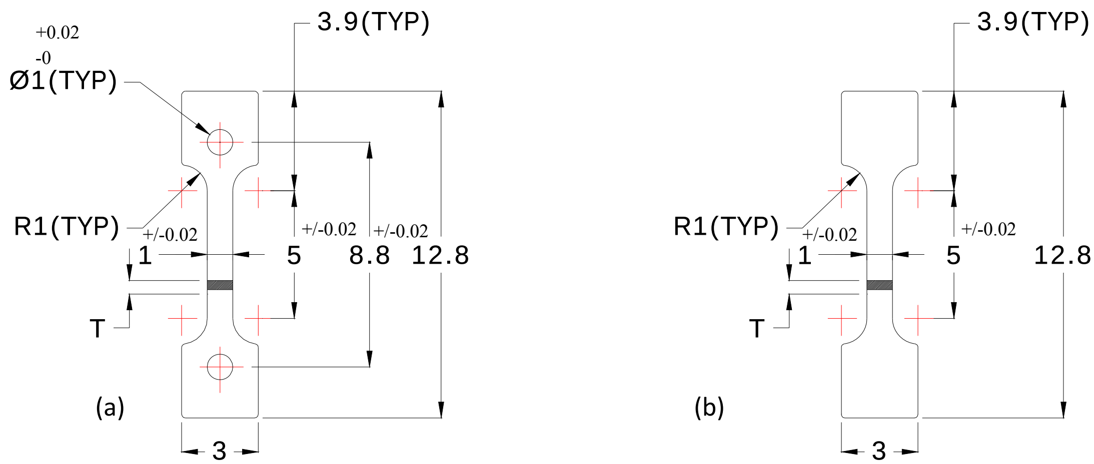


*Fig. 3.7: Dimensional details of miniature tensile test specimens (a) with pin-holes and (b) without pin-holes*

**Design of gauge section:** The other issue of miniature tensile specimen is the non-conformity of ductility data between miniature specimen and standard specimen. The gauge length plays a major role in measurement of ductility of the tensile test specimen. In order to address this issue, it needs a little-bit deliberation, as given below.

The elongation measurement of tensile specimens consists of two components; first, the uniform elongation up to necking, and second, the localised elongation once necking begins. The extent of uniform elongation depends upon the metallurgical condition of material and the effects of specimen size and shape on the development of the neck. Fig. 3.8 shows the variation of local elongation along with the gauge length of a prominently necked tensile specimen [70]. It is seen that shorter the gauge length the greater the influence of localised elongation at the neck on the total elongation of the gauge length. The total elongation is given as

*Final Length -Initial Length =uniform elongation + local elongation at necking*

$$i.e.\ L_f - L_0 = e_u L_0 + \alpha \quad (3.1)$$

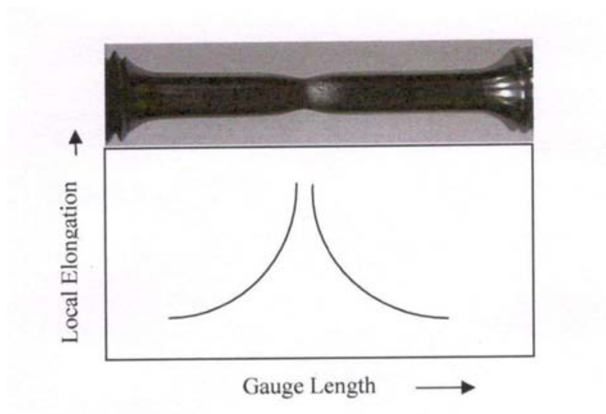


*Fig. 3.8: Dependence of ductility data on gauge length [70]*

The tensile elongation is given as

$$e_f = (L_f - L_0)/L_0 = e_u + \alpha / L_0 \quad (3.2)$$

A number of attempts have been made to rationalize the strain distribution in tensile test and based on which it has been concluded that geometrically similar specimens develop geometrically similar necked region. By applying Barba's law, $\alpha=\beta\sqrt{A_0}$, [70], where $A_0$ is the initial area of cross-section and $\beta$ is a coefficient, the elongation, given in equation (3.2), becomes

$$e_f = e_u + \beta\sqrt{A_0} / L_0 \quad (3.3)$$

The equation shows that for measurement of ductility properties of different-sized specimen the ratio $L_0/\sqrt{A_0}$ for sheet specimen and $L_0/D_0$ for round specimen must be maintained [70].

As per ASTM 370 and E8M, $L_0/D_0$ for round specimen is 4 and 5, respectively, whereas for sheet type specimens this ratio of $L_0/\sqrt{A_0}$ varies from 2.8 to 14.1. The $L_0/\sqrt{A_0}$ ratio for miniature specimens used by Panayotou et al [9] and Hamilton et al. was found to be 10, whereas it was 7.9 used by Jung et al [17] and Dai el al [31].

In present case, the miniature specimen needed to be geometrically similar to the sub-size specimen, as shown in Fig. 3.5b, in order to have comparable elongation data. The sub-size specimen, Fig. 3.5b, has gauge length of 9.5mm, gauge width of 3mm and thickness of 1mm, which gives $L_0/\sqrt{A_0}=5.48$. It can be seen that by fixing the thickness of 0.3mm, the gauge length becomes 3mm as per $L_0=5.48\sqrt{A_0}$. Therefore, the gauge length of the miniature specimen was taken as 3mm. However, it must be noted that as thickness plays a role in deciding $L_0/\sqrt{A_0}$ ratio and thus this value of gauge length is a tentative value, which needs to be confirmed by experimental, metallurgical and numerical analyses, as given in section 3.6.

## 3.5 Test Setup

### *3.5.1 Testing machine & video extensometer*

As the gauge length of miniature specimen was 3 mm, it was not possible to mount any mechanical extensometer. In many of the previous works [6, 7, 9], the extension measurements were done using the crosshead travel. In general, the measurement of elongation using the crosshead travel gives lower value of extension due to the effective smaller length of necking region, as is clear from Fig. 3.8. This effect was also experimented by Dobi and Junghans [32] as mentioned in section 2.2.4 of chapter-2. It was concluded by them that for correct stress-strain curve the elongation should be measured directly on the specimen.

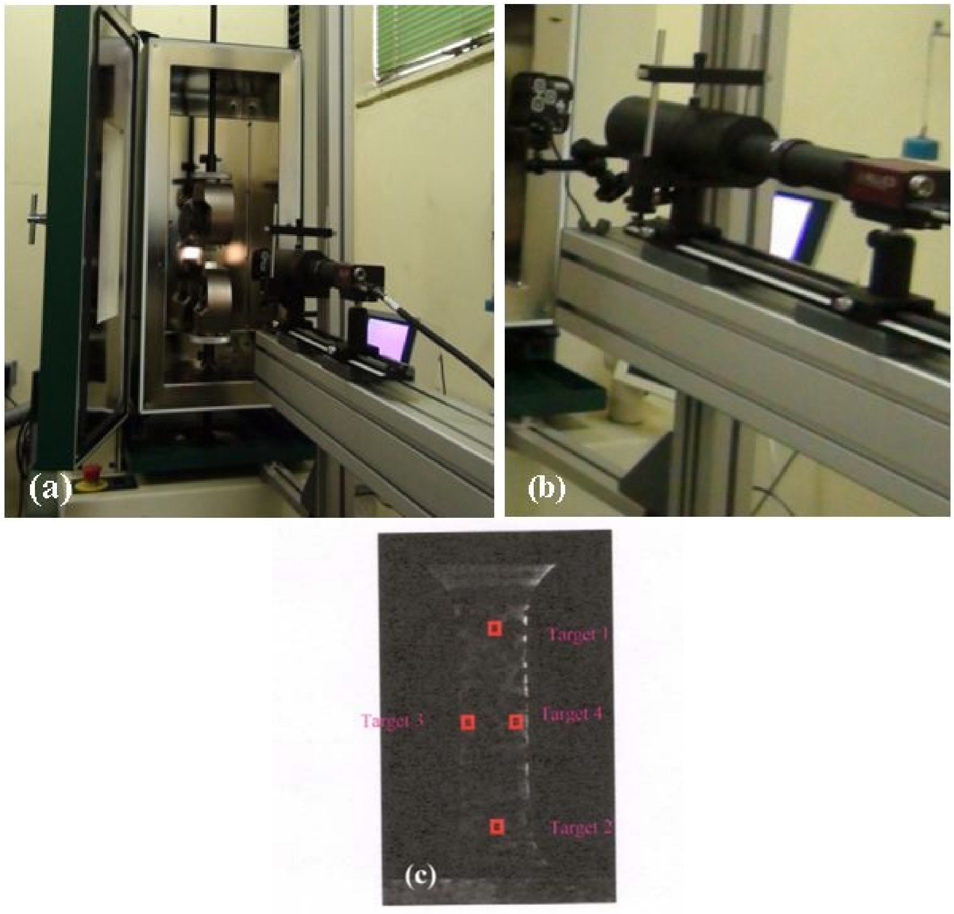


*Fig. 3.9: (a) Universal testing machine mounted with video extensometer, showing (b) camera and (c) digital marking of test specimen*

The need to measure strain value directly on the specimen has inspired researchers to use non-contact type extensometers [28]. In present case, the tensile test machine was mounted and coupled with video extensometer, Fig. 3.9a. The camera of the video extensometer had fixed focus, Fig. 3.9b, and was used for measurement of gauge section extension and its distribution. The video extensometer works on the principle of pattern recognition technique. The test specimen was marked with contrast patterns prior to loading in the machine. The camera tracks the marked targets on the test specimen, Fig. 3.9c, and works as an extensometer, which gives the strain values during the test.

### *3.5.2 Special test grips*


*Fig. 3.10: (a) Tensile Test fixtures for pin-holed specimens, (b) specimens with pin-holes, (c) test fixture for shoulder-supported test specimens and (d) specimens which are shoulder loaded*

Special test grips, as shown in Fig. 3.10a and 3.10c, were developed for gripping the miniature test specimen. Shoulder supported grips, Fig. 3.10c, provided better support than a pinned grips, Fig. 3.10a [29]. The pinned specimen, Fig. 3.10b, had two problems; first, two holes were to be made on the test specimens with required positional and dimensional accuracy which proved to be a difficult task, and the second, there were chances of the holes getting deformed during the test, adding error to the elongation data. Therefore, the shoulder support grips were used for specimens as shown in Fig. 3.10d, which eliminated the drawbacks of pinned specimens.

### 3.6 Determination of minimum thickness of miniature tensile specimens

For optimization of thickness of test specimens a set of experiments, as given in para 3.6.1, were conducted in which the specimens thickness was varied while keeping the width and gauge length fixed, for getting the comparable results with standard size specimens. The detail dimensions of two types of miniature specimens are shown in Figs. 3.11a and 3.11b. The specimen geometry, for miniature tensile test specimen required the gauge length of 3mm. Based on this requirement, miniature specimen of two different parallel lengths; 5mm for 20MnMoNi55 steel and CrMoV steel and 3mm for SS304LN, were used for the study. The reason for selecting smaller parallel length of SS304LN is explained below.

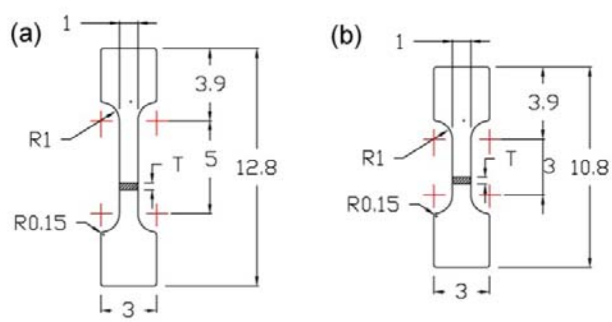


*Fig. 3.11: Dimensional Details of Miniature Test Specimens from (a) 20MnMoNi55 and CrMoV Steels, and (b) SS304LN*

As explained earlier, the video extensometer was used for measuring the strain data of the miniature test specimens, by way of identifying two points on the gauge section and tracking these points until fracture of the specimen. Due to high elongation of the SS304LN material, these points used to be so smeared and spread that the camera could not track them till the end of the experiments. Due to this reason, specimens from SS304LN material had 3mm parallel length; and markings for the gauge length were done on the pins of the grips.

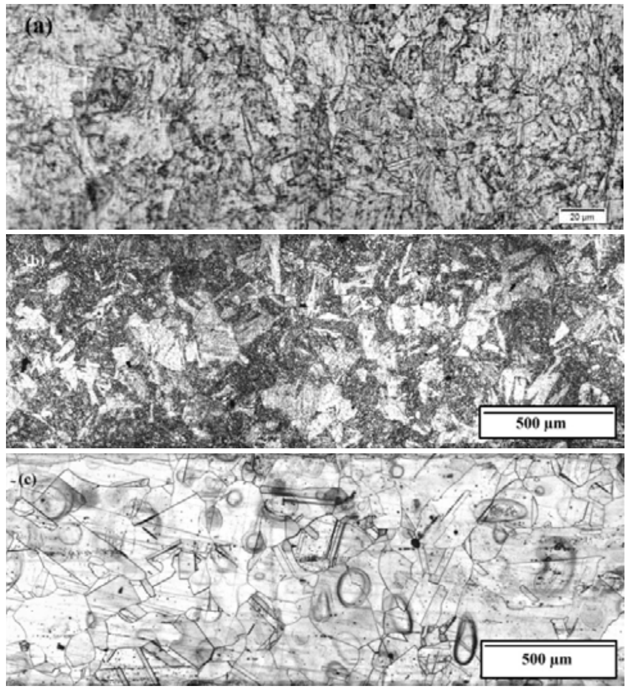


| Material | 20MnMoNi55 | CrMoV Steel | SS304LN |
|---|---|---|---|
| Grain Size | 12.23 µm-15.6 µm | 68.1 µm-79.03 µm | 151.34µm-171.32µm |

*Fig. 3.12: Micrographs for grain size measurement across gauge cross-section of miniature tensile test specimens from (a) 20MnMoNi55 (b) CrMoV ferritic steel and (c) SS304LN materials*

The specimens were prepared using wire cut EDM process and manually polished using 1200, 2400, 4000 grit size SiC paper to have mirror-finish surface. Following this procedure, specimens of thicknesses 0.15mm to 0.4 mm were prepared in steps of 0.05mm for all the three materials. The grain size of the three materials were measured, micrographs of which are shown in Fig. 3.12. The grain sizes of 20MnMoNi55 were found to be in range of 12.23µm-15.6 µm, for CrMoV steel it was 68.1 µm-79.03 µm and for SS304LN it was found to be in range of 151.34 µm-171.32 µm. For study of thickness effect and to optimize the thickness of such specimens, three specimens of each thickness size were subjected to tensile test at a strain rate of $1x10^{-3}$/s at 28°C test temperature.

### *3.6.1 Experimental results and discussions*

Tensile tests were conducted on miniature specimens, having 1mm width but with varying thicknesses, 0.15, 0.2, 0.25, 0.3, 0.35 and 0.4mm. The stress-strain graph of all these experiments are as shown in Fig. 3.13. It was observed that for thinner specimens, yielding and failure took place early in comparison to thicker specimens, resulting in lesser value of strength and ductility data for the former. This behaviour is prominent in 0.15 and 0.2 mm thick specimens among all the three materials.

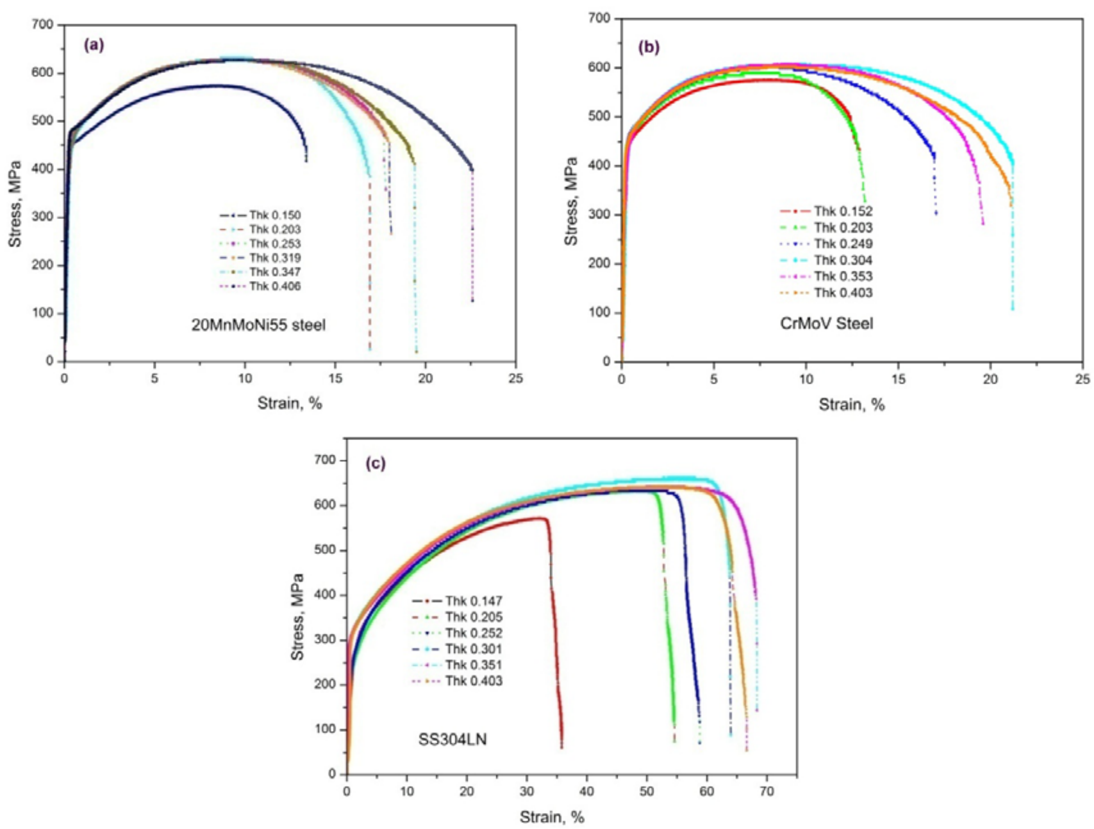


*Fig. 3.13: The engineering stress – strain plot for varying thicknesses for (a) 20MnMoNi55 steel, (b) Cr-Mo-V steel and (c) SS304LN obtained using miniature test specimens*

In order to assess the reason of early failure of thinner specimens and to understand the type of fracture taking place in various thicknesses of specimens, further analyses were carried out on the broken test specimen, using photographs and fractographs. Photographs of fractured specimens with different thicknesses are shown in Fig. 3.14-3.16 for 20MnMoNi55 steel, CrMoV steel and SS304LN, respectively.

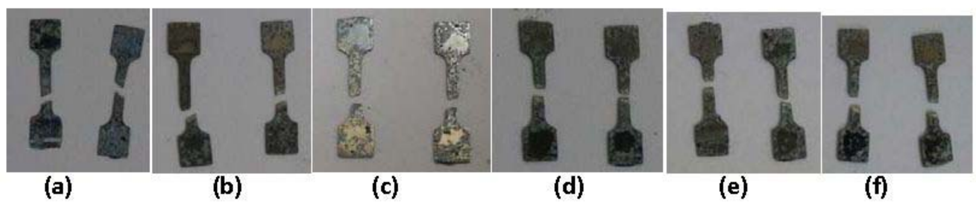


*Fig. 3.14: Photographs of miniature tensile specimen of 20MnMoNi55 for thicknesses (a) 0.15mm, (b) 0.2mm, (c) 0.25mm, (d) 0.3mm, (e) 0.35mm and (f) 0.4mm*

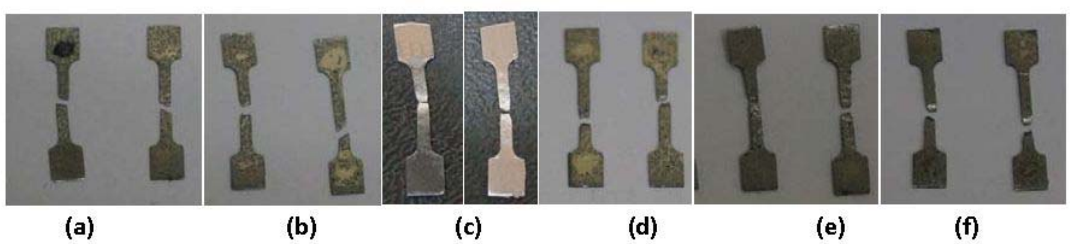


*Fig. 3.15: Photographs of miniature tensile specimen of CrMoV ferritic steel for thicknesses (a) 0.15mm, (b) 0.2mm, (c) 0.25mm, (d) 0.3mm, (e) 0.35mm and (f) 0.4mm*

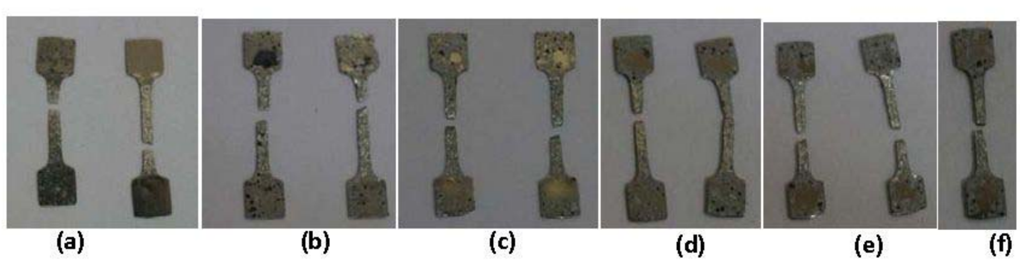


*Fig. 3.16: Photographs of miniature tensile specimen of SS304LN for thicknesses (a) 0.15mm, (b) 0.2mm, (c) 0.25mm, (d) 0.3mm, (e) 0.35mm and (f) 0.4mm*

These images were analyzed using IMAGE software to find out variations in geometries of the broken neck regions; viz. diffused neck length, neck angle and fracture angle, as per the nomenclature shown in Fig. 3.17a.

The criterion for checking the existence of sufficient volume in gauge section is suggested by the fracture angle; higher the fracture angle suggesting a shear type of failure, like plain stress condition existing at the fracture zone. It is found that for specimens of thickness 0.15mm and 0.2mm, the fracture angle for specimens from 20MnMoNi55 steel are in range of 19.3°-26.7°, whereas the same for CrMoV steel and for SS304LN are in range of 19.9°-23.4° and 9.8°-14.9°, respectively. Other specimens, having thickness 0.25 to 0.4mm, failed in the angle range of 5.5°-11.8°, 4.4°-8.6° and 2.3°-6.7° for 20MnMoNi55 steel, CrMoV steel and SS304LN, respectively for the three materials. The summary of these data are given in Table 3.3 and the fracture behaviour in terms of included neck angle, fracture angle and neck length is given in Figs. 3.17b, 3.17c, 3.17d and Fig. 3.18.

The included neck angle indicates the resistance of material during necking; higher neck angle indicates higher resistance of the material against failure and a ductile nature of failure is observed. This also suggests the existence of sufficient volume of material in the gauge section to resist the necking. It is observed, in Table-3.3, that the neck angle is quite small for the thickness 0.15 and 0.2 mm but increases appreciably when the thickness of the test specimen is increased beyond 0.25mm. In absence of sufficient volume in the gauge section, the test specimens fail early suggesting a brittle type of failure. Yet another criterion for judging the adequacy of material volume in the gauge section is the neck length, which includes a diffuse neck length (occurring in rectangular cross section) and a localized neck, Fig. 3.19. As shown in Table-3.3, in case of thinner specimens, i.e. 0.15 and 0.2mm, the neck lengths are smaller in all the three materials suggesting the absence of sufficient volume of material in the gauge section, due to which early necking could not be prohibited. These three parameters, fracture angle, neck angle, and neck length, are useful in determining the minimum thickness of the gauge portion in miniature tensile specimen.

***Table-3.3: Neck length, neck angle and fracture angle for varying thicknesses of test specimens***

| | **Materials** | | | | | | | | |
|---|---|---|---|---|---|---|---|---|---|
| Nominal Specimen Thickness (mm) | **20MnMoNi55** | | | **CrMoV** | | | **SS304LN** | | |
| | Avg. Neck Length (mm) | Avg. Neck Angle (°) | Avg. Fracture Angle (°) | Avg. Neck Length (mm) | Avg. Neck Angle (°) | Avg. Fracture Angle (°) | Avg. Neck Length (mm) | Avg. Neck Angle (°) | Avg. Fracture Angle (°) |
| 0.15 | 0.18 | 4.4 | 26.7 | 0.23 | 21.9 | 23.2 | 0.31 | 6.2 | 9.8 |
| 0.2 | 0.41 | 10.9 | 19.3 | 0.16 | 21.7 | 19.9 | 0.41 | 6.2 | 14.9 |
| 0.25 | 0.45 | 22 | 11 | 0.7 | 27.2 | 8.6 | 0.71 | 14.7 | 6.7 |
| 0.3 | 0.53 | 21.5 | 11.8 | 0.89 | 32.2 | 4.4 | 0.88 | 17.6 | 3.1 |
| 0.35 | 0.46 | 31.1 | 9.2 | 0.63 | 28.7 | 6.7 | 0.82 | 14.6 | 2.3 |
| 0.4 | 0.59 | 31.3 | 5.5 | 0.64 | 27.5 | 8 | 0.64 | 16.7 | 7.1 |

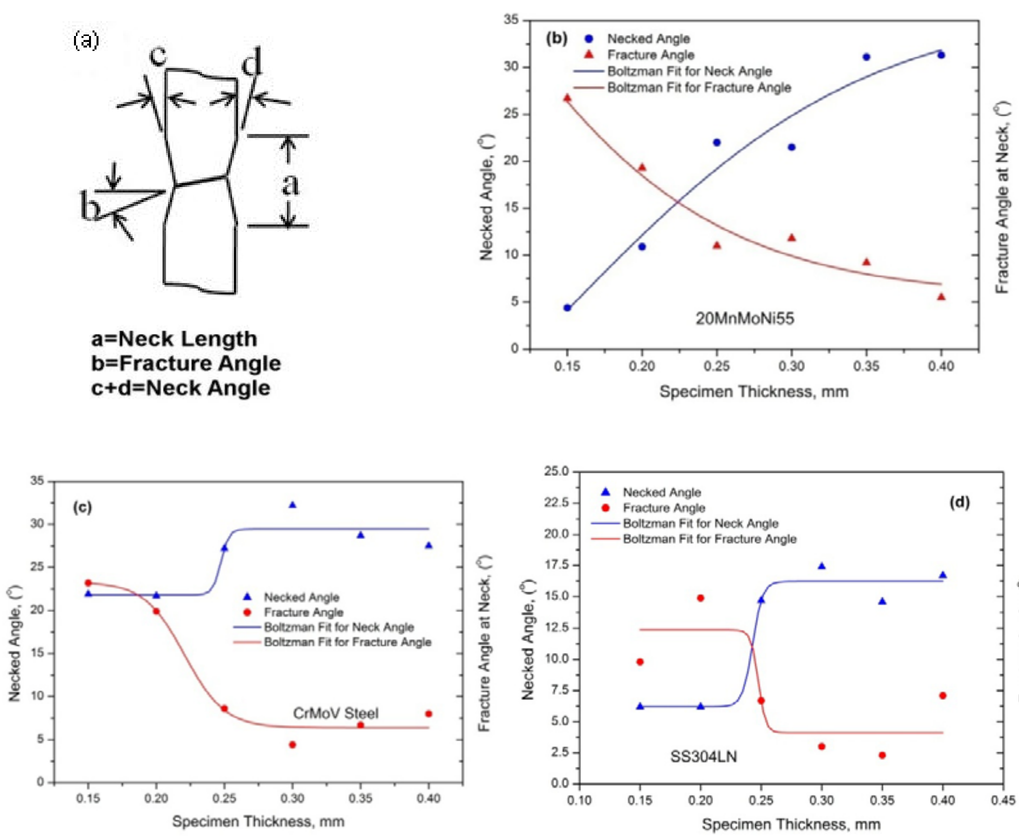


*Fig. 3.17: (a) Nomenclature of neck angle and fracture angle and graphs showing these angles for (b) 20MnMoNi55 steel (c) CrMoV steel and (d) SS304LN*

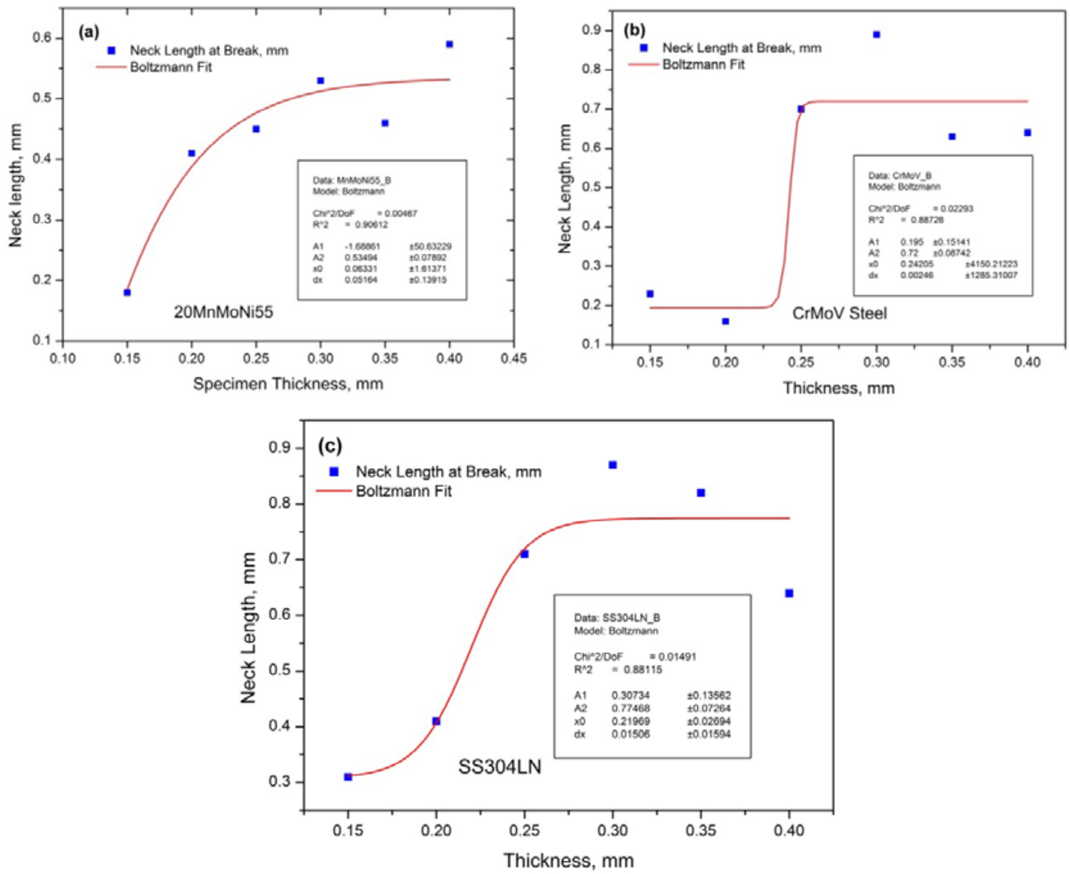


*Fig. 3.18: Graphs showing the necked length for (a) 20MnMoNi55 steel, (b) CrMoV steel and (c) SS304LN*

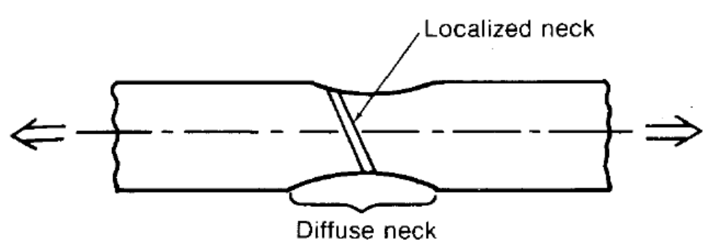


*Fig. 3.19: Necking behavior in rectangular tensile test specimens [70]*

The reduction of the YS and UTS for thinner specimens, Fig. 3.13, can be explained by the Ashby's model [70]. In a polycrystalline material, Fig. 3.20, the grains constrain each other to accommodate the misfit between them in the form of geometrically necessary dislocations, which induce the long-range back stress filed. For yielding to take place, the applied stress,

$\sigma_{APP}$, has to overcome the back stresses, $\sigma_{1B}$, $\sigma_{2B}$ and $\sigma_{3B}$ in directions 1, 2 and 3, as shown in Fig. 3.21. At the same time, the back stress components normal to the surface should be relaxed to satisfy the plane stress condition. For specimen of sufficient thickness, the crystals within the specimen are able to resist the applied tensile stresses, as discussed above, by creating back stresses; however, for thinner specimens there are less or relaxed induced back stresses in the thickness direction, $\sigma_{3B}\approx 0$, Fig. 3.21, to resist the yielding. Thus, the relaxed back stresses reduce the yield strength and UTS of thinner specimens [30].

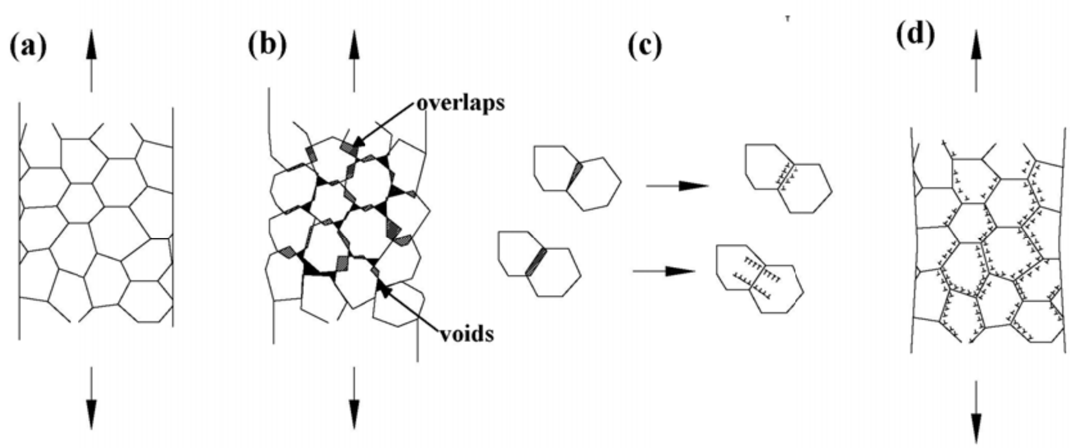


*Fig. 3.20: Ashby's model of deformation of polycrystalline material (a) Polycrystalline material deforms in macroscopic uniform way, produces overlap and voids at boundaries (b) These can be corrected by introducing geometrically necessary dislocations at (c) and (d). Here statistical dislocations have not been shown [70]*

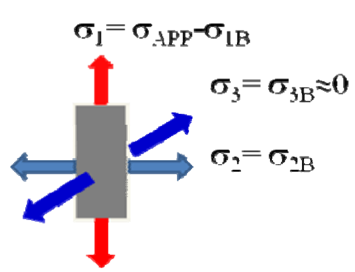


$\sigma_{APP}$=Applied stress

$\sigma_{1B}$=Back stress in applied stress direction

$\sigma_{2B}$=Back stress in width direction

$\sigma_{3B}$=Back stress in thickness direction

*Fig. 3.21: Maximum resolved shear stress in tensile test specimen*

Lesser value of $\sigma_{3B,}$ which is approximately equal to zero in case of thinner specimens, as explained above, is also responsible for low ductility values. Preferential straining in thickness direction takes place due to maximum resolved shear stresses being higher in thickness direction, i.e. $\tau_{1\text{-}3} \geq \tau_{1\text{-}2}$, as shown in Fig. 3.21 and given in equation-3.4 [30]. The plastic deformation is localized in thickness direction even before the development of plastic instability. Necking takes place when strain in thickness direction becomes equal to the critical strain for plastic instability. After the initiation of plastic instability, the elongation increment (total elongation-uniform elongation) reduces in thin specimens. This causes lesser value of total strain

$$\tau_{1-3} = \frac{\sigma_1 - \sigma_3}{2} \geq \tau_{1-2} = \frac{\sigma_1 - \sigma_2}{2} \qquad (3.4)$$

The mechanical response of miniature tensile specimens was also studied by normalising the thickness data with grain sizes of the three kinds of materials. Mechanical properties data, for the 20MnMoNi55, CrMoV and SS304LN materials, were plotted with respect to thickness/grain size, i.e. t/d, as shown in Fig. 3.22. It was found that the YS, UTS and uniform elongation data almost stabilized corresponding to t/d values as 16, 3.4 and 1.5, for the respective materials; however, the total elongation of the materials kept on increasing for increasing value of thicknesses. The reason for continuous increasing of total elongation for specimens of higher thicknesses is due to availability of more than sufficient volume of material in the gauge section. The available extra volume of material is allowing the specimen to elongate till the volume of material, at the neck, is able to sustain the growth and resist fracture. For thinner specimens this resistance ceases faster in comparison to thicker specimens because the failure of former is dominated by shear deformation while later fail by voids formation and their coalescence.

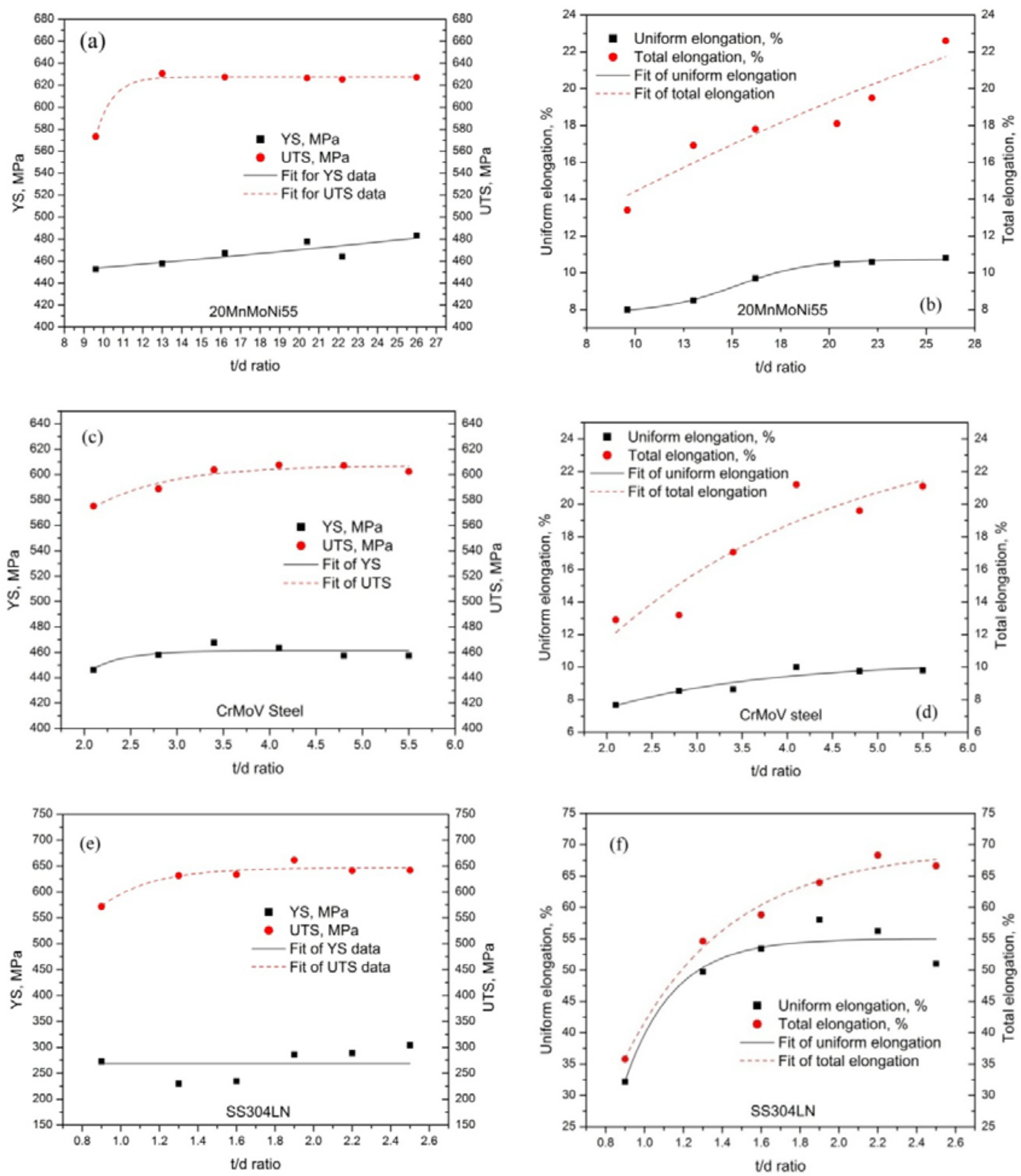


*Fig. 3.22: The plots of strength and ductility data with t/d ratio for (a & b) 20MnMoNi55 steel, (c & d) Cr-Mo-V steel and (e & f) SS304LN materials, obtained using miniature test specimens*

Plastic deformation mechanism has further been analysed for change in strain hardening rate, n, with t/d ratio for all the three kinds of materials, as shown in Fig. 3.23. It is found that initially 'n' values are smaller, in all the cases, and rise with increasing value 't/d' ratio and then stabilises. The threshold values of t/d for stabilising ‘n’ values for materials 20MnMoNi55, CrMoV steel and SS304LN have been found to be approximately near to 11, 3.7 and 1.2 respectively. These values of t/d are smaller than the corresponding t/d values (16, 3.4 and 1.5) that were determined for getting stabilised data of strength and ductility, which suggest that we are getting stabilised data of strength and ductility corresponding to 16, 3.4 and 1.5 values of t/d, as discussed above. These experimental values were further examined using finite element method, using pure mechanics approach, i.e. without incorporating any damage module into the analysis, which is described in section 3.6.3.

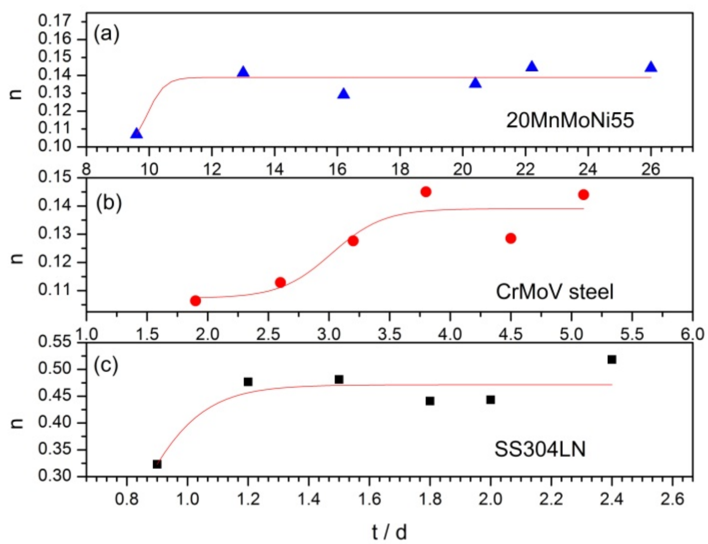


*Fig. 3.23: The plots of strain hardening data with t/d ratio for (a) 20MnMoNi55 steel, (b) Cr-Mo-V steel and (c) SS304LN materials, obtained using miniature test specimens*

### *3.6.2 Fractographic analyses of tested specimens*

This behaviour of failure of varying thickness of the test specimens was also verified using fractographs, as shown in Figs. 3.24-3.26. These images appear very close to each other but it is seen that thinner specimen show elongated micro-voids along the fracture surface and shallower dimples, whereas symmetric micro-voids, equi-axed, deeper and wider dimples are seen for higher thickness specimens. Also, within a void there are fibrous features representing resistance to void growth, which appear to be increasing with increase in specimen thickness, resulting in higher ductility and strength data with increasing thicknesses of the specimens.

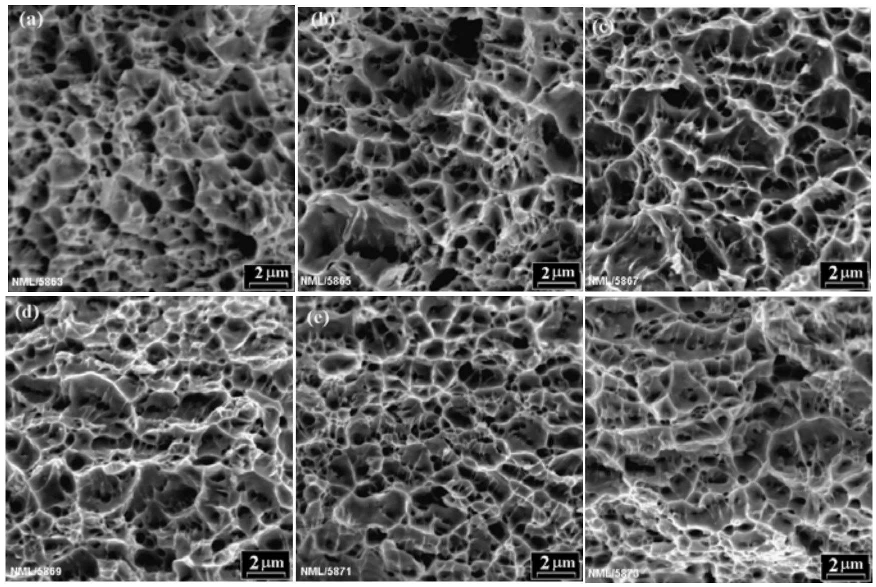

*Fig. 3.24: Fractographs of miniature tensile specimen of 20MnMoNi55 for thicknesses (a)0.15mm, (b)0.2mm, (c) 0.25mm, (d) 0.3mm, (e) 0.35mm and (f) 0.4mm*

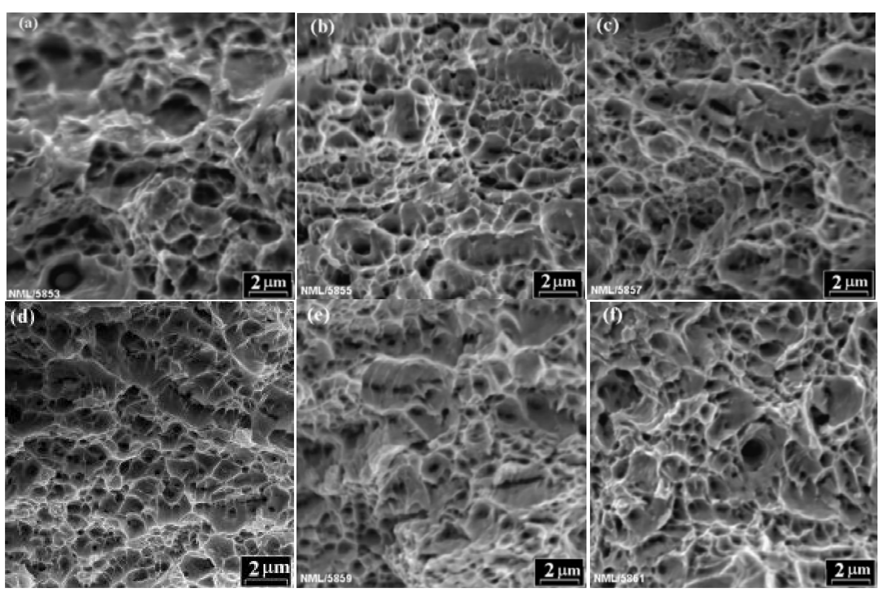

*Fig. 3.25: Fractographs of miniature tensile specimen of CrMoV ferritic steels for thicknesses (a) 0.15mm, (b) 0.2mm, (c) 0.25mm, (d) 0.3mm (e) 0.35mm and (f) 0.4mm*

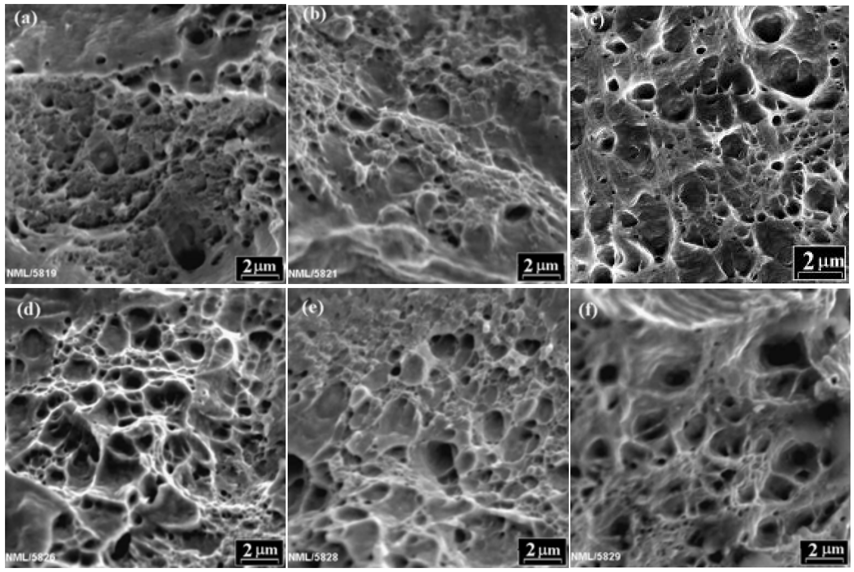


*Fig. 3.26: Fractographs of miniature tensile specimen of SS304LN for thicknesses (a) 0.15mm, (b) 0.2mm, (c) 0.25mm, (d) 0.3mm, (e) 0.35mm and (f) 0.4mm*

### ***3.6.3 Finite element analysis***

For modeling the behaviour of miniature specimen during tensile test, a model utilising half symmetry of the actual tensile specimen was developed as shown in Fig. 3.27. About twenty thousand 8-noded brick elements were used for meshing. Gauge length of the specimen was map-meshed while the shoulder sections were free-meshed with brick elements. For modeling nonlinear material behaviour, von-Mises plasticity model with isotropic material hardening method was used. Because of the large-scale deformations involved during necking, geometric non-linearity was also accounted for in the finite element formulation.

Multi-linear material hardening procedure used in the model is shown in Fig. 3.28. For modeling stresses beyond UTS from experimental data, model of the form shown in equation below was used with a few data points prior to UTS.

$$\sigma = K\varepsilon^{n}, \text{ where K = 886.75 and n =0.113} \qquad (3.5)$$

This equation prescribes the stress-strain relationship beyond UTS up to which we have experimental data. This is necessary for modeling behaviour after initiation of necking when very high localised strains are developed in the model.

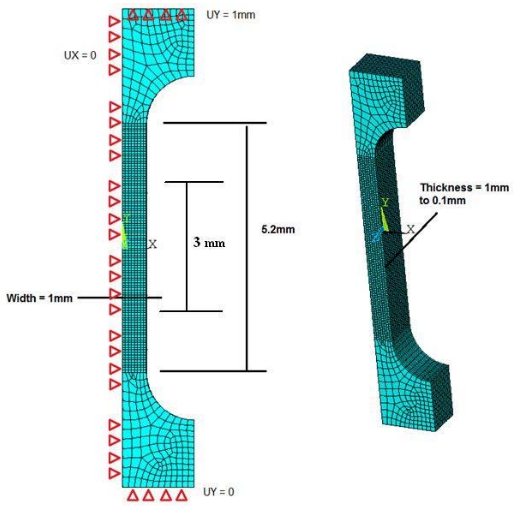


*Fig. 3.27: Meshed FE model and dimensions*

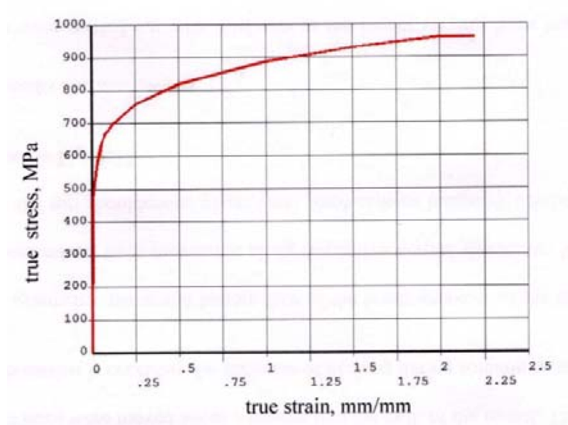


*Fig. 3.28: Multi-Linear material property data used for modeling*

For inducing necking after UTS, the nodes on middle plane, in the gauge length, lying on one of the outer surfaces were moved about a micron into the bulk of the model. This very small geometric deformation is necessary for initiation of necking during solution process.

The nodes on symmetric plane and bottom face of the lower shoulder of the half-symmetry model were constrained form movement along respective normal directions. While the top most plane at the top shoulder was given 1mm displacement boundary condition along its normal as shown in Fig. 3.27.

### 3.6.4 FEM results and discussions

FEM analyses were carried out with thickness of the model varying from 1mm to 0.1mm with other dimensions kept constant. Fig. 3.29 shows contour plots of the necking phenomena in various thickness test specimens. Fig. 3.28 shows engineering stress versus engineering strain for different model thicknesses.

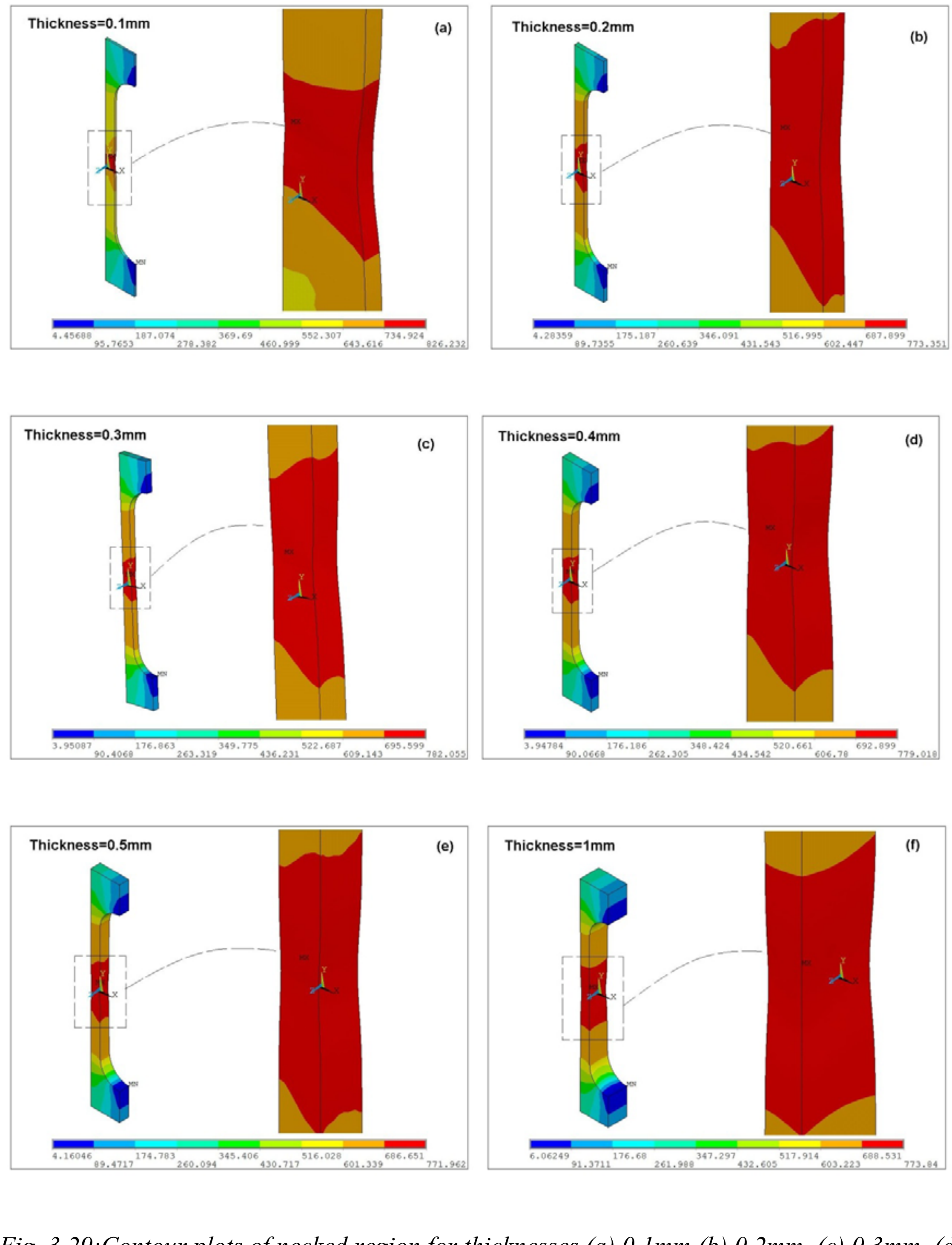


*Fig. 3.29:Contour plots of necked region for thicknesses (a) 0.1mm (b) 0.2mm, (c) 0.3mm, (d) 0.4mm, (e) 0.5mm and (f) 1mm*

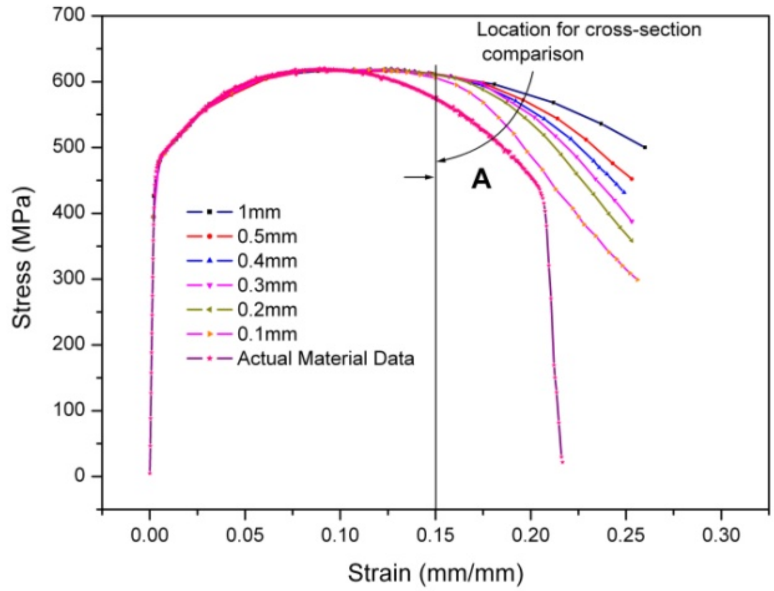


*Fig. 3.30: Comparison of stress-strain plots for various thicknesses using FEM with experimental data*

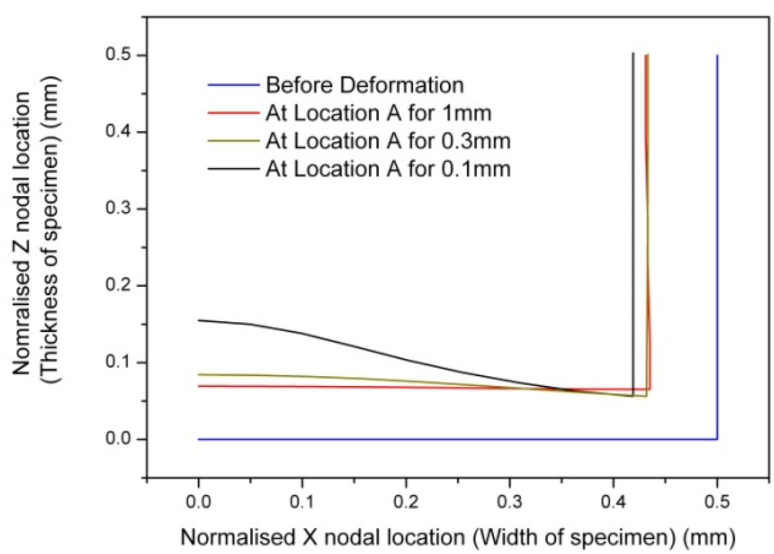


*Fig. 3.31: Normalised quarter-symmetric cross-section at necking for various thicknesses*

It must be noted that the plots match with the stress strain behaviour of full size experimental tensile test till the UTS. After UTS decreasing thickness of the specimen, especially below about 0.3mm, alters the stress strain behaviour. It is imperative to note that for the present FE model that does not take into account formation of micro voids or any damage model at the necked region, the results much further after necking is not generally correct. Thus, a point identified by marker line ‘A’ in the figure, is used for comparison of the plots of different thicknesses. The location ‘A’ is chosen such that the FE plot for 1mm thick specimen is in complete agreement with the experimental data. At this location it is seen that the FE plots for decreasing thicknesses matches well with the experimental data except for 0.2mm and 0.1mm models. For these models it is seen that the strength decreases much faster than other thicker models.

Reason for the considerable variation in plot for thinner specimen in comparison to the other thicker specimens seems to be due to the variation of tri-axial stresses developed at the neck cross section for different thicknesses and non- availability of sufficient volume of material to counter the load. Fig. 3.31 illustrates the way the quarter symmetric cross section deforms at the neck for various thicknesses corresponding to location ‘A’ in Fig. 3.30. All the plots are normalised, in Fig. 3.31, to the same dimensional scale for better clarity. It can be easily seen that till a thickness of 0.3mm, the reduction in cross section at the neck is fairly uniform with a slight inward curvature of the corresponding face. But for 0.1mm thickness neck, the inward curvature is significantly higher in the thickness direction. This sudden decrease in thickness at the centre of the wider face of the specimen leads to higher localised strains at centre, which further leads to earlier micro-void formation at the region and decreased strength.

### *3.6.5 Closures on determination of minimum thickness of miniature tensile specimens*

Tensile tests were conducted with an aim to determine the minimum thickness required in the gauge section of miniature tensile test specimens in order to get data comparable to standard test specimens. Miniature tensile test specimens, with uniform width of 1mm and varying thicknesses from 0.15 to 0.4mm from three different materials were used for the experiments. It was found that 0.3mm thickness, corresponding to t/d values as 16, 3.4 and 1.5 for 20MnMoNi55, CrMoV steel and SS304LN materials, respectively, was able to give the YS, UTS and uniform elongation data almost stabilised, however, the total elongation data of all the materials kept increasing. The reason for continuous increasing of total elongation for specimens of higher thicknesses is due to availability of more than sufficient volume elements of material in the gauge section, which is allowing the specimen to elongate till the volume of material, at the neck, is able to sustain the growth and resist fracture. These experimental values were also successfully verified using finite element method, using pure mechanics approach.

## 3.7 Experiments & validation of miniature tensile test data

### *3.7.1 Experimental procedure*

Based on findings of section 3.6, miniature tensile specimens of 0.3mm thickness were used for experimental verification of their tensile results with standard sub-size specimens, as shown if Fig. 3.5b. Other dimensions of the gauge section of the miniature specimen were 1mm width x 3mm gauge length. Miniature and sub-size tensile specimens were fabricated from the same lots of three materials. The sub-size specimens and miniature specimens were made geometrically similar by maintaining the geometrical ratio $L/\sqrt{A}=5.48$. Three specimens each from sub-size and miniature size tensile specimens were tested at room temperature and at same strain rate of $1x10^{-3}$ per second. Video extensometer was used for recording strain data and load cell of 1kN was used for load measurement. All the tensile tests were conducted at room temperature with a strain rate of $1x10^{-3}$ per second. The results from miniature as well as sub-size test specimens have been summarised in Table-3.4 and they have been compared in Figs. 3.32a, 3.32b and 3.32c for 20MnMoNi55, CrMoV and SS304LN steels, respectively. Scatter in UTS, YS properties, uniform and total elongation properties for 20MnMoNi55 steel, Cr-Mo-V steel and SS304LN for sub size and miniature test specimens is shown in Fig. 3.32d.

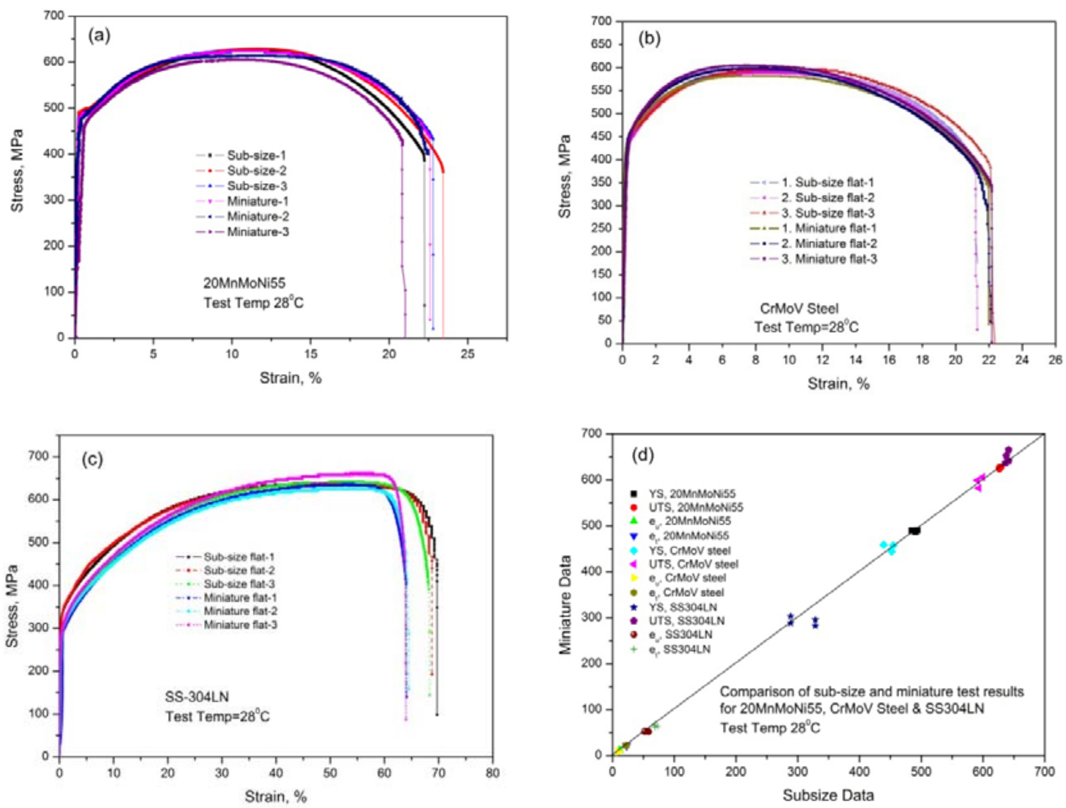


*Fig. 3.32: The engineering stress – strain plot, obtained using Sub-size and Miniature specimens; for (a) 20MnMoNi55 steel (b) CrMoV Steel and (c) SS304LN and (d) their respective variations in strength and elongation properties*

### 3.7.2 Comparison of experimental results with sub-size data

Average values of three specimens of each type, miniature and sub-size and from all the three materials were used for comparison. Comparison of YS data, obtained using miniature specimens, varied in the range of -5.86% (for SS304LN) and 1.11% (for CrMoV steel) in comparison to sub-size data. The UTS data from miniature specimen matched with sub-size data for 20MnMoNi55 steel and maximum deviation 0.34% was found for CrMoV steel. The uniform elongation data varied in the range of -7.21% (for CrMoV steel) and 6.09% (for 20MnMoNi55 steel). The total elongation data varied in the range of -6.82% (for SS304LN) and 1.84% (for CrMoV steel).

***Table-3.4: Comparison of tensile test results of sub-size and miniature specimens***

| | YS, MPa Sub-size | YS, MPa Mini | UTS, MPa Sub-size | UTS, MPa Mini | $e_u$, % Sub-size | $e_u$, % Mini | $e_f$, % Sub-size | $e_f$,% Mini |
|---|---|---|---|---|---|---|---|---|
| | | | | 20MnMoNi55 | | | | |
| Test-1 | 491 | 487 | 627 | 624 | 11.5 | 12.3 | 22.3 | 22.6 |
| Test-2 | 494 | 490 | 629 | 628 | 11.4 | 12.8 | 23.4 | 22.5 |
| Test-3 | 485 | 490 | 627 | 627 | 11.5 | 11.5 | 22.8 | 21 |
| Average | 490 | 489 | 627 | 627 | 11.5 | 12.2 | 22.8 | 22.0 |
| % error | | -0.2% | | 0 | | 6.09% | | -3.50% |
| | | | | CrMoV | | | | |
| Test-1 | 452 | 444 | 593 | 582 | 9.4 | 9.5 | 21.3 | 22.0 |
| Test-2 | 439 | 459 | 591 | 599 | 8.7 | 8.7 | 21.3 | 22.1 |
| Test-3 | 455 | 458 | 599 | 606 | 10.9 | 8.9 | 22.4 | 22.1 |
| Average | 449 | 454 | 594 | 596 | 9.7 | 9.0 | 21.7 | 22.1 |
| % error | | 1.11% | | 0.34% | | -7.21% | | 1.84% |
| | | | | SS304LN | | | | |
| Test-1 | 315 | 300 | 638 | 637 | 54.2 | 54.2 | 69.7 | 64.1 |
| Test-2 | 318 | 284 | 636 | 625 | 53.9 | 58.2 | 68.8 | 64.5 |
| Test-3 | 289 | 284 | 641 | 662 | 56.2 | 58.0 | 68.3 | 64.0 |
| Average | 307 | 289 | 639 | 641 | 54.8 | 56.8 | 68.9 | 64.2 |
| % error | | -5.86% | | 0.31% | | 3.64% | | -6.82% |

### *3.7.3 Validation of miniature specimen test data by finite element analysis*

The experimental results from miniature specimens were also validated using finite element analysis. The finite element modeling and computations were conducted using finite element software. The 2-D finite element model of quarter shape of the miniature test specimen was used due to geometric symmetricity, as shown in Fig. 3.33a. The test specimen was modeled with four-noded quadrilateral plane stress elements because the thickness of the body or domain is small relative to its lateral (in-plane) dimensions. Mapped meshing was adopted for the gauge length while other sections were free meshed with emphasis given to the number of elements in the gauge section and shoulder sections of the specimen. Geometric nonlinearity was also modeled on top of material non-linearity. In order to represent the experimental setup, the loading pin was simulated for providing load to the specimen. The loading pin was treated as 2-D rigid body with friction coefficient of zero. Due to symmetricity only one pin was modeled and the motion in X-direction was arrested. However, it was allowed to experience displacement in the Y direction as in the experimental situation. Contact elements were defined between the loading pin and the shoulder contact line of the specimen model. A concentrated force was applied to the reference point of the pin in the Y direction. The load was applied through the amplitude field in a linear fashion i.e. at time zero, the load value is zero and at time t=1 the load is maximum. All these prescribed conditions were applied in the respective reference node of load pins.

**(a) Material modeling**

In the elastic analysis of simulation, the material properties of the columns were defined by elastic modulus and Poisson's ratio. In the nonlinear analysis stage, material nonlinearity or plasticity was included in the FEM using a mathematical model known as the associated plasticity flow rule with von-Mises yield criterion. In the finite element simulation of miniature specimen, the plastic properties are defined together with the isotropic hardening rule. It means that the yield surface size changes uniformly in all directions such that the yield stress increases in all stress directions as plastic straining occurs. In the incremental plasticity model true stresses and true plastic strains of a conventional test specimen were specified. This is because, during the tensile test, the cross-section area of the sample decreases due to elongation, while each subsequent increase of sample length takes place over an already elongated sample length. The true stress-true strain defines the flow curve appropriately, as they represent the basic flow characteristics of the material. The incremental plasticity model requires the true stress-strain curve from the point corresponding to the last value of the linear range of the engineering stress-strain curve to the ultimate point of the stress-strain curve.

### (b) FEA results and discussions

A concentrated load of 300 N (for two pins load would be 600N) was applied on the reference node of the pin in a linearly varying manner i.e. at time t=0, the load was zero and at time t=1, the load applied was (300N). For each time step, both the loads taken by the specimen and the corresponding elongation in the specimen was stored in the software. Fig. 3.34 shows the true stress-true strain curves obtained by the FE simulation of specimen and experimental results, which are in good agreement.

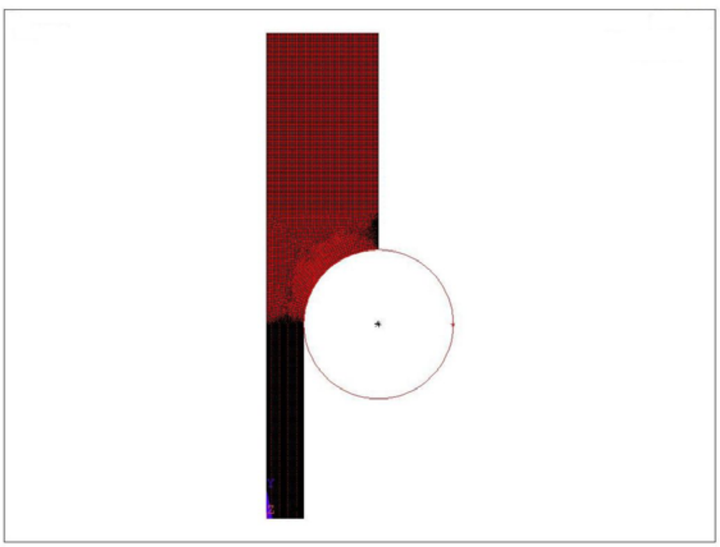

*Fig. 3.33a: Geometric modeling and meshing of quarter symmetry of miniature tensile test specimen*

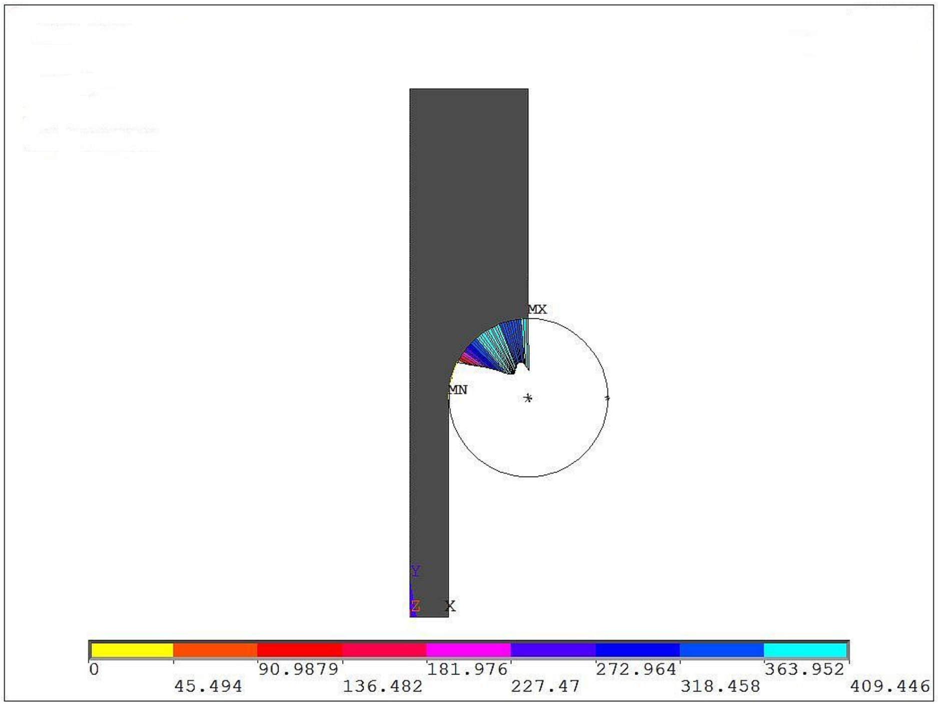


*Fig. 3.33b: Contact pressure distribution at the specimen shoulder at 300N load*

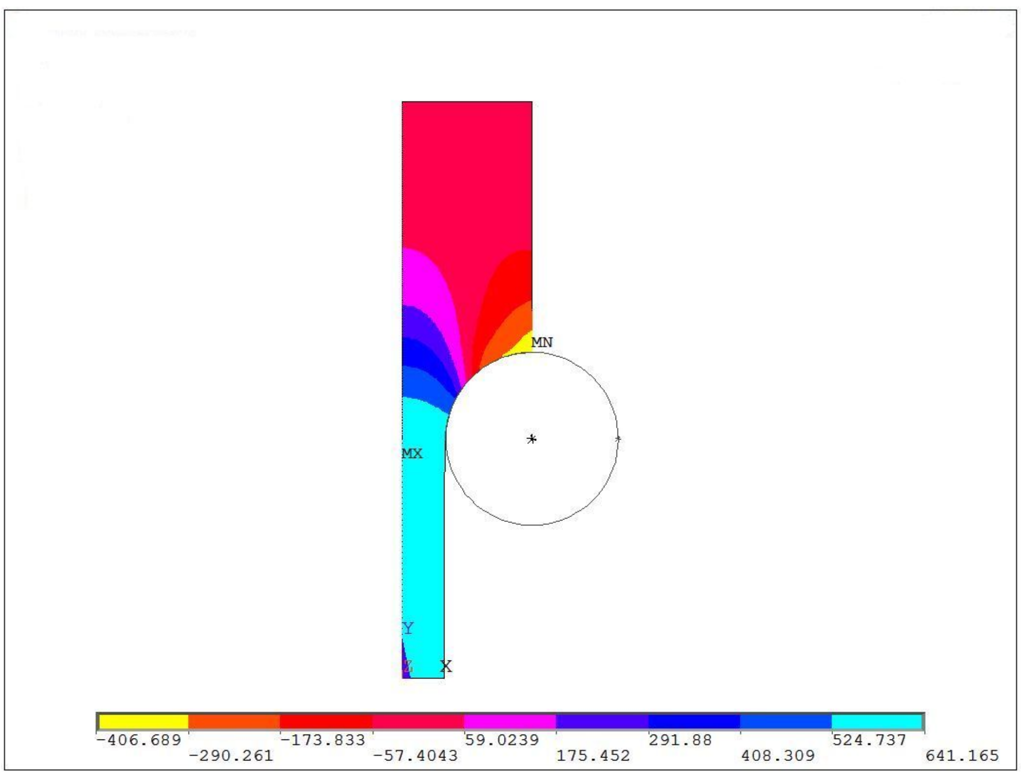


*Fig. 3.33c: Stress distribution at 300N load*

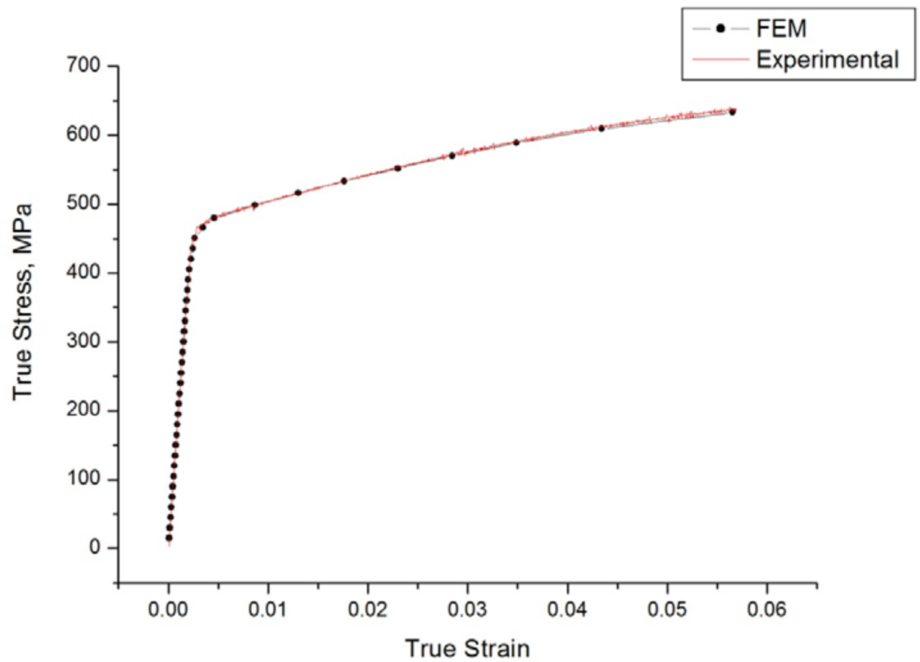


*Fig. 3.34: Comparison of true stress–true strain curves obtained experimentally and from FE analysis*

### 3.8 Closures

Based on the above experimental and numerical analyses, following conclusions could be drawn from this chapter:

- For in-service SSCs, boat sampling technique is useful as it scoops metal samples (boat samples) in a non-destructive manner.
- Boat sample of size 25mm x 40mm x 3mm can be used for extracting various types of miniature specimens, viz. tensile, small punch test, charpy and fatigue specimens.
- Geometric design of miniature tensile specimens was finalised based on the requirement that minimum 6-8 numbers of specimen could be extracted from the boat sample.

- Minimum thickness of miniature tensile specimen was evaluated by experiments, FEM analyses and fractography on miniature tensile specimens of thicknesses varied from 0.15mm to 0.4mm for the 20MnMoNi55, CrMoV steel and SS304LN materials.
- Minimum thickness of miniature tensile specimen was found to be 0.3mm for the given three materials, whose grain-sizes varied from 12 microns to 171 microns. Corresponding to t/d values were found to be 16, 3.4 and 1.5 for 20MnMoNi55, CrMoV steel and SS304LN materials, respectively.
- The finalised dimensions of miniature tensile specimen's gauge section were 1mm width x 0.3mm thickness and 3mm gauge length.
- Tensile test results from these miniature specimens could give data comparable to sub-size data. The true stress – true strain curves obtained experimentally and through FEM analysis of miniature specimen were also in good agreement.
- For tapping the potential of miniature tensile test technique, there is a need for a coherent international effort for standardizing the technique and adopting this as standard practice for the mechanical property evaluation.

# CHAPTER-4

# Small Punch Test and Development of Correlation for Ultimate Tensile Strength

## 4.1 Introduction

As discussed in chapter-3, boat samples can be used for extraction of small punch test (SPT) specimens, as shown in the schematic, Fig. 3.3. Disks of 10mm diameter or 10x10 sq. mm are also used for conducting the SPT experiments, however, in present case disks of 3mm diameter has been used based on the requirement that a comparatively larger numbers of SPT specimens can be extracted from the boat sample. The driving force for development of SPT was the need to evaluate mechanical properties from minimal irradiated volume of material due to various involved advantages. Development of the technique for evaluation of new materials' properties was advantageous too as significantly large number of tests could be performed using such lesser volume of material.

In SPT, the disk specimen is clamped within a die assembly, as shown in Fig. 4.1, and is pressed by a punch in a position controlled manner with an increasing load. This results in generation of load-displacement curve, as shown in Fig. 4.2. This load-displacement curve has typically four zones, named as elastic bending (zone I), plastic bending (zone II), membrane stretching (zone III) and failure (zone IV). The curve has been thought of as an indication of the material properties as it is generated as a response of material against application of load. This thought has resulted in development of a number of correlations for evaluation of yield strength (YS), ultimate tensile strength (UTS), elongation, creep and fracture properties etc.

Even though SPT does not give direct mechanical properties as the universal tensile test does, its ability to evaluate these properties, based on the correlations has made it attractive. It is also a fact that some of these correlations have established themselves, such as correlation for YS, but at the same time, some are yet to be established. Not able to establish a universal set of such correlations till date, has made the SPT rather more challenging and attractive. Due to these reasons, with progress of time, many researchers have joined the field and have put their efforts to establish the universal set of correlations for estimation of mechanical properties.

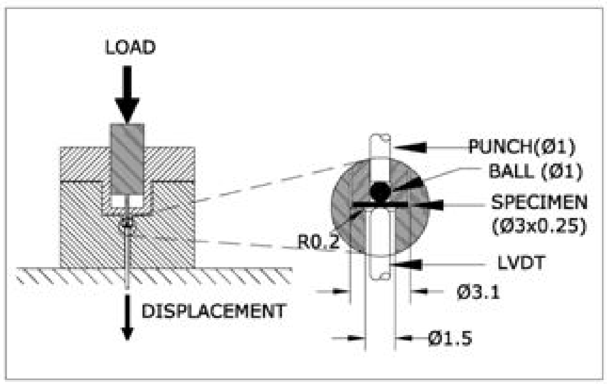


*Fig. 4.1: Small punch test (SPT) setup*

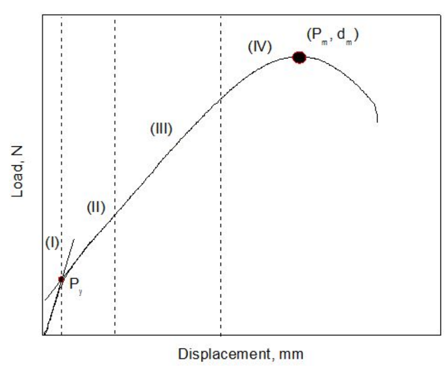


*Fig. 4.2: Typical SPT load vs. displacement curve with different zones*

One such correlation is for evaluation of ultimate tensile strength (UTS) using SPT, which has been an open issue since the development of the technique. Various correlations of UTS developed by different researchers [45, 48, 49, 52, 53] have been discussed in section 2.3.1. The larger plastic strains, in tri-axial state of stress during SPT, make the translation to the equivalent uniaxial parameter less certain. Correlations based on maximum value of load in load-displacement curve, $P_{max}$, have been used by many [41, 54 ], but those are also in disagreement [16, 20, 42, 54] as the point corresponding to $P_{max}$ does not represent a necking situation as in case of UTS, in a uniaxial tensile test. In this chapter, an attempt has been made for locating necking zone, which appears prior to $P_{max}$ [20, 54], through experiments and FEM analyses. Experimental results on disk specimens from 20MnMoNi55, CrMoV ferritic steel and SS304LN materials along with FEM analyses suggested that load corresponding to 0.48mm displacement is very close to the necking zone, and gives best fit for a UTS correlation.

## 4.2 Materials for Study

The same block of 20MnMoNi55 and CrMoV low alloy steels, as discussed in section 3.3, were used for the experiments in this chapter, however, different block of SS304LN was used. The mechanical properties of these materials were determined by fabricating sub-size round and flat tensile test specimens, as shown in Fig. 4.3, and conducting tensile test at varying range of temperature. The mechanical properties of the materials are given below, in Table-4.1.

***Table- 4.1: Mechanical properties of materials taken for study***

| Temp | 20MnMoNi55 | | | | CrMoV steel | | | | SS304LN | | | |
|---|---|---|---|---|---|---|---|---|---|---|---|---|
| °C | YS | UTS | Elongation, % | | YS | UTS | Elongation, % | | YS | UTS | Elongation, % | |
| | MPa | MPa | Uniform | Total | MPa | MPa | Uniform | Total | MPa | MPa | Uniform | Total |
| 25 | 484 | 629 | 10.4 | 22.8 | 471 | 610 | 10.2 | 20.8 | 245 | 584 | 67.6 | 75.9 |
| 100 | 451 | 582 | 8.1 | 18.2 | 425 | 544 | 7.4 | 19.3 | 178 | 455 | 56.8 | 71.3 |
| 200 | 433 | 573 | 6.8 | 14.9 | 400 | 516 | 7.0 | 18.2 | 137 | 404 | 44.2 | 56.5 |
| 250 | 453 | 600 | 8.1 | 19.3 | 399 | 514 | 6.4 | 16.7 | 132 | 387 | 43.1 | 54.8 |
| 300 | 457 | 621 | 8.4 | 17.9 | 394 | 503 | 6.2 | 15.8 | 118 | 395 | 43.7 | 52.0 |

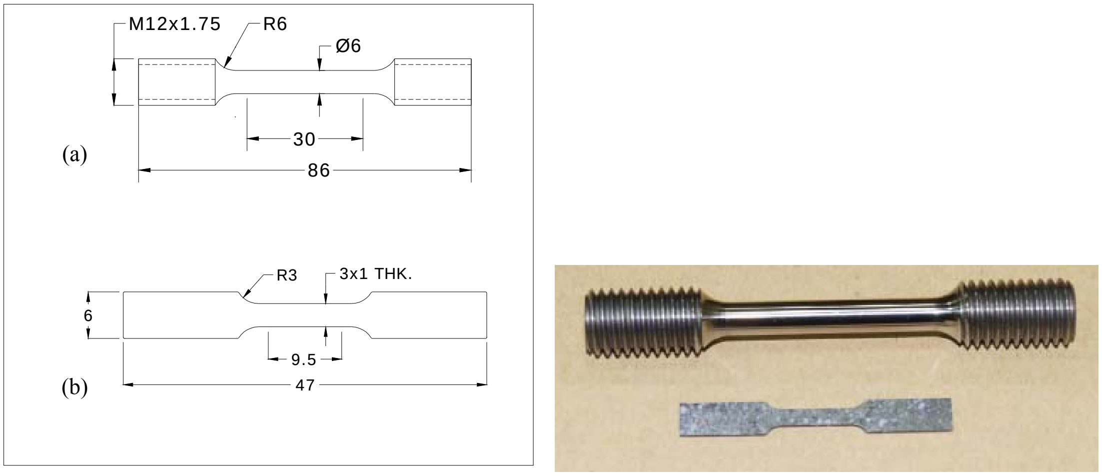


(c)

*Fig. 4.3: Dimensional details of (a) sub-size round specimen, (b) sub-size flat specimen and (c) their photographs*

## 4.3 SPT test setup

SPT test setup, Fig. 4.4, was fabricated with a provision for mounting LVDT. However due to connectivity issues for high temperature tests, the LVDT could not be used below the test specimen, as suggested earlier; and the LVDT mounted on the crosshead of the punch was used instead, Fig. 4.5.

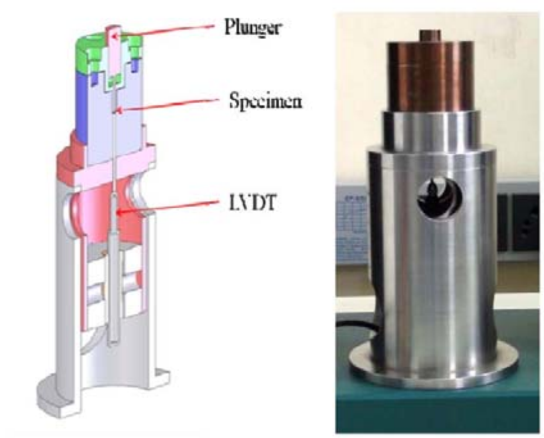


*Fig. 4.4: SPT Test setup with a provision of LVDT mounting at the bottom of disk*

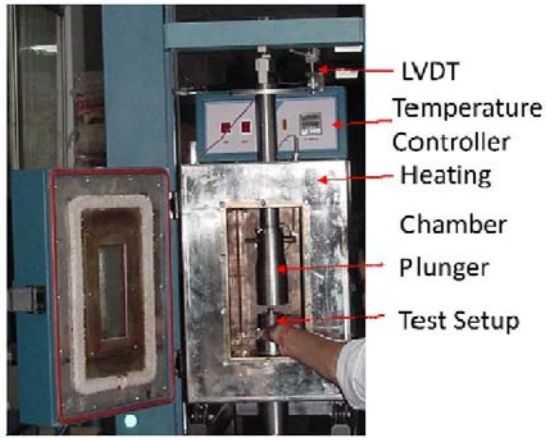


*Fig. 4.5: SPT Test setup with LVDT mounted on the moving punch cross head*

### 4.4 Experimental procedure

Initially, the disks of 10mm diameter were fabricated using EDM process and were polished with 1000, 1200, 2400, 4000 grit papers prior to final diamond polishing for 0.25 micron surface finish with a thickness of 0.25mm (+/-0.002mm). Later, the 10mm disk was then used to punch out test specimens of 3mm dia and thickness of 0.25mm (+/-0.002mm). These test specimens were subjected to SPT on a 5kN test machine with a load cell of capacity 1000N. A displacement controlled rate of 0.2mm per minute was applied till 90% load drop. More than 70 small punch tests were conducted, in total, at 25°C, 100°C, 200°C, 250°C and 300°C test temperatures for all the three material with three tests at each temperature for each material. Two hours soaking time was given for high temperature tests of both types, tensile and SPT.

### 4.5 Experimental results and discussions

The SPT graphs for the three materials for varying test temperatures are given in Fig. 4.6. Most of the failures were found at the circumference of the specimens as shown in Fig. 4.7.

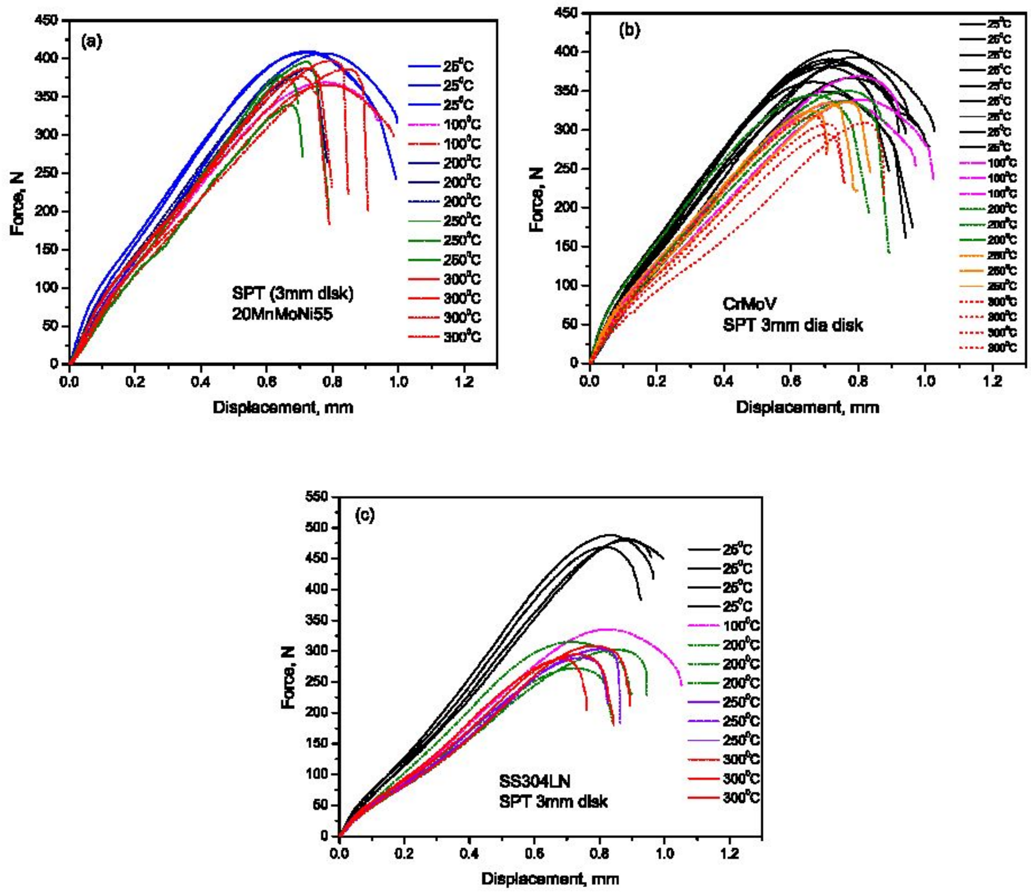


*Fig. 4.6: SPT graphs at different test temperatures as shown for (a) 20MnMoNi55, (b) CrMoV Steel and (c) SS304LN*

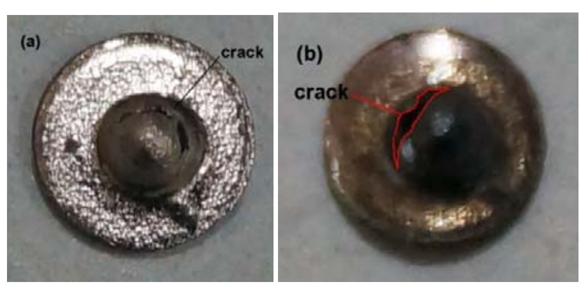


*Fig. 4.7: Showing 20MnMoNi55 test specimen tested at temperature (a) 25℃ and (b) 200℃. All test specimens failed at the circumference*

As discussed earlier, $P_{max}$ in SPT does not correspond to a state of stress similar to necking zone of tensile test, in present study it has been tried to find out the necking zone on the SPT curve, which can be considered for evaluation of UTS. There may be two ways to find out the necking zone; experimentally and analytically. Experimentally, this can be done by loading to a number of definite displacement values and removing the specimens for surface inspection through high resolution digital imaging. But this method might have many limitations, such as consistency, repeatability and reliability of specimen thickness, surface finish, mounting the test specimen in the SPT test setup, alignment of specimens with the punch, loading pattern of machine while in test etc. Apart from these human error is inherent part of every experiment. Further it has been reported that during initial phase of loading (zone-I in Fig. 4.2), is very sensitive to the alignment issue, due to which this zone does not show consistency in the SPT graphs even for very close similarity between test specimens. Practical limitations always play a vital role in distinguishing any two specimens and they can never be exactly similar. In summary, it is easier said than done to adopt the experimental way of verifying the SPT graph to find out the necking zone. Therefore the alternate easier way, described below, was adopted in this study, in which a help was taken from commercially available finite element software to find out a point on the SPT curve, which may behave like necking zone and can be used for development of correlation for UTS evaluation.

### 4.6 Finite element analysis

The finite element analysis of SPT was done based on an axi-symmetric model due to the symmetry of the test specimen. Further simplification was based on noting that the ball and the hardened lower and upper portions of the die are parts that undergo negligible deformation in comparison to the test specimen. Hence, these parts were assumed to behave as non-deformable bodies in the finite element analyses. For meshing the axi-symmetric specimen geometry, four-noded quadrilateral elements were used as these quadrilateral elements are capable of solving for large geometric deformation and material non –linearity.

Material yield condition was modelled using von-Mises yield criterion as the loading is monotonic in nature; the yield surface expansion or material hardening was assumed to be multi-linear isotropic. Further it may be noted that the modelling was done only for room temperature condition.

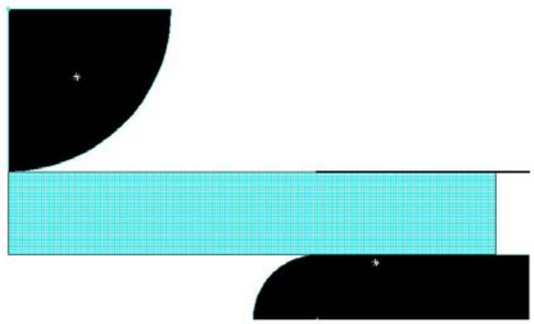

*Fig. 4.8: Axi-symmetric SPT finite element mesh*

The Young's modulus and Poisson's ratio were given as additional inputs for the analysis. Contacts between different surfaces were modelled using contact elements, based on Augmented Lagrangian contact algorithm, defined between various mating surfaces. For modelling friction between the contacting surfaces a friction coefficient of 0.3 was defined between the ball and punch. The finite element model was subjected to mesh independence analysis and the final meshed finite element model is shown in Fig. 4.8. The material properties used for the three different SPT materials are shown in Fig. 4.9. It must be noted that during SPT FE analyses, material undergoes considerable plasticity much beyond ultimate tensile strength for a given material. For generating material data beyond ultimate tensile strength point, it becomes necessary that an extrapolation scheme be developed, that without much loss in accuracy, represents actual material behaviour. In the present analyses, the material is assumed to behave according to logarithmic extrapolation as given below,

$$\sigma = K\varepsilon^{n} \qquad (4.1)$$

where, K and n are constants that depend on plastic material characteristics beyond yield point.

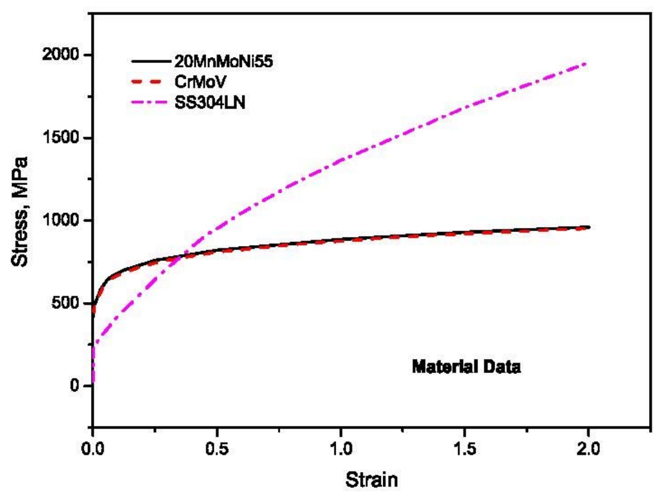


*Fig. 4.9: Material property data used for FEM.*

On the finite element model the left side line is automatically assigned zero radial displacement for axi-symmetric analysis configuration. The bottom of the meshed geometry is constrained from downward movement by the rigid contact element definition on the die at the same time the rigid contact elements on the top part of the die provides constraint to motion of the disk model in the upward direction.

After post processing the results of finite element analysis, plots in Fig. 4.10, show comparison of experimental force versus displacement data for 20MnMoNi55, CrMoV and SS304LN disk material. This analysis was carried out with 0.3 friction coefficient value. It was noticed in separate analyses that the Finite Element plot deviated considerably, especially in the maximum force developed area with the experimental data for lower values of friction coefficient. As can be seen, the contour plots in Fig. 4.11-4.13, that the surface of the punch slides considerably with the disk in latter portions of punch displacement where friction effects become significant. It can be noticed that the graphs are in good agreement with 0.3 as the friction coefficient value.

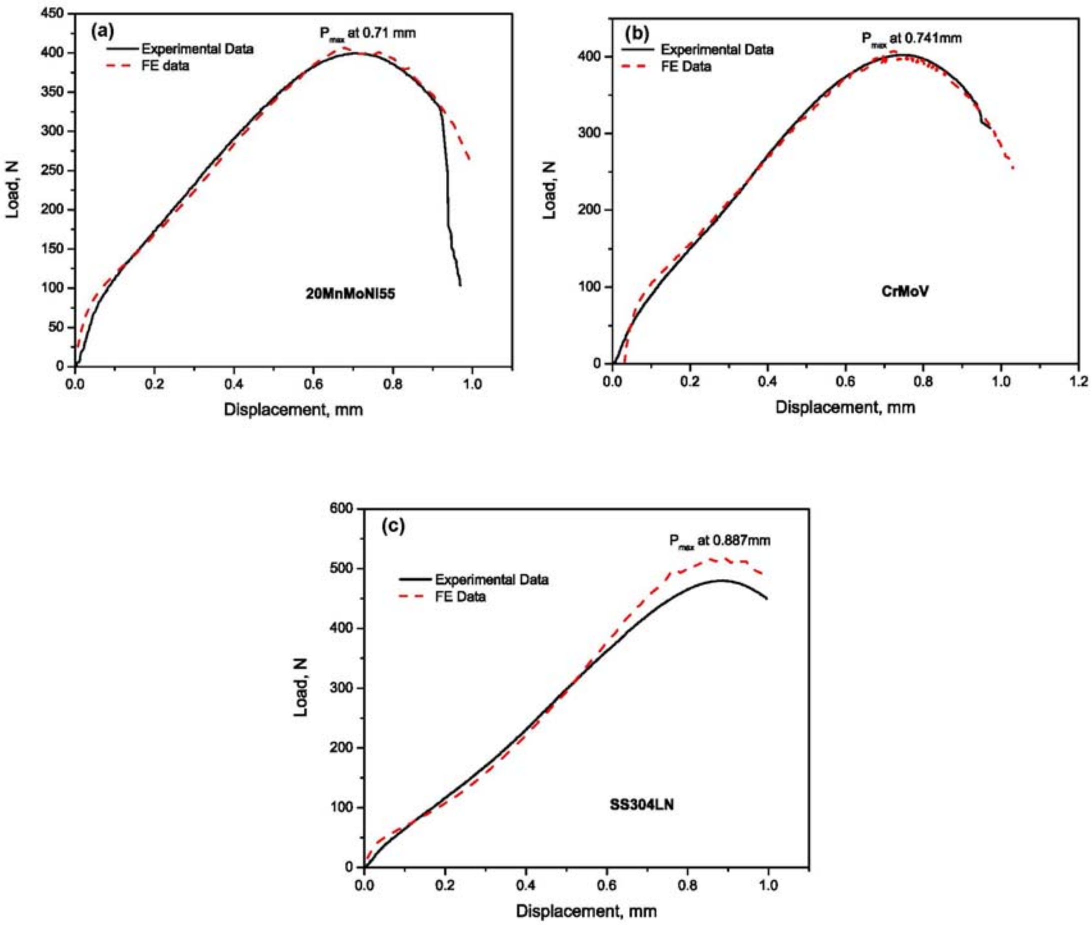


*Fig. 4.10: Plots of experimental and FE results for variation of punch force with punch displacement for (a) 20MnMoNi55 (b) CrMoV steel and (c) SS304LN disk material.*

It may be noted that for SS304LN material, the maximum force developed as calculated from the FE results are significantly higher than what is experimentally observed. This may be attributed to the fact that SS304LN material, because of its higher ductility, develops significant plastic strain on the disk above 70% in excess of 0.6mm punch travel. This relatively higher plastic deformation leads to permanent material damage in the form of generation of cracks and voids much further ahead of punch travel distance at which maximum force is generated. In finite element modelling no such permanent material damage was solved, which in other words means that the finite element model behaves stronger than actual under the punch and hence develops higher force. Also, it may be noted that for SS304LN material, the portion of the graph beyond the maximum force generated location is rather short in comparison to other steels considered here indicating much earlier formation of voids and cracks in the disk.

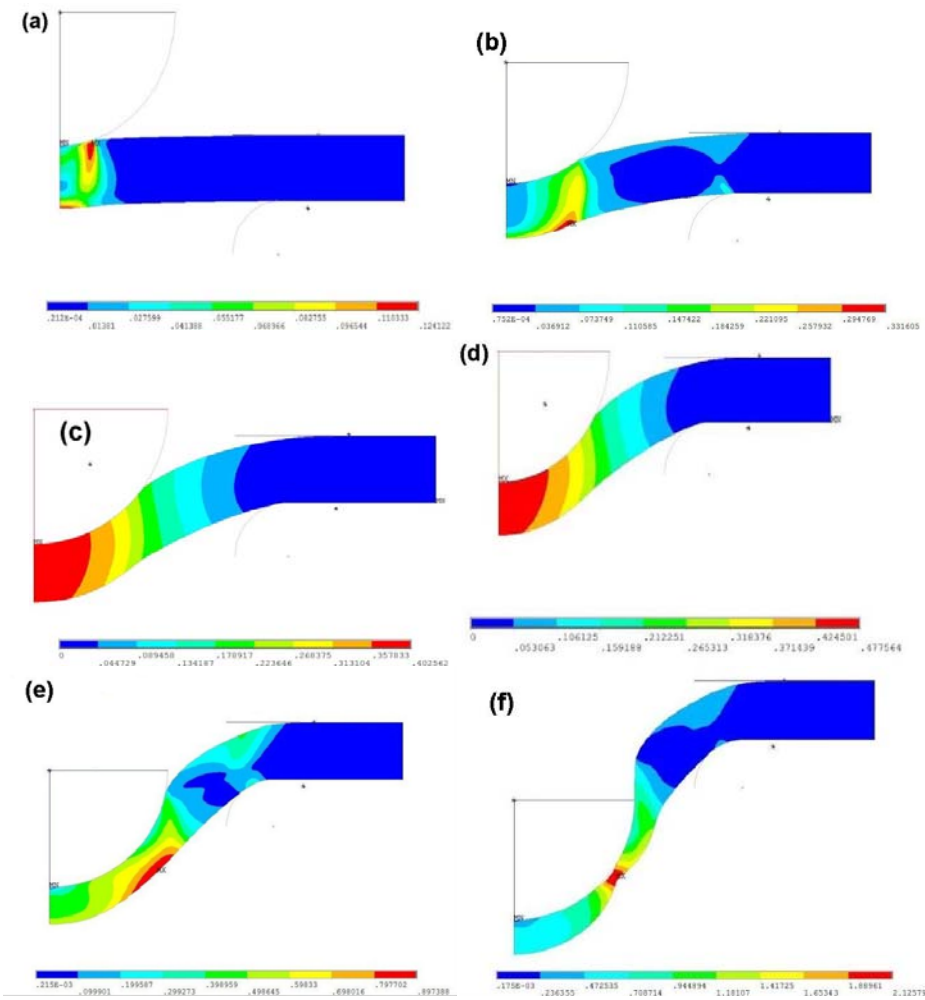


*Fig. 4.11: Contour plots of 20MnMoNi55 for von-Mises total strain on FE model under punch travel distance of (a) 0.03mm, (b) 0.2mm, (c) 0.4mm, (d) 0.48 mm, (e) 0.7mm and (f) 1mm.*

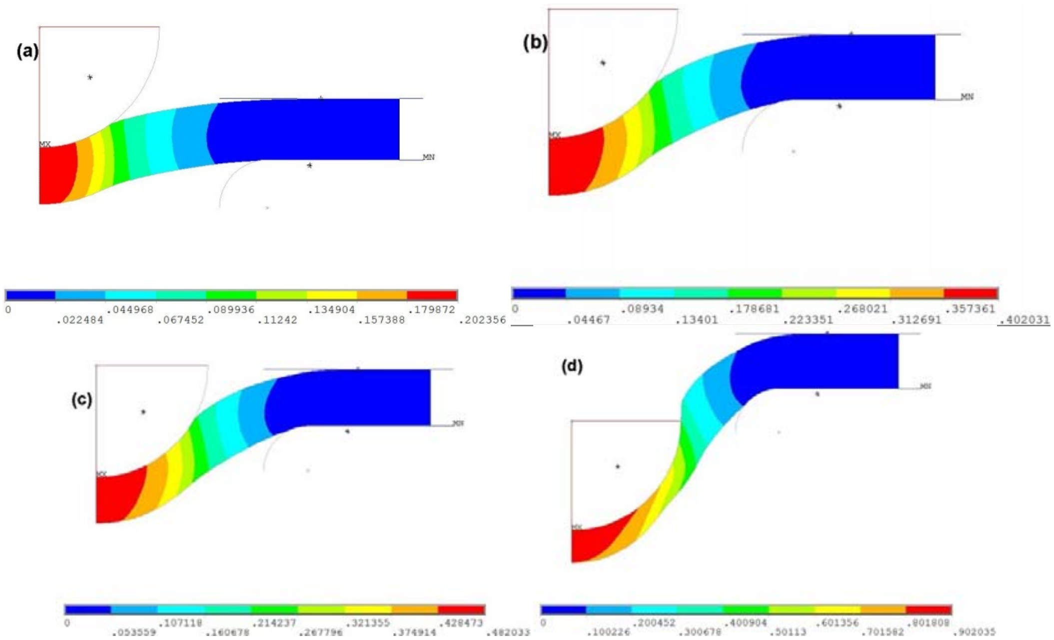


*Fig. 4.12: Contour plots for CrMoV steel for von-Mises total strain on FE model under punch travel distance of (a) 0.2mm, (b) 0.4mm, (c) 0.48 mm and (d) 0.9mm.*

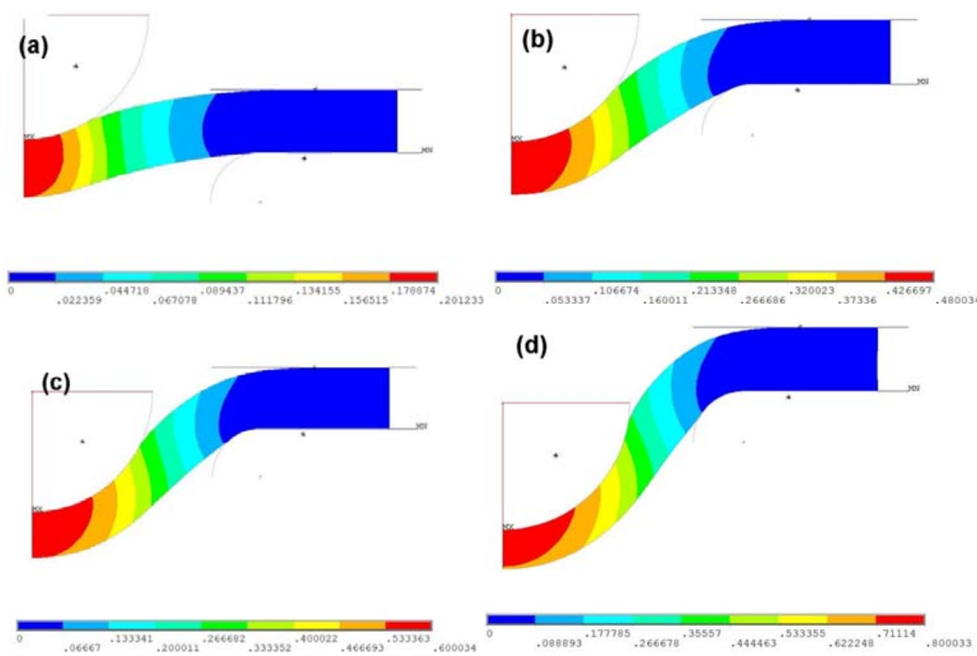


*Fig. 4.13: Contour plots for SS304LN for von-Mises total strain on FE model under punch travel distance of (a) 0.2mm, (b) 0.48mm, (c) 0.6 mm and (d) 0.8mm.*

## 4.7 Analyses for necking of the SPT disk

Figs. 4.11-4.13 show the deformation of the disk, for the three materials, under the punch during various stages of punch travel. These figures indicate that during initial stages of punch travel, the deformation of the disk involves more bending and less of stretching. As the deformation progresses under the punch travel, the stretching initiates which give rise to a noticeable decrease in thickness of the disk between the punch centre and material still inside the upper and lower halves of the die. Decrease in thickness further increases to a pronounced thinning under further punch travel and finally ends in failure along the thinned portion. It must me pointed out at this time that significant portions of the material below the punch undergoes considerable plasticity, for example, in excess of 50% for punch travel of about 0.7mm in case of 20MnMoNi55. A computer code was written to identify the location and the thickness of the thinnest section along the radial direction on the specimen for different punch travels. The code essentially extracts the nodal displacements of the top surface nodes to the nodes on the lower surface. Then calculates the least distance between the top surface node to the bottom surface node and plots the same for all top surface nodes against radial displacement from centre of the disk. The lowest distance indicated on such graph can be identified as the thinnest portion on the disk for a given punch travel. Figs. 4.14a, b and c show such plots for the three materials.

Fig. 4.15a shows the variation of the minimum thickness on the disk with different punch travel distances for the three materials. This was plotted with the intention to find the punch travel distance at which the thickness begins to decrease rapidly, indicating necking similar to that observed in uniaxial tensile specimen tests. From Fig. 4.15b it can be noted that the minimum disk thickness decreases with the punch travel and also that beyond about 0.5mm punch travel the rate of change of minimum thickness decreases rapidly with further increase in punch travel.

Further, from Fig. 4.15a, it can be noted that the radial location of the minimum thickness on the disk, observed at an average of about 0.28mm for 20MnMoNi55 and CrMoV steel (except for some stretching caused by the punch), on the disk also does not change significantly with increase in punch travel. For SS304 the radial location of the minimum thickness on the disk is observed at an average of about 0.38mm. Further analysis, from Fig. 4.15b, it can be noted that the pattern of minimum thickness reduction on radial location for the three materials are identical, even though these materials are not so identical, particularly SS304LN is highly ductile in comparison to the other two. This indicates that degree of necking increases progressively at the same location on the disks of all the materials.

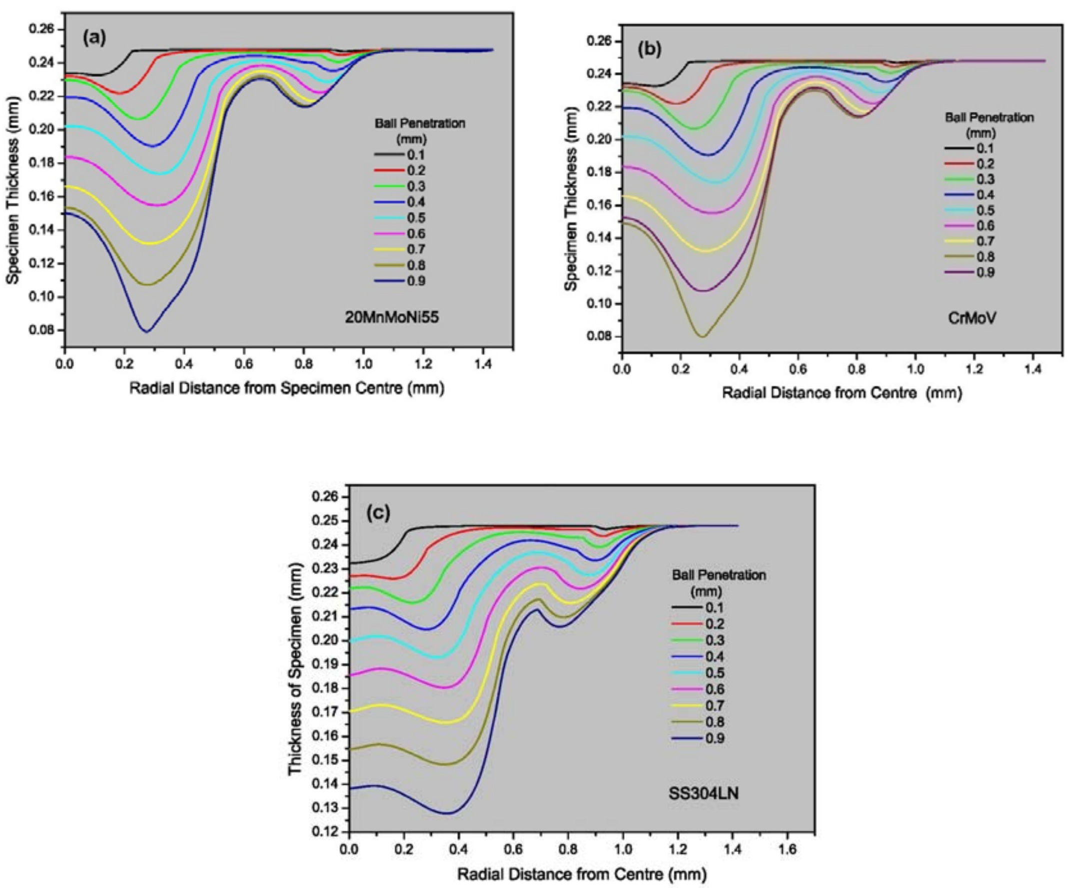


*Fig. 4.14: Plots of thickness of disk at various radial locations for different punch travel distances for a) 20MnMoNi55, (b) CrMoV Steel and (c) SS304LN*

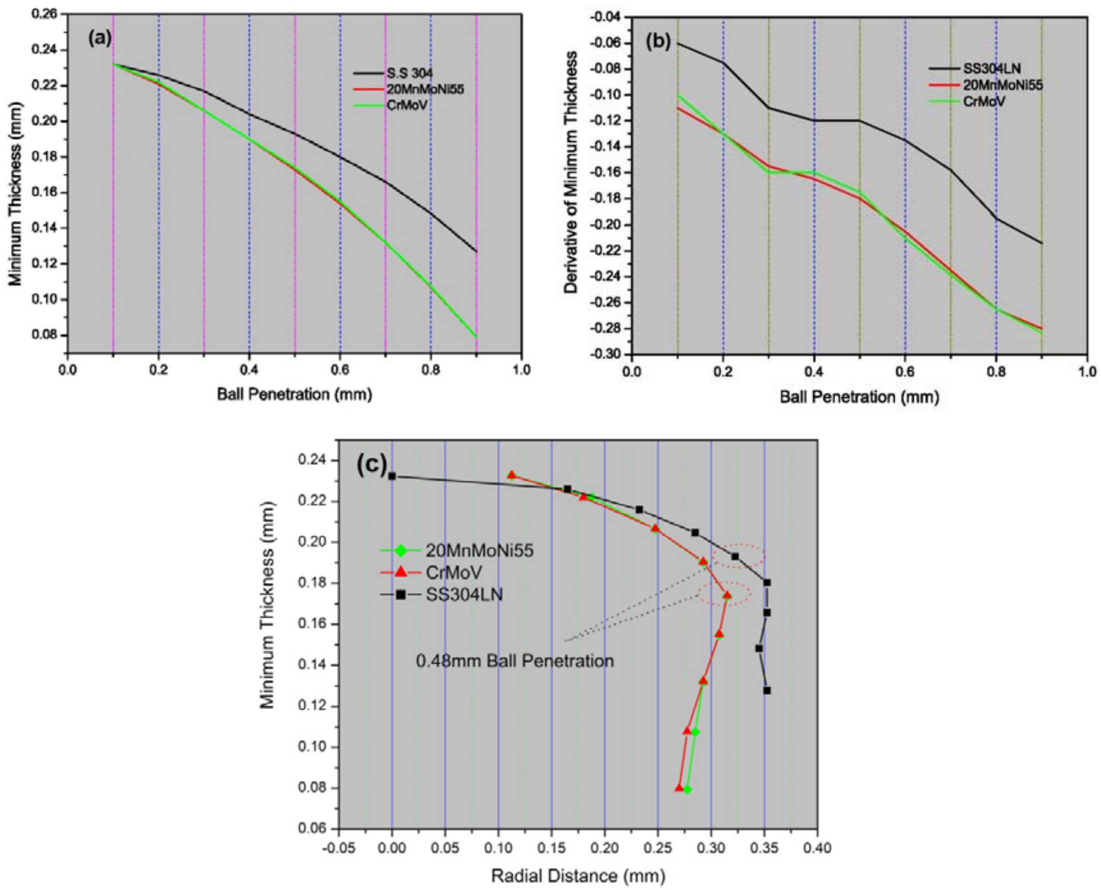


*Fig. 4.15: (a) Variation of minimum thickness on the disk with punch travel distance (b) Derivative of minimum thickness on the disk with punch travel and (c) Location of minimum thickness vs. radial distance.*

Further analysis performed close to 0.5mm punch travel has indicated that the rate of change of minimum thickness starts to change significantly at 0.48mm. So it can be approximately assumed that the necking zone may be at 0.48mm of displacement for all the three materials. This analysis was done for room temperature tests, however, being the same test setup and same thickness of test specimen, it may be logical to conclude that the necking zone may be at 0.48mm for all tests and for all materials. Therefore a load corresponding to 0.48mm displacement may be considered as load at UTS and the same can be used for derivation of correlation for UTS for all the three materials.

The reason for necking taking place at 0.48 mm in all the three materials can be explained considering the membrane stretching phenomena in zone-3, in the test specimens. The specimen has the freedom, based on its ductility, to stretch within the annular space between the punch and die. The less ductile material will not have comparatively more uniform stretching across its whole cross-section unlike the ductile material. This behavior of specimen is also visible in the FE contour plots of three materials in Figs. 4.11 to 4.13, where it can be seen that SS304LN has uniform thinning throughout its cross-section till 0.8mm of displacement. So this behavior might be attributed more towards the material deformation within the constraints of punch-die assembly than only the materials behavior.

The other reason may be explained based on the corollary with the necking phenomena in uniaxial tensile test, where necking or localized deformation begins when the increase in stress due to decrease in cross sectional area of the specimen becomes greater than the increase in load-carrying ability of the material due to strain hardening. In SPT also similar phenomena is happening in the membrane stretching zone, where uniform wall-thinning is taking place till approximately 0.48mm of ball penetration and the minimum thickness point is moving away from centre, Fig.4.14c, however after necking, .i.e. in the vicinity of 0.48mm, the minimum thickness points are moving towards the centre for the two less ductile materials. These phenomena can be explained in terms of strain-hardening. As the ball is penetrated further after necking, i.e. after of 0.48mm, strain hardening is making the zone stronger in comparison to their adjacent material and during further penetration, necking is taking place at a place which is below the ball and towards the centre. In this way, the points are moving closer towards the centre till a fracture takes place. However, for SS304LN material, the movement of minimum thickness away from centre is till 0.6mm of ball penetration and there is no shifting towards the centre, rather it is almost constant thereafter.

Since SS304LN is a highly ductile material in comparison to the other two materials, this phenomenon is different in this case.

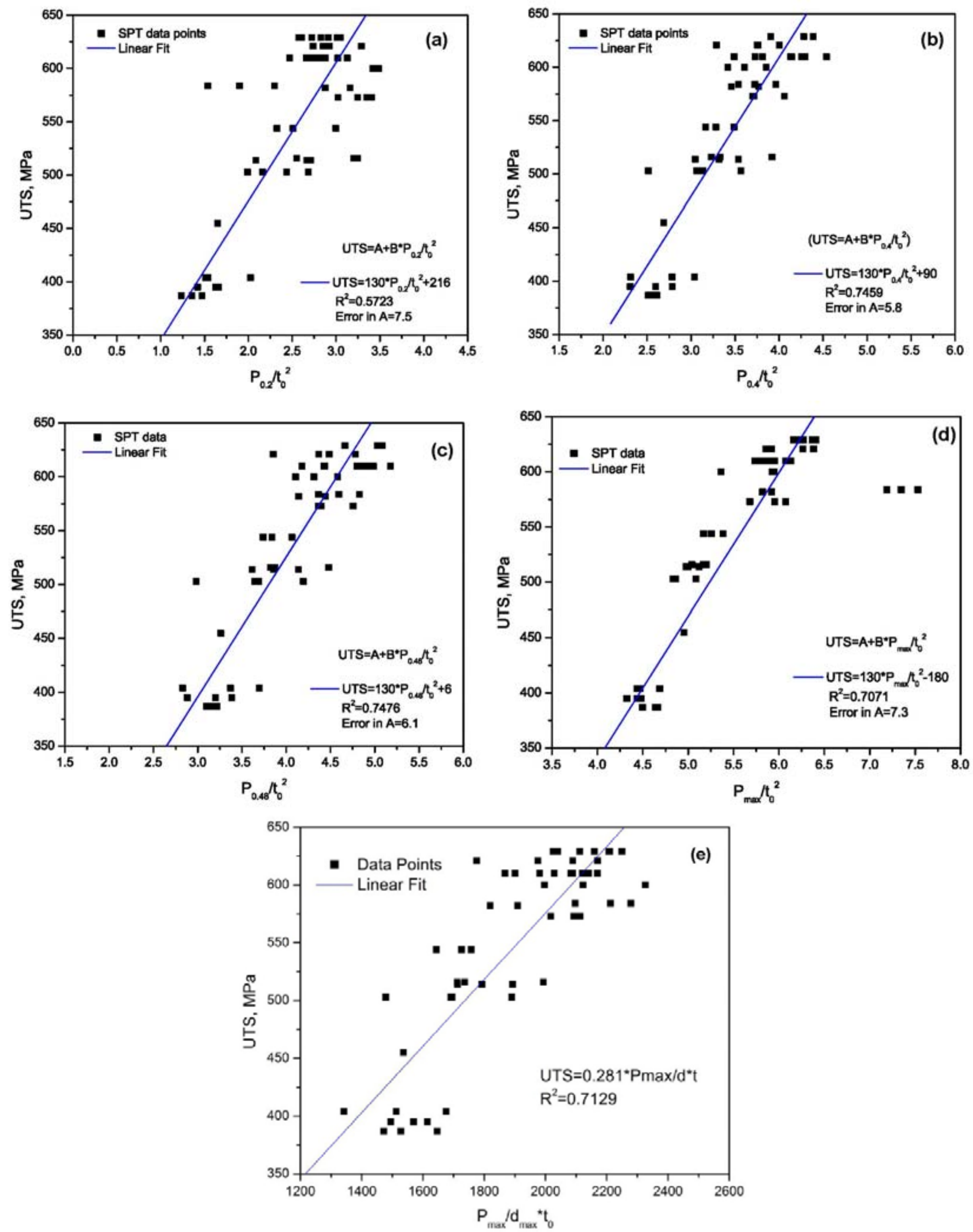


*Fig.4.16: Correlation between UTS and (a) $P_{0.2}/t_0^2$ (b) $P_{0.4}/t_0^2$ (c) $P_{0.48}/t_0^2$ (d) $P_{max}/t_0^2$ and (e) $P_{max}/t_0 * d_{max}$.*

## 4.8 Discussions and evaluation of UTS correlation

Based on the FE analyses, it was decided to locate $P_{0.2}$, $P_{0.4}$, $P_{0.48}$ and $P_{max}$ on all load-displacement plots of all the materials. These points were corresponding to displacements of 0.2mm, 0.4mm, 0.48mm and maximum load, in that order. These many numbers of points were selected to have an idea if there was any converging or any other types of patterns emerging out. Values of $\frac{P_{0.2}}{t_0^2}$ , $\frac{P_{0.4}}{t_0^2}$ , $\frac{P_{0.48}}{t_0^2}$ and $\frac{P_{max}}{t_0^2}$ were found out for each plot and these values were plotted against UTS values, obtained from uniaxial tensile tests, to establish correlations between the two. A linear fit of these data were found as shown in Fig. 4.16.

The following linear relationship were obtained between SPT and UTS for the three materials, based on the probable necking zones at displacements of 0.2mm, 0.4mm, 0.48mm and displacement corresponding to $P_{max}$:

$$UTS=130*\frac{P_{0.2}}{t_0^2}+216 \tag{4.2}$$

$R^2$=0.5723,

$$UTS=130*\frac{P_{0.4}}{t_0^2}+89 \tag{4.3}$$

$R^2$=0.7459,

$$UTS=130*\frac{P_{0.48}}{t_0^2}+6 \tag{4.4}$$

$R^2$=0.7476

$$UTS=130*\frac{P_{max}}{t_0^2}-320 \tag{4.5}$$

$R^2$=0.7071

$$\text{UTS}=0.281*\frac{P_{max}}{d_{max}*t_0} \tag{4.6}$$

$R^2=0.7129$

As is seen, linear fits have been carried out for all the set of data corresponding to 0.2mm, 0.4mm, 0.48mm and displacement corresponding to $P_{max}$ values. It can be seen, linear fit with fixed slope of 130, as used by various authors [11, 36, 37], has the maximum fit of data points. Further as was concluded through FE analysis, the data corresponding to 0.48mm has the maximum fit ($R^2=0.7476$), which is closely followed by data corresponding to 0.4mm ($R^2=0.7459$), however the data corresponding to displacements corresponding to $P_{max}$ has lesser fit ($R^2=0.7071$). The displacements corresponding to $P_{max}$ values are 0.71mm (for 20MnMoNi55), 0.741mm (for CrMoV steel) and 0.887mm (for SS304LN).

Due to the fact that average value of tensile properties have been used for deriving the correlation in Fig. 4.16, there appear a lot of data scatter in all the graphs and so $R^2$ value are very poor. In such a case, a way to look for the best fit may be to look for the even distribution of data points across the linear fit and their symmetry. Here, even though $P_{max}$ may look to be best fit due to data points being very close to each other, but closer look conveys that the data points are more evenly distributed in $P_{0.48}$ curve. The $R^2$ values also suggest that $P_{0.48}$ has the best fit among all.

This confirms our assumptions that considering a point in the necking zone, which begins much earlier than $P_{max}$, a better correlation can be obtained for UTS. In present study, this point is at 0.48mm, which may vary minutely for a different set of the punch-die assemblies; however it is found to be independent of materials, as is seen here. Even though, at 0.48 mm displacement also, a lot of data scatter is observed as in other cases also. This may be due to three different types of materials being used in study, as it has been reported; ductility plays a major role in SPT graph. Here also ductility of SS304LN is much higher than the other two materials. The other reasons for large scatter of data may be due to various sources of error, like a) specimen geometry and surface finish, b) test fixture tolerances and c) testing method, collection & interpretation of data and human error, etc. For the same size of specimen data, the specimen should be representative of whole body. For uniform microstructure this source of error is minimal. In addition, the disk specimen should be prepared in a consistent and reproducible geometry and surface finish. The thickness of 0.25mm has been controlled within ±0.002 mm to minimise this type of error. Surface finish is particularly important for disk bend test as the strain is maximum at the surface and the polishing up to 0.25microns using diamond polishing was done to minimise the error. The alignment of punch and die axes of test fixture, tolerances, centring and clamping of specimen in the test fixture are other sources of error. The dimensions and geometrical tolerances of test fixture developed, were precisely controlled to minimise the error, however, the inherent deviations might have caused some error in test results. The test method includes the accuracies involved in measurement of test speed, displacement, data acquisition etc., which must be consistent with the theoretical understanding. The acquisition of data was based on computer software with LVDT range of ±2mm with accuracy of ±0.001mm. Calibrated load cell of 1kN with accuracy of 1% was used for measurement of the load.

### 4.9 Closures

Following are the conclusions from this chapter:

- Small disks of 3mm diameter were found to be suitable to be extracted from a boat sample, or small volume of material.

- Small punch tests were carried out on 3mm diameter x 0.25mm thick disks using 1mm diameter balls, within a test setup, consisting of a punch and specimen holder assembly.

- The tests were carried out on 20MnMoNi55, CrMoV and SS304LN steel specimen for a range of test temperatures.

- Finite element analyses were carried out and found to be in good agreement with the experimental results of SPT.

- FEM contours were analysed at different displacement values of the punch to find out necking regions of the SPT disk specimens.

- For the given test setup, disk specimen size and test conditions, the necking zones of the SPT disks are found to be very close to 0.48mm displacement,

- It has been found that correlation of UTS using SPT is best suited if the data corresponding to necking zone, i.e. corresponding to punch displacement of $P_{0.48}$, is used in comparison to $P_{max}$ or any other value.

- Thus, the new UTS correlation, for 3mm diameter and 0.25mm thick disks, was given as : UTS=130*$\frac{P_{0.48}}{t_0^2}$ +6

# CHAPTER-5

# Applicability of Miniature Test Techniques in Indian BWRs

## 5.1 Introduction

Chapter-1 discussed about the industrial needs for development of miniature test techniques, followed by standardization of miniature tensile specimens in chapter-3 and development of UTS correlation for SPT in chapter-4. This chapter aims towards applicability of miniature test techniques, as envisaged in chapter-1, in Indian perspective.

In India, there are requirements from various industries, like petroleum industries, heavy water industries and nuclear power plants for assessing the existing mechanical properties of their various equipment. The major requirement is from two units of BWRs, operating in Tarapur, India, for assessing the existing mechanical and metallurgical conditions of H4A weld locations of their core shrouds, based on the various reported incidents of cracking of these welds in overseas reactors, as discussed in section 5.3. For the purpose, it was decided to physically obtain metal samples from the H4A location in the core shroud for further analyses. To serve the purpose, a scooping technique, named as boat sampling technique (BST) was developed [73]. This chapter gives brief description of the BST, full-scale mock-up trials at Tarapur reactor site of Indian BWR, extraction of miniature test specimens from the dummy boat sample, conducting tensile and small punch tests on the miniature specimens from the boat sample and their comparison with standard test results.

## 5.2 Core shroud

Core shroud of BWR is a cylindrical vessel, made by a series of circumferential or horizontal welds named as H1, H2, H3, etc. It consists of top & bottom grid plates, which provide lateral support to the fuel assemblies, and maintains core geometry during operational transients and postulated accidents to permit control rods insertion. It partitions feed water in the reactor vessel down-comer annulus region from cooling water flowing through the reactor core.

While in operation, the core shroud experiences radiation field, high temperature and various static & dynamic loads, resulting in degradation of mechanical and fracture properties of the material; leading to reduction in safe operating margin. Many of the welds and the adjoining HAZ regions of core shroud are known to be susceptible to various forms of Stress Corrosion Cracking (SCC) due to simultaneous presence of aqueous environment, high temperature and tensile stress.

## 5.3 Cases of core shrouds cracking world over

Many cases of core shrouds cracking have been reported from countries like Germany, Sweden, USA, Japan, etc. [74-78] during the year 1990 to 1994. Most of the cracking phenomena were Intergranular stress corrosion cracking (IGSCC) of SS304 type of steels due to chromium depletion at grain boundaries, presence of oxidizing environments and influence of local stresses [78,79]. SS316L was developed in 1977, which has excellent resistance to sensitization and this was assumed to be the only solution for SCC in those days [80]. Many core shrouds, earlier made of SS304 were replaced with SS316L material, viz. Fukushima Daiichi Unit 3 (1998), Fukushima Daiichi Unit 2 (1999), Tsuruga Unit 1 (2000), Fukushima Daiichi Unit 5 (2000), Shimane Unit 1 (2001) and Fukushima Daiichi Unit 1 (2001) [81, 82], and so on.

The cracking of pressure vessel nozzles made of SS316L, in 1985, and later cracking of core shrouds made of SS316L changed the perception of low-carbon SS being the solution for SCC and study in this area started in 1992 [80]. The study revealed that the SCC of low carbon SS was attributed to the depletion of Chromium and enrichment of Nickel and Silicon at grain boundaries as a result of radiation induced segregation (RIS), increase in surface hardness of the material and its sensitivity to SCC [83]; combined effects of high residual stresses associated with the shroud construction, the presence of a more aggressive, oxidising environment in the core and to micro-structural changes in the material [84]; cold work and surface deformation, surface treatment causing surface roughness and hardening [78, 80, 83, 84]; and, residual stresses generated during manufacturing and machining [78, 85] of core shroud.

The irradiation assisted stress corrosion cracking (IASCC) is another form of SCC, which is more prone to occur after the core shrouds see a threshold value of neutron fluence. For austenitic stainless steels in normal water chemistry of BWR environment the threshold value is suggested as $5x10^{24}$ $n/m^2$, for high energy neutron (E>1MeV), however experiments have shown this value may be even lower as $2x10^{24}$ $n/m^2$[85] for commercial purity SS. It is caused due to exposure to neutron irradiation for extended periods, which changes the microstructure, due to radiation hardening effect; and microchemistry due to RIS of the SS; and degrades their fracture properties [86-89].

Later it was concluded that all grades of SS and environmental conditions are susceptible to SCC in high temperature water, whether de-aerated or aerated, high or low $H_2$, theoretically pure water or contaminated, lower or higher temperature [90]. However, the kinetics of SCC growth varies enormously with stress intensity, yield strength, degree of sensitization, water chemistry, irradiation, temperature etc. The role of yield strength is especially important because it changes with surface cold work, bulk cold work, weld shrinkage strain, and irradiation hardening. It was also argued that the role of metallurgical strengthening mechanism might have a similar effect [90]. Further, it is stated that as core shrouds are subjected to relatively low fluence and most cases of core shroud cracking have been attributed to classical IGSCC of thermally sensitized stainless steels. Because of the applied stresses on the shroud are also very low, the nature of the cracking experienced by the core shrouds might be strongly influenced by the residual stresses associated with the core shroud welds [91].

Although safety analysis done by concerned agencies for the potential significance associated with the core shroud cracking does not pose a high degree of risk in short-term. However, in long term, it is a safety concern because of the uncertainties associated with the behavior of core shrouds with 360° cracks, under accident conditions and because it could eliminate a layer of defense in depth [91]. Therefore, regular and reliable monitoring for degradation of core shroud material and its weld regions is a requirement, which should be followed religiously.

## 5.4 Indian BWRs at Tarapur

The twin reactors of Tarapur Atomic Power Station (TAPS) are dual cycle reactor with primary and secondary loop with installed capacity of 210MWe each unit, however later both units were re-rated to 160 MWe and are operating only on primary loop. TAPS core shrouds have been constructed from various heats of SS304 cylinders by way of a number of horizontal welds, as shown in Fig. 5.1. Table-5.1 provides the chemical composition of various heats of material used in construction of core shrouds of TAPS 1 and 2. The core shrouds have completed 27 effective full power years and it is expected that the material of the shrouds would have undergone irradiation hardening during its service. It is also expected that they might have worked out surfaces near welds, formed during its construction about 47 years ago, resulting in hardened surface. Due to irradiation-hardening and hardened worked-out surfaces, the core shrouds might be susceptible to cracking by SCC. It is pertinent to mention that there is no surveillance programme for TAPS core shroud to monitor its health. Hence, a need was felt to develop a technique of scooping out small coupons, machining miniature samples from the coupon for mechanical property evaluation and micro-structural characterization, and assess the health of the core shroud material, as has been done in various reactors abroad [80, 83, 92].

***Table 5.1: Chemical composition (wt%) of various heats of TAPS core shroud material***

| Sl No. | C | Mn | P | S | Si | Cr | Ni | Mo |
|---|---|---|---|---|---|---|---|---|
| Heat 1 | 0.055 | 1.640 | 0.025 | 0.018 | 0.5 | 18.58 | 9.57 | 0.24 |
| Heat 2 | 0.058 | 1.21 | 0.019 | 0.013 | 0.54 | 18.9 | 9.38 | |
| Heat 3 | 0.048 | 0.85 | 0.027 | 0.024 | 0.54 | 18.59 | 9.30 | 0.24 |
| Heat 4 | 0.044 | 1.2 | 0.016 | 0.012 | 0.8 | 18.20 | 9.06 | |
| Heat 5 | 0.052 | 1.15 | 0.014 | 0.004 | 0.72 | 18.70 | 9.04 | |
| Heat 6 | 0.068 | 1.24 | 0.018 | 0.015 | 0.46 | 18.89 | 9.07 | |

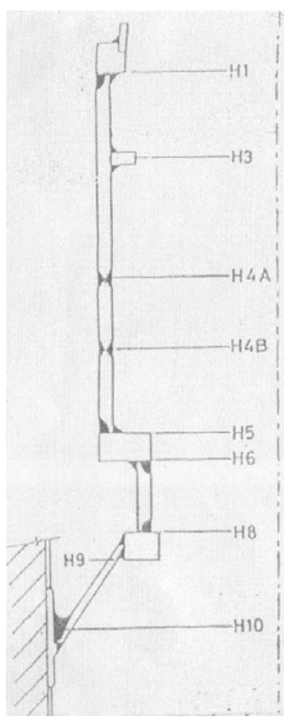


*Fig. 5.1: Horizontal welds of TAPS core shroud.*

## 5.5 Development of boat sampling technique for TAPS 1 & 2 core shrouds

Boat sampling technique for TAPS reactor was developed for scooping out boat-shaped metal sample from the core shroud in a remotely and non-destructive manner. The technique, utilizes a scooping device, known as ‘Sampling Module’, shown in Fig. 5.2a, which operates under water-filled condition of reactor and grinds out a boat-shaped sample from the core shroud. The sampling operation is an internal grinding operation and the sample is obtained by spinning the cutter, Fig. 5.2b, about its axis of symmetry, Fig. 5.2c, while slowly advancing it about a perpendicular axis to feed the cutter into the parent material. The abrasive coated cutter generates a 1mm wide kerf through the material while scooping. Depending upon the operating asymmetries, the actual kerf width may vary. The depth of the depression left in the base material is known as scooped region and is equivalent to the sample thickness plus the kerf width. The scooping operation is non-destructive as the contour of the scooped region merges smoothly with the surface profile of the core shroud and there is no loss of integrity or reduction in service life of the core shroud. The scooped material, known as ‘boat sample’, is used to carry out required mechanical & metallurgical tests. Since the core shroud is full of water to minimize the radiation dose to personnel, various motors or drives, used in the sampling module are provided with water-sealed muffles. The overall process of scooping is remotely controlled and operable with the help of a number of sensors and control elements.

### *5.5.1 Sampling module*

The sampling module consist of a sampling cutter, Fig. 5.2a, driving motor, feeding motor, control for the motors, feedback sensors for speed and position monitoring, sample enclosure and thickness control device etc. The driving motor rotates the cutter at 8000 rpm, which is monitored with the help of a hall-sensor based tachometer. The feed motor advances or retracts the cutter in a controlled manner, which senses position by the potentiometer based sensor degrees and displayed in the human machine interface console of the control panel, Fig. 5.3.

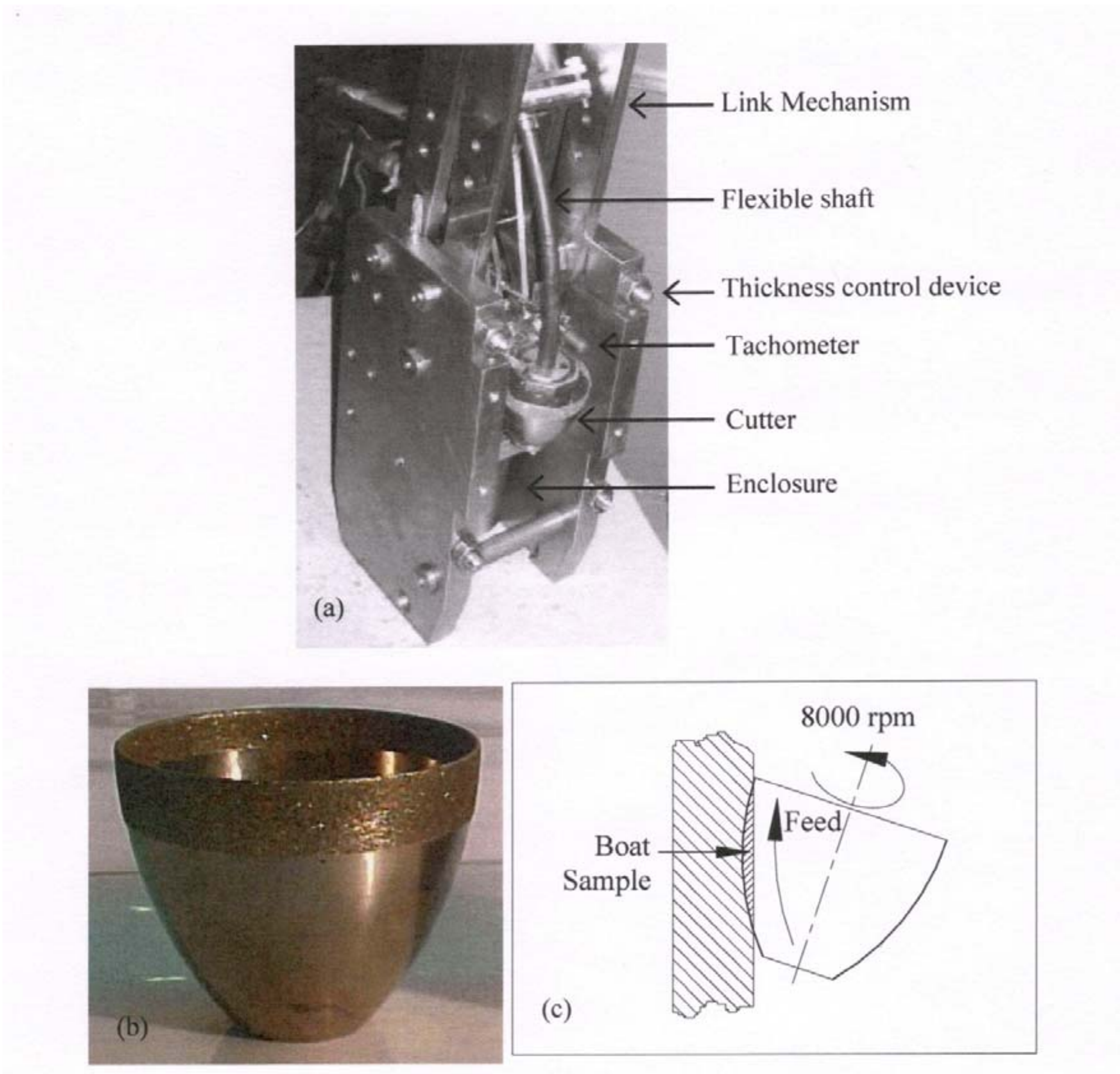


*Fig. 5.2: (a) Sampling module with its various components, (b) Sampling cutter and (c) A metal sample is obtained by spinning the cutter about its axis of symmetry, while slowly advancing it about a perpendicular axis to feed the cutter into the parent material*

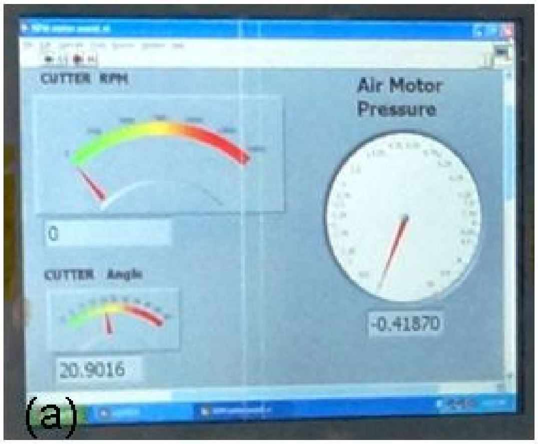

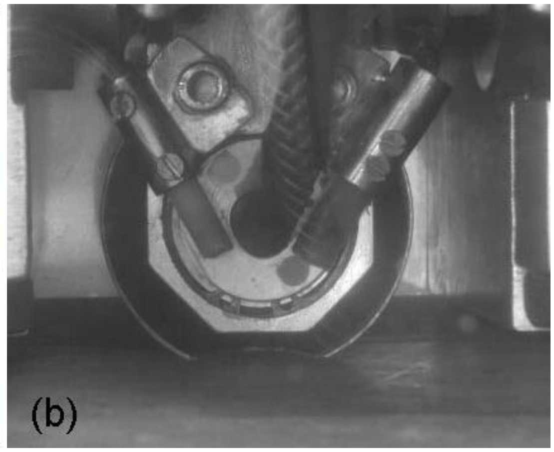


*Fig.5.3: (a) Display in the human machine interface console of the control panel showing cutter RPM, cutter position and supply air pressure to air motor and (b) camera view while sampling operation*

The sampling module is provided with an enclosure for protection against escaping of boat sample due to centrifugal force, just after its detachment from the shroud wall. The thickness of the boat sample can be controlled by thickness controlling device in the module.

### *5.5.2 Sampling cutter*

The sampling cutter is cup-shaped and is coated with cubic boron nitride abrasive for grinding operation. Cubic Boron Nitride (CBN) is the second hardest known material, only diamond being harder than CBN and is synthesized from hexagonal boron nitride under conditions similar to those used to produce synthetic diamond from graphite. Its properties of high thermal stability and resistance to chemical attack make it suitable for machining of ferrous materials, in areas where diamond abrasives are not normally employed. CBN is known for thermal resistance up to a temperature of 1000°C, like diamond up to 650°C. CBN is free from carbon and does not have any reaction with steel. This property of CBN makes it the ideal for grinding of hardened steel. The nature of bonding of the coating on the cutter is very important. The electroplated bond was selected based on the requirement of cutter geometry. The coating of CBN is single layer and CBN was deposited uniformly over the steel body of the cutter by the process of electroplating. The higher speed is preferable for high speed grinding process. The size of chips sheared by abrasive grain in electroplated CBN grinding wheel decreases as the cutting speed is increased. This improves grinding efficiency and makes the wheel grind cooler. A large proportion of available power is utilized into shearing chips and less is wasted as heat. High speed grinding machines have short cycle time but highest material removal rate to maximize productivity. They are usually equipped with automated parts loading/unloading.

The grit size was selected along with the bond to suit the component to be ground and surface finish requirement. The performance of grinding by the electroplated cutters is measured in terms of Specific Volume ground value, which is ratio of Volume of parent material removed in $mm^3$ to the Area available in cutter for grinding in $mm^2$.

### *5.5.3 Boat samples*

A boat sample, shown in Fig. 5.4a, removed from a flat surface, is elliptical in shape and has approximate dimension as Y=40mm long, X=25mm wide and T=3mm thick at centre. The contour of scooped region, shown in Fig. 5.4b, is smooth merging with the parent material and has approximate dimensions as H=45mm long, W=30mm wide and D=4.5mm depth at centre.

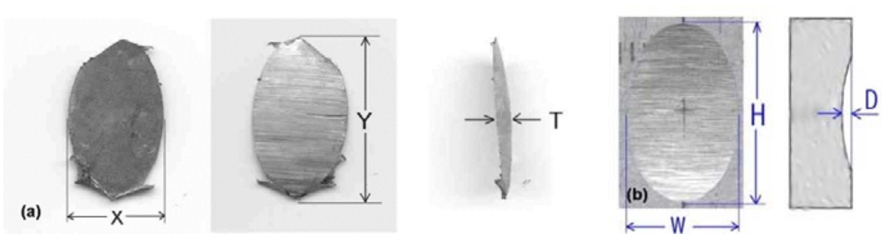


*Fig. 5.4: Geometry of (a) boat sample and (b) scooped region*

At the end of the sampling operation, the boat sample falls in the cutter shell by gravitation mode or in the housing of the sampling module, which is collected remotely. Fine mesh powder is generated due to grinding action during sampling which is lost in the pool water.

### *5.5.4 Sample collection system*

a) Sample: After sampling operation is complete, sample is collected in the cutter shell or falls within the housing of the sampling module. The sample is collected either with the help of tong or by gravitational method.

b) Metal Powder: During Sampling operation, along with the boat sample, fine mesh powder of approximate size of 200 mesh is generated due to grinding action. A housing has been provided in the sampling module for collecting the powder within it, however, based on the experience of the sampling operation so far, the powder is lost in the water pool due to the high speed of the cutter. Hence, it seems that powder, generated during the sampling operation cannot be collected inside the housing.

### *5.5.5 Mock-up trials and qualification of sampling technique*

Various sampling mock up trials were conducted to obtain boat samples from plate, weld and HAZ regions, some are shown in Fig. 5.5, and dimensional details of the sample and scooped regions are given in Table-5.2. These tests were conducted to qualify the technique and for study of the following:

- Dimensional Study of Sample and Scooped Region
- Surface Finish of Sample and Scooped Region
- Life Test of Cutter and flexible shaft
- Optimisation of Sampling Duration

- Ultrasonic Examination
- Visual Examination of Scooped Region
- Fluorescent Dye-Penetrant Test of Scooped Region to find out any crack due to sampling operation
- Micro-Hardness test of the region to study any hardness change due to sampling operation

The dimension and volume of the sample are ensured to be sufficient to carryout mechanical and metallurgical tests.

The qualification of sampling technique included the individual qualification of sampling module components, viz. cutter, flexible shaft, feed motor, drive motor and motor muffles; sample; scooped region; integrated system and operational procedure based on the safety and operation requirements. The sampling cutter was subjected to circularity test, run out test; the flexible shaft was subjected to life test for 8 hours of operation at 8000 rpm; the motors were subjected to torque margin measurement and the muffles of motors were subjected to leak test.

**Circularity Test**: Circularity within 0.05 mm at any points on the cutter was achieved according to estimation to minimise kerf width.

**Run out Test**: Run out in the feed direction should be minimum (within 0.1mm) to minimise kerf width.

**Stability Test:** The complete device was tested at speed of 10000 RPM to verify the stability under high rotational speed.

**No load test of Air motor:** 10000 RPM at 80 psi (5.7 kg/cm$^2$) air pressure

**Endurance test of flexible shaft:** The flexible shaft in “C” shape was found safe in operation for eight hour operation at 8000 RPM.

**Leakage Test**: Muffles on air motor and on stepper motor have been provided for under water operation. These muffles, whether under static or operating condition, have been designed as leakage proof for safe operation.

A full scale mock up facility, Fig. 5.6a, was created for the 15 metre deep under-water operation. The sampling module was attached to the handling manipulator, Fig. 5.6b, for operation in the core shroud. The mock-up trials were successfully conducted to reaffirm its capability for actual core shroud sampling operation. The sampling operation was monitored through camera apart from the features available in the sampling module.

(a)

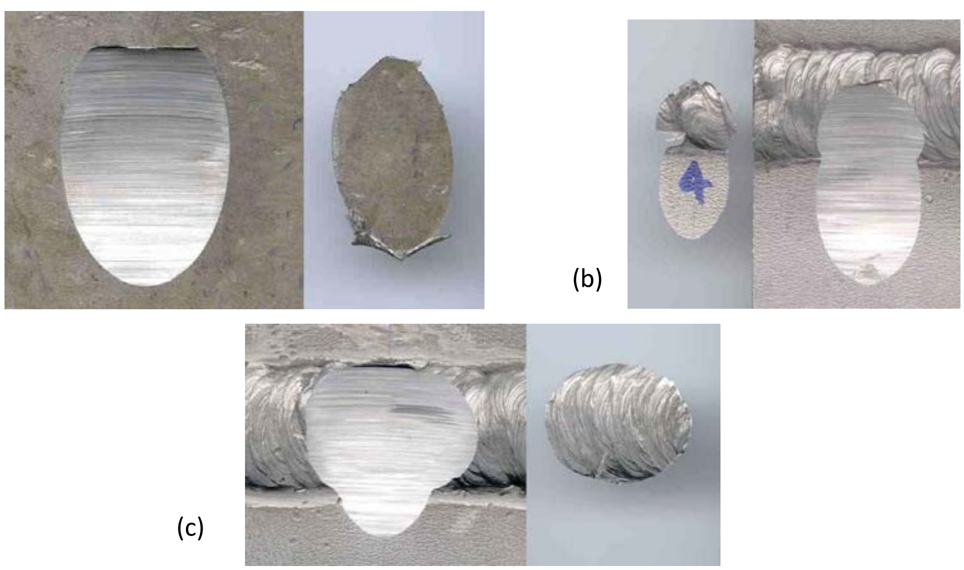


*Fig.5.5: Boat Samples obtained during qualification trials of sampling operation (a) Sample from flat stainless steel plate, (c) Sample from HAZ of welded flat SS plate and (d) Sample from weld region of flat SS Plate*

***Table 5.2: Scooping trials on different material conditions***

| Parent Material | Dimensions (in mm) | |
|---|---|---|
| | Boat Sample (X*Y*T) | Scooped Region (H*W*D) |
| SS-304 | 20x34x1.8 | 39.5x27.6x3.5 |
| HAZ of SS304 | 17x38x2.7 | 48x25x3.5 |
| Weld SS304 | 25.4x31.5x4.4 | 36x36x6.9 |

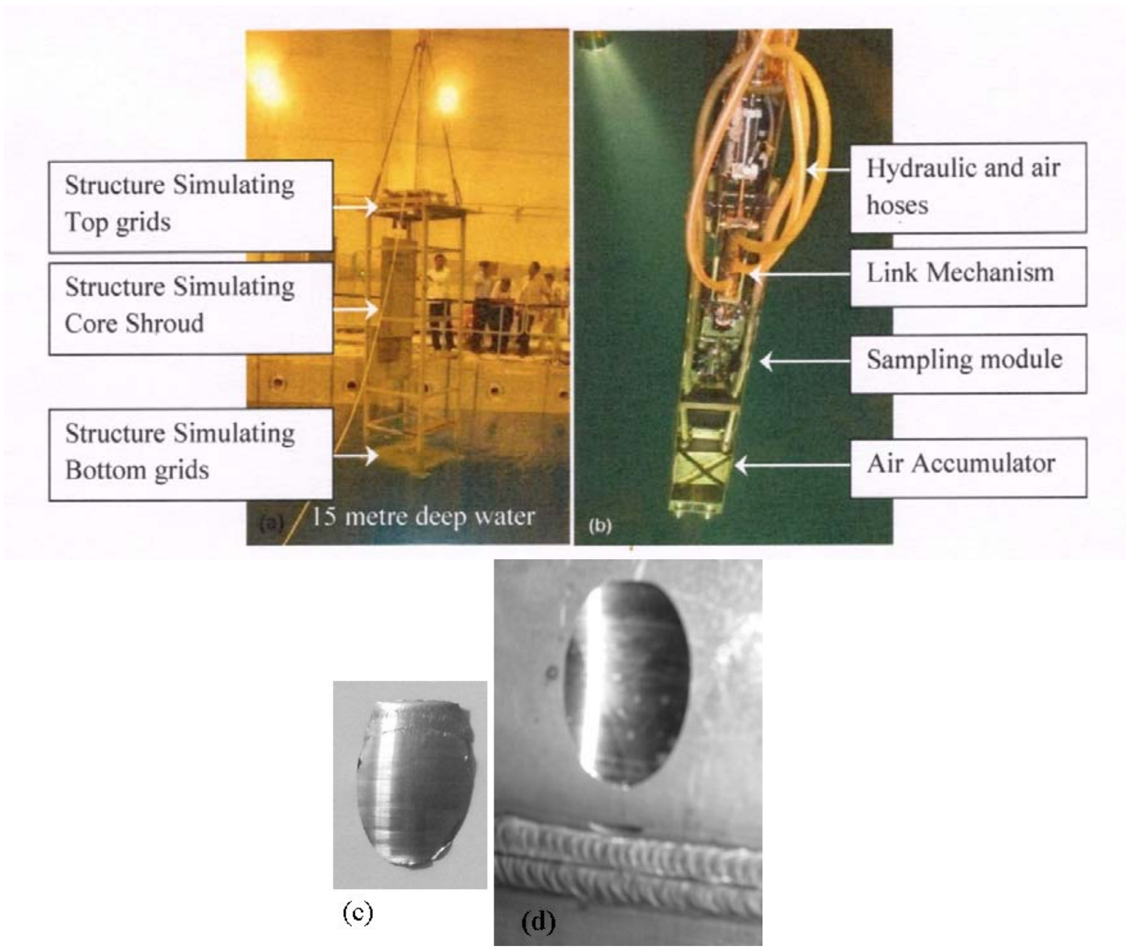


*Fig. 5.6: A full scale mock up trials were conducted at TAPS in (a) a water pool under 12metre head using simulated upper & lower grids structures and simulated core shroud, (b) Integrated assembly of Sampling Module and Handling Manipulator and (c) boat sample from simulated core shroud (d) scooped region created in the simulated core shroud*

## 5.6 Fabrication of miniature specimens from boat samples

Post process of boat sample involves preparation of a various types of miniature test specimens and evaluation of mechanical properties using them. Dummy boat sample, scooped from SS304, having chemical composition given in Table-5.3, were subjected to EDM for fabrication of various types of miniature test specimens as shown in Fig. 5.7b. Miniature tensile specimen of gauge length 3mm, small punch test specimen of diameter 3mm, miniature hour-glass shaped fatigue test specimen of 3mm diameter, and miniature Charpy impact test specimen were fabricated from the dummy boat sample. The specimens were polished using SiC paper in wet condition up to 4000 grit size to obtain scratch free surfaces. SPT disk specimens were finished using 0.25micron diamond paste.

***Table 5.3: Chemical composition of material used for dummy boat sample and experiments on miniature tensile and SPT from the sample***

| Material | C | Cr | Ni | Mo | S | P | Co | Si | Mn | Cu | N |
|---|---|---|---|---|---|---|---|---|---|---|---|
| SS304 | 0.061 | 18.02 | 8.17 | 0.26 | 0.012 | 0.026 | 0.13 | 0.40 | 1.72 | 0.35 | 0.041 |

*Fig 5.7: Preparation of miniature test specimens from dummy boat sample by EDM*

## 5.7 Experiments with tensile specimens from boat sample and validation

To ensure the usefulness of miniature test techniques it is important to have comparable results of miniature tests and conventional tests with respect to the mechanical properties, viz. UTS, YS and elongation. Validation of mechanical properties obtained from miniature tensile specimen was done by comparing them with the results of sub-size tensile specimens, Fig. 5.8, which were made from the same block of material.

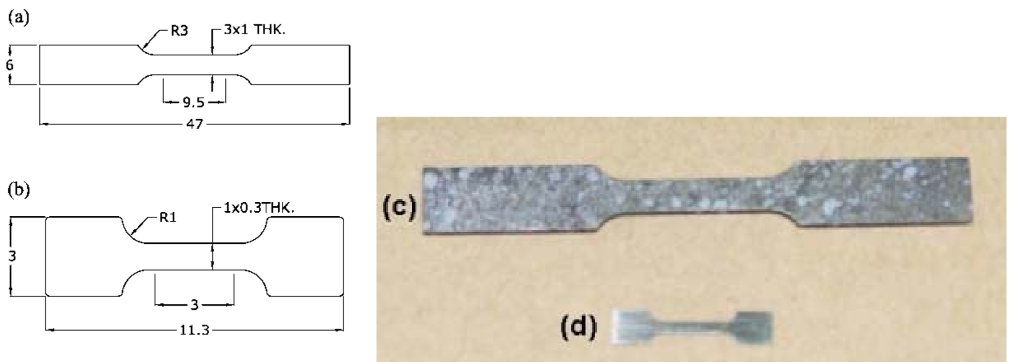


*Fig. 5.8: Dimensional details of (a) Sub-size flat specimen and (b) Miniature tensile test specimens and respective photographs in (c) and (d)*

Tensile tests were conducted at room temperature at a strain rate of $10^{-3}$ per sec on miniature size test specimens, prepared from boat samples of SS304 materials. The tests were conducted on screw driven machine. The strain values were measured using single camera video extensometer. The sub-size specimens from the same block were also tested under similar conditions. The results are summarized in Table-5.4 and Fig 5.9. For miniature specimen the UTS and YS values are in the range of 725-751 MPa and 423-471 MPa in comparison to respective sub-size values as 727-741MPa and 438-455MPa. The minimum UTS values for both the cases are very close to each other while the minimum YS values are within 3.5% range. The percentage uniform elongation and total elongation values for miniature specimen are 46.2-59.6 and 58.6-74.3, in comparison to respective sub-size values as 46.6-62.7 and 64.5-75. The minimum uniform percentage elongation for both the cases are very close to each other, however the minimum total percentage elongations are within 10% range. Due to high ductility of SS304 material, during testing, there is overall stretching in the parallel section of the specimen and there is continuous strain hardening till the failure and there is not much deformation after necking. Therefore uniform elongation values are very close to total elongation values. Overall, it can be concluded that the results obtained by miniature test specimens are comparable with those obtained by conventional sub-size test specimens within a very close error band. With the precise control of surface finish of test specimen, dimensional deviations, alignment of test fixtures, better strain measurement, the error band can be further minimized. It can be emphasized that BST and miniature tensile test methods have the potential for successful implementation at TAPS core shroud or any other pressure vessel, which needs an urgent attention of its life management issues.

***Table 5.4: Test results of tensile specimens made out of dummy boat sample***

| | Sub-size specimen | | | Miniature Specimen | | | | | |
|---|---|---|---|---|---|---|---|---|---|
| Specimen No. | 1 | 2 | 3 | 1 | 2 | 3 | 4 | 5 | 6 |
| YS, MPa | 438.3 | 449.1 | 454.6 | 423.3 | 438.5 | 435.0 | 424.6 | 435.0 | 471.0 |
| UTS, MPa | 741.4 | 736.3 | 727.2 | 750.9 | 728.1 | 727.3 | 726.6 | 745.1 | 724.9 |
| Uniform Elongation, % | 54.5 | 62.7 | 46.6 | 52.6 | 49.5 | 46.5 | 52.0 | 59.6 | 46.2 |
| Total Elongation, % | 75.0 | 68.1 | 64.5 | 69.0 | 58.6 | 59.2 | 66.9 | 74.3 | 59.3 |

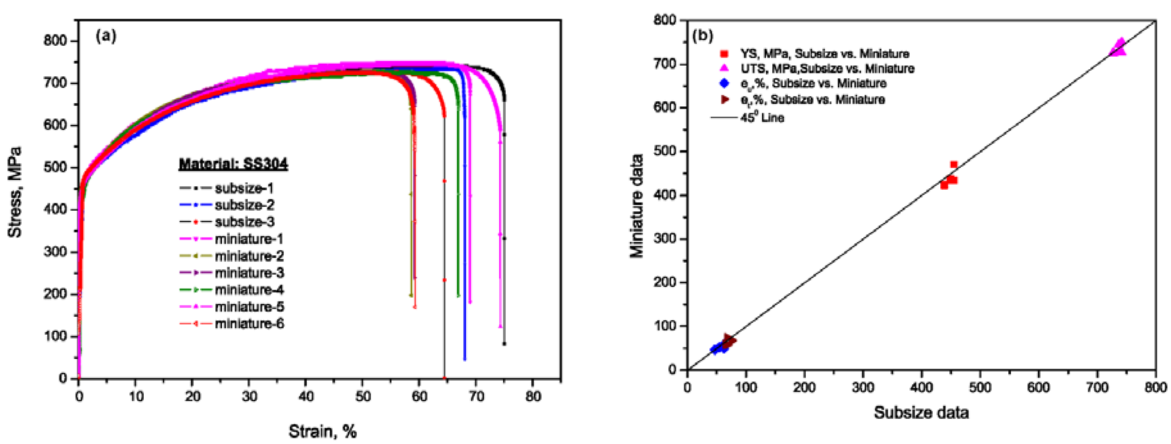


*Fig. 5.9: (a) The engineering stress – strain plot obtained using sub-size and miniature specimens for SS304 and (b) Scatter in YS and UTS, uniform and total elongation data of miniature specimens in comparison to sub-size specimens for SS304*

## 5.8 SPT experiments on specimens from boat sample and validation

Small punch tests were also conducted on specimens made out from dummy boat sample. The load-displacement plots for three specimens are shown in Fig. 5.10. The UTS values were obtained using newly developed correlation as per equation-4.4, mentioned in chapter-4. The UTS values were also obtained using Mao's correlation, as per equation-4.5 in chapter 4. All these data are summarised in Table 5.5. The UTS values, obtained from both the correlations are compared with the average of tensile data from sub-size specimen, as mentioned in Table 5.4. As per this table, the average UTS value for the material is 735MPa. It is found that the UTS values obtained using the new correlation has error of 9.35%, whereas the UTS obtained using Mao correlation has error of 12.24%.

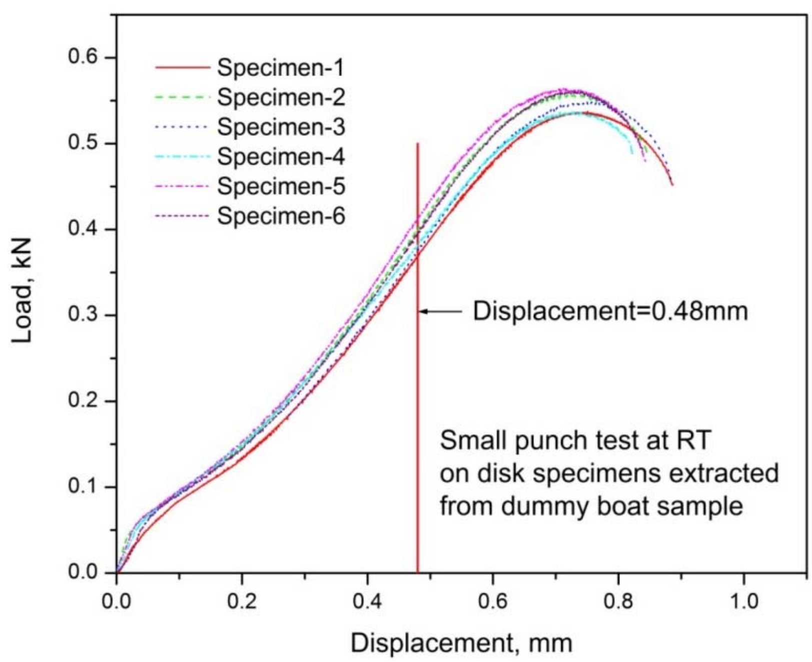


*Fig. 5.10: Load-displacement plots obtained using SPT specimen from dummy boat sample from SS304 plate*

*Table 5.5: Test results of SPT specimens from dummy boat sample*

| Specimen No. | Thickness (mm) | $P_{0.48}$ kN | $P_{max}$ kN | UTS (as per new correlation) MPa | UTS (as per X Mao's correlation) MPa |
|---|---|---|---|---|---|
| 1 | 0.2528 | 0.4113 | 0.5420 | 842.6 | 782.6 |
| 2 | 0.250 | 0.3993 | 0.5634 | 836.5 | 851.7 |
| 3 | 0.2524 | 0.3955 | 0.5567 | 813.1 | 816.0 |
| 4 | 0.2526 | 0.3808 | 0.5444 | 781.8 | 789.1 |
| 5 | 0.2512 | 0.3749 | 0.5707 | 778.4 | 855.7 |
| 6 | 0.2506 | 0.3691 | 0.5676 | 770.1 | 854.9 |
| Average Value | | | | 803.8 | 825.0 |
| Error in the UTS values | | | | 9.35% | 12.24% |

## 5.9 Closures

Following conclusions are from this chapter:

- Industrial applicability of Miniature Test Technique was probed with an illustration of probable deployment of the technique at Indian BWRs for scooping metal sample from core shrouds of TAPS 1 and 2. The system was successfully tested and qualified in shop floor trials and full-scale mock-up trials at TAPS.
- The mock boat samples were used to machine out miniature tensile and small punch test specimens, as per dimensions standardised in chapter-3.
- The tensile properties obtained using miniature specimens were found to be in agreement within 10% with the results from standard sub-size test specimens.
- SPT experiments were conducted on the disk specimens obtained from dummy boat sample and UTS values were evaluated using the UTS correlation, developed in

chapter-4. The UTS value obtained by new correlation was 9.35% higher, while the same obtained by Mao's correlation was 12.24% higher.

- This chapter conveys the potential of miniature test techniques as ageing management methodology for industrial application.

# CHAPTER-6

# Conclusions, Contributions and Future work

## 6.1 Conclusions

This thesis is focused on the use of miniature tensile test and small punch test techniques to meet specific data requirements for materials and components. It is understood that there are industrial needs for the development of miniature test techniques. From the literature, it is also clear that many designs of miniature tensile specimens have user driven requirements and there is no "perfect” or “universally agreed" design finalized yet. For small punch test there is no consensus on UTS correlations, which are based on $P_{max}$ value in Load-displacement plot. The present work aimed towards addressing these issues related to miniature tensile and small punch test techniques using two pressure vessel materials, 20MnMoNi55 and CrMoV steel; and one piping materials SS304LN; and following are the conclusions:

- Minimum thickness required for miniature tensile specimen, to match the mechanical properties from standard test specimen was found to be 0.3mm for the given materials.
- The tensile properties obtained using miniature specimens were found to be in agreement within 10% with the results from standard sub-size test specimens.
- Finite element analyses were carried out to find out necking regions of the SPT disk specimens. For the given test setup, disk specimen size and test conditions, the necking zones of the SPT disks are found to be very close to 0.48mm displacement, which is much earlier than displacements corresponding to $P_{max}$ values, which are

0.71mm (for 20MnMoNi55), 0.741mm (for CrMoV steel) and 0.887mm (for SS304LN).

- UTS were evaluated by conducting SPT experiments on the disk specimens obtained from dummy boat sample. The UTS value obtained by new correlation was 9.35% higher, while the same obtained by Mao's correlation was 12.24% higher.

- This study conveys the potential of miniature test techniques as ageing management methodology for industrial application. For tapping the potential of miniature tensile test technique, there is a need for a coherent international effort for standardizing the technique and adopting this as standard practice for the mechanical property evaluation.

## 6.2 Contributions

Following are the contributions from this work:

- Specimen geometry of miniature tensile test was finalised as 3mm gauge length, 1mm width and 0.3mm thickness.

- A new UTS correlation, based on the necking region of the SPT disk specimens of 3mm diameter and 0.25mm thickness, is given as :

  $$UTS=130*\frac{P_{0.48}}{t_0^2}+6$$

- Boat sampling technique was developed for scooping of boat sample from any in-service component in a non-destructive manner.

### 6.3 Future scope of work

Following future work may be targeted towards achieving the objectives of miniature test techniques:

- Various designs of miniature tensile specimen have been developed over the last thirty years to meet various commercial objectives. In most of the cases, the data interpretation has either reached an acceptable stage for specific materials important for the industry or approximate methods are being refined. As a future work, more experimental studies on different materials should be carried out as more test data become available for verification based on Round Robin experiments, which will help in standardisation of the experimental methods to ensure accurate and reproducible tests.

- The present study was carried out were on isotropic materials, which were from pressure vessel and piping applications. Similar work may be carried out on anisotropic material to study the effect of miniaturisation on the tensile properties. Pressure Tubes material, Zr-2.5%Nb, of 220MWe and 700MWe PHWRs, would be a good choice for the future work. The anisotropic properties of the Zr-2.5%Nb material would be possible using miniature tensile specimens, in axial, circumferential and radial directions.
- The miniature specimen test techniques can be extended for evaluation of mechanical properties in functionally graded materials (FGMs). The FGMs are a new kind of inhomogeneous composite materials which have a smooth and continuous variation of material properties along one or more directions [93, 94].

# References:


1. D. Tabor, ‘The hardness of metals’, Clarendon Press, London, 1951
2. B. S. Shabel and R. F. Young, ‘A new procedure for the rapid determination of yield and tensile strength from hardness tests’, in J. F. Bussiere et al. (eds.), Non-destructive characterization of materials II, Plenum Press, New York, (1987) 335-343
3. M. O. Lai, K. B. Lim, ‘On the prediction of tensile properties from hardness tests’, J.Mater.Sci.26, (1991) 2031-2036
4. Martin Gasco and Gejza Rosenberg, ‘Correlation between hardness and tensile properties in ultra-high strength dual phase steels-short communication’, Materials Engineering 18 (2011) 155-159
5. D. Blagoeva, N. Taylor, R. Hurst, ‘State-of-the-art report on application of miniaturized testing techniques to support life management decisions for nuclear plants’, JRC 42138, EUR 23221 EN, ISSN 1018-5593, 2007
6. N.F. Panayotou, R.J. Puigh, E.K. Opperman, ‘Miniature specimen tensile data for high energy neutron source experiments’ Journal of Nuclear Materials 103 & 104 (1981) 1523-1526
7. R. L. Klueh, Miniature Tensile Test Specimens for Fusion Reactor Irradiation Studies, Nuclear Engineering and Design/Fusion 2 (1985) 407-416
8. G. E. Lucas, ‘The development of small specimen mechanical test techniques’, Journal of Nuclear Materials 117 (1983) 327-339
9. N. F. Panayotou, S. D. Atkin, R. J. Puigh and B. A. Chin, ‘Design and use of Nonstandard Tensile Specimens for Irradiated Materials Testing’ STP-888 (1986) 201-219
10. A. Kohyama, K. Hamada and H. Matsui, ‘Specimen size effects on tensile properties of neutron irradiated steels’ , Journal of Nuclear Materials, 179-181 (1991) 417-420

11. M. P. Manahan, A. Browning, S. Argon and O. K. Harling, ‘Miniaturised disk bend test technique development and application’, ASTM STP 888, (1986) 17-49

12. G. R. Odette, M. He, D. Gragg, D. Klingensmith and G.E. Lucas, ‘Some recent innovations in small specimen testing’, Journal of Nuclear Materials, 307-311 (2002) 1643-1648

13. G. E. Lucas, G. R. Odette, M. Sokolov, P. Spatig, T Yamamoto and P Jung, ‘Recent progress in small specimen technology’, Journal of Nuclear Materials, 307-311 (2002) 1600-1608

14. G. E. Lucas, G. R. Odette, H. Matsui, A. Moslang, P. Spatig, J. Rensman and T. Yamamoto ‘The role of small specimen test technology in fusion materials development’, Journal of Nuclear Materials’, 367-370 (2007) 1549-1556

15. G. E. Lucas, G. R. Odette and J. W. Sheckherd, ‘Shear punch and micro hardness tests for strength and ductility measurements’ ASTM STP 888, (1986) 112-139

16. J. Kameda and X. Mao, ‘Small punch test and TEM-disc testing techniques and their application to the characterisation of radiation damage’, Journal of material science, 27(1992) 983-989

17. P. Jung, A. Hishinuma, G. E. Lucas and H. Ullmaier, ‘Recommendation of miniaturized techniques for mechanical testing of fusion materials in an intense neutron source’, Journal of Nuclear Materials 232 (1996) 186-205

18. Y. Kohno, A. Kohyama, M. L. Hamilton, T. Hirose, Y. Katoh, F. A. Garner, ‘Specimen size effects on the tensile properties of JPCA and JFMS’ Journal of Nuclear Materials’, pp 283-287 (2000) 1014-1017

19. Yuanchao Xu, Guangshen Ning, Changyi Zhang, Qingkai Yu and Yanping Xu, ‘Application of the miniature specimen technique to material irradiation tests and

surveillance for reactor components' International Journal of Pressure Vessels and Piping 77 (2000), pp 715-721

20. E. N. Campitelli, P. Spatig, R. Bonade, W. Hoffelner and M. Victoria, 'Assessment of the constitutive properties from small ball punch test: experiment and modeling' Journal of nuclear materials, 335(2004), 366-378

21. W. R. Corwin and G. E. Lucas, 'The use of small-scale specimens for testing irradiated material', ASTM Special Technical Publication 888, PCN 04-888000-35, Albuquerque, Sept. 1983

22. W. R. Corwin, M. H. Fahmy and W. L. Server, 'Small specimen test techniques applied to nuclear reactor vessel thermal annealing and plant life extension', ASTM Special Technical Publication 1204, PCN 04-012040-35, Jan. 1992

23. W. R. Corwin, S. T. Rosinski, Eric van Walle, editers, 'Small Specimen Test Techniques' ASTM Special Technical Publication 1329, July 1998, ISBN0-8031-2476-7

24. Mikhail A. Sokolov, John D. Landes, Glenn E. Lucas, editors, 'Small Specimen Test Techniques: 4th Volume', ASTM Special Technical Publication 1418, 2002

25. M. A. Sokolov, Guest editor, 'Small Specimen Test Techniques: 5th Volume', ASTM Special Technical Publication 1502, January 2007

26. Mikhail A. Sokolov and Enrico Lucon, Editors, 'Small Specimen Test Techniques: 6th Volume', ASTM Special Technical Publication 1576, January 2014,

27. A. Kohyama, K. Asakura and N. Igata, 'Mechanical property changes in ferritic steels by 14MeV neutron bombardment', Journal of Nuclear Materials, 141-143(1986) 921-925

28. J. D. Lord, B. Roebuck, R. Morrell, T. Lube, ‘Aspects of strain and strength measurement in miniaturised testing for engineering metals and ceramics’ Materials Science and Technology, 26 (2010) 127-148

29. Ivan Klevstov, Andrei Dedov and Artjom Molodstov, ‘Measurement of tensile and yield strength of boiler steels by small punch and tensile test methods’, Estonian Journal of Engineering, 2009, 15, 2, 99-107

30. T. S. Byun, J. H. Kim, S. H. Chi and J. H. Hong, ‘Effect of specimen thickness on the tensile deformation properties of SA508 Cl.3 Reactor Pressure Vessel Steel’, ASTM SPT 1329, (1998) 575-587

31. Y. Dai, G. W. Egeland, S. Long, ‘Tensile properties of EC316LN irradiated in SINQ to 20 dpa’, Journal of Nuclear Materials’, 377 (2008) 109-114

32. D. Dobi and Eva Junghans, ‘Determination of the tensile properties of specimens with small dimensions’, Kovine, Zlitine, Technologije 33(1999) 6

33. A.V. Sergueeva, J. Zhou, B. E. Meacham, D. J. Branagan, ‘Gage length and Sample size effect on measured properties during tensile testing’, A526 (2009), Mat.Sc and Engg A, 79-83

34. Jin Weon Kim, Kyoungsoo Lee, Jong Sung Kim, Thak Sang Byun, ‘Local mechanical properties of alloy 82/182 dissimilar weld joint between SA508 Gr.1a and F316SS at RT and 320°C, Journal of Nuclear Materials, 384 (2009) 212-221

35. A. Dedov and I. Klestov, ‘Comparison of direct and indirect methods of tensile properties determination for post-exposed power plant steels’ Annals of DAAAM for 2012 & proceedings of the 23$^{rd}$ International DAAAM symposium, Vol 23, No. 1, ISSN 2304-1382

36. Ellen M Rabenberg, B. J. Jaques, B. H. Sencer, F. A. Garner, P. D. Freyer, T. Okita and D. P. Butt, ‘Mechanical behaviour of AISI 304SS determined by miniature test

methods after neutron irradiation to 28dpa', Journal of Nuclear Materials, 448 (2014) 315-324

37. T. S. Byun, K. Farrell, E. H. Lee, J. D. Hunn and L. K. Mansur, 'Strain hardening and plastic instability properties of austenitic stainless steels after proton and neutron irradiation', Journal of Nuclear Engineering, 298 (2001) 269-279

38. ManSoo Joun, Jea Gun Eom, Min Cheol Lee, 'A new method for acquiring true stress-strain curves over a large range of strains using a tensile test and finite element method', Mechanics of materials, 40(2008) 586-593]

39. M. P. Manahan, A. S. Argon, O. K. Harling, 'The development of a miniaturized disk bend test for the determination of post irradiation mechanical properties', Journal of nuclear materials, 103 & 104 (1981), 1545-1550

40. G. E. Lucas, A. Okada, M. Kiritani, 'Parametric Analysis of Disk Bend Test', Journal of nuclear materials, 141-143 (1986), 532-535

41. X. Mao and H. Takahashi, 'Development of a further-miniaturized specimen of 3mm diameter for TEM disk (ϕ3 mm) small punch test', Journal of nuclear materials, 150(1987), 42-52

42. Hideaki Takahashi, Tetsuo Shoji, Xinyuan Mao, Yoshikazu Hamaguchi, Toshihei Misawa, Masahiro Saito, Tatsuo Oku, Tsuneo Kodaira, Kiyoshi Fukaya, Hiroshi Nishi and Masahide Suzuki, 'Recommended practice for small punch testing of metallic materials', JAERI-M-88-172, Sept 1988

43. V.. Vorlicek, L. F. Exworthy and P. E. J. Flewitt 'Evaluation of miniaturised disc test for establishing the mechanical properties of low-alloy ferritic steels', Journal Of Materials Science (1995) Volume 30, Issue 11, 2936-2943

44. E. Fueury and J. S. Ha, 'Small punch tests to evaluate the mechanical properties of steels for steam power plant: I. Mechanical strength', International Journal of pressure vessel and piping 75 (1998) 699-706

45. C. Q. Chen, J. G. Sun and Y.C. Xu, 'Neutron irradiation hardening of ODS alloy tested by miniature disk bend test method', Journal of nuclear materials, 283-287 (2000), 1011-1013

46. M. B. Toloczko, M. L. Hamilton and G. E. Lucas, 'Ductility correlations between shear punch and uniaxial tensile test data', Journal of nuclear materials, 283-287 (2000), 987-991

47. Zhao-Xi Wang, Hui-Ji Shi, Jian Lu, Pan Shi and M Xian-Feng, 'Small punch testing for assessing the fracture properties of the reactor vessel steel with different thicknesses', Nuclear Engineering and Design 238 (2008) 3186–3193

48. Yoon-Suk Chang, Jong-Min Kim, Jae-Boong Choi, Young-Jin Kim, Min-Chul Kim and Bong-Sang Lee, 'Derivation of ductile fracture resistance by use of small punch specimens' Engineering Fracture Mechanics, 75 (2008) 3413-3427

49. I. Klestov, A. Dedov and A. Molodtsov, 'Using of small punch test for determination of tensile properties for power plant steels' 6$^{th}$ International DAAAM Baltic Conference Industrial Engineering, 2008, Estonia

50. Szabolcs Jónás, Szabolcs Szávai, Péter Rózsahegyi and Róbert Beleznai, 'Determination of material properties using small punch test', University of Miskolc

51. Ma Young Wha and Kee Bong Yoon, 'Assessment of tensile strength using small punch test for transversely isotropic aluminium 2024 alloy produced by equal channel angular pressing', Material Science and Engineering A527 (2010) 3630-3638

52. M. Madia, S. Foletti, G. Torsello and A. Cammi, ‘On the applicability of the small punch test to the characterisation of the 1CrMoV aged steel: Mechanical testing and numerical analysis’, Engineering Failure Analysis 34 (2013) 189-203
53. Kai-shu Guan, Tong Xu, Xiao-cheng Zhang, Zhi-wen Wang, ‘Effect of microdefects on load-deflection of small punch test by experimental investigation and finite element analysis’, International Journal of Pressure Vessel and Piping , 110, (2013), 14-16
54. T. E. Garcia, C. Rodriguez, F. J. Belzunce and C. Suarez, ‘Estimation of the mechanical properties of metallic materials by means of small punch test’, Journal of Alloys and Compounds 582 (2014) 708-717
55. S. P. Singh, S. Bhattacharya and D. K. Sehgel, ‘Evaluation of high temperature mechanical strength of Cr-Mo grade steel through small punch test technique’, Engg Failure Analysis 39 (2014) 207-220
56. J. Rodríguez, García Cabezas, E. Cárdenas, F. J. Belzunce, and C. Betegón., ‘Mechanical Properties Characterisation of Heat Affected Zone using small punch test’, Welding Journal, Sept 2009, 88, 188-192
57. A. D. Amayev, V. I. Badanin, A. M. Kryukov, V. A. Nikolayev, M. E. Rogov and M. A. Sokolov, ‘Use of sub-size specimens for determination of Radiation embrittlement of operating reactor pressure vessels’, ASTM STP1204, 1993, pp 424-439
58. M. Valo and R. Ahlstrand, ‘Application of reconstitution welding technique for studying base metal of a Novoronesh unit-1 trepan sample’, ASTM STP1204, 1993, 440-456
59. Kundan Kumar, K. Madhusoodanan and B.B. Rupani, ‘Miniature Specimen Technique as an NDT Tool for Estimation of Service Life of Operating Pressure

Equipment' Proceeding of the International Conference & Exhibition on Pressure Vessels and Piping, "OPE 2006 – CHENNAI", 7-9, February 2006, Chennai, India

60. K. Miyahara, C. Tada, T. Uda, N. Igata, 'The Effects of grain and specimen sizes on mechanical properties of Type 316 Austenitic stainless steel', Journal of Nuclear Materials, 133 &134 (1985) 506-510
61. M. Klein, A. Hadrboletz, B. Weiss, and G. Khatibi, 'The size effect on the stress-strain, fatigue and fracture properties of thin metallic foils', Material Science and Engineering, A319-321 (2001) 924-928
62. L.V. Raulea, A.M. Goijaerts, L.E. Govaert, F.P.T. Baaijens, 'Size effects in the processing of thin metal sheets', Journal of Material Processing Technology 115(2001)44-48
63. T. Fülöp, W.A.M. Brekelmans and M.G.D. Geers, 'Size effects from grain statistics in ultra-thin metal sheets', Journal of Materials Processing Technology 174(2006)233-238
64. S X Li & G R Cui,' Dependence of strength, elongation and toughness on grain size in metallic structural materials', Journal of Applied Physics 101, 083525 (2007)
65. G. Partheepan, D. K. Sehgal and R. K. Pandey, 'Design and usage of simple miniature specimen test setup for the evaluation of mechanical properties', Int J. Of microstructure and materials properties, Vo. 1, No. 1, (2005) 38-50
66. G. Partheepan, D. K. Sehgal and R. K. Pandey, 'Finite element application to estimate In-service material properties using miniature specimen', Int. Journal of Aerospace and Mechanical Engineering 2:2 2008, 130-136
67. R. V. Prakash and S. Arunkumar, 'Evaluation of damage in materials due to fatigue cycling through static and cyclic small punch testing', Small specimen Test Techniques:6$^{th}$ volume, STP 1576 (2015), pp. 168-186

68. W. Sharpe and R. O. Fowler, ‘A novel miniature tension test machine’, ASTM STP-1204, 1993, 386-401

69. M. L. Hamilton., M. A. Blotter and D. J. Edwards, ‘Evaluation of Miniature Tension Specimen Fabrication Techniques and Performance’, ASTM SPT 1204, 1993, pp 368-385

70. G. E. Dieter, ‘Mechanical Metallurgy’, McGraw Hill Education (India) Pvt. Ltd., ISBN-13:978-1-25-906479-1

71. A. Okada, ‘Tension Test System for Irradiated Small Specimens operated by remote control’, ASTM STP-1204, 1993, 324-335

72. A. Kohyama, S. Sato, and K. Hamada, ‘An automated tensile machine for small specimens heavily neutron irradiated in FFTF/MOTA’, ASTM STP-1204, 1993, 356-367

73. Kundan Kumar, K. Madhusoodanan, R. N. Singh, J. K. Chakravartty, B. K. Dutta, and R. K. Sinha, “Development and Validation of In-Situ Boat Sampling Technique for Mechanical Property Evaluation and Life Management of TAPS Core Shroud”, International Journal of Engineering Research & Technology (IJERT) ISSN: 2278-0181, Vol. 3, Issue 7, July-2014

74. Stress Corrosion Cracking in Light Water Reactors: Good Practices and Lessons Learned, IAEA Nuclear Energy Series, Sept 2011, No. NP-T-3.13

75. Status Report: Intergranular Stress Corrosion Cracking of BWR Core Shrouds and Other Internal Components, NUREG-1544, March 1996, USNRC

76. S. Ooki, Y. Tanaka, K. Takamori, S. Suzuki, S. Tanaka, Y. Saito, T. Nakamura, T. Kato, K. Chatani, and M. Kodama, ‘Study on SCC growth behavior of BWR core shroud’ Proceedings of the 12th International Conference on, Environmental Degradation of Materials in Nuclear Power System –Water Reactors –Edited by T.R.

Allen, P.J. King, and L. Nelson TMS (The Minerals, Metals & Materials Society), 2005, 365-378

77. H. Yamashita, 'SCC growth behavior of BWR core shroud materials' International Journal of Pressure Vessels and Piping 85 (2008) 582–592
78. Karlsen Wade, 'Localized deformation as a key precursor to initiation of intergranular stress corrosion cracking of austenitic stainless steels employed in nuclear power plants' Journal of Nuclear Materials 406 (2010) 138–151
79. Kamaya Masayuki and Haruna Takumi, 'Influence of local stress on initiation behaviour of stress corrosion cracking for sensitized 304 stainless steel' Corrosion Science 49 (2007) 3303–3324
80. Yuichi Okamura, Akihiro Sakashita, Toshihiko Fukuda, Hironobu Yamashita and Tsuneo Futami, 'Latest SCC Issues of Core Shroud and Recirculation Piping in Japanese BWRs', Transactions of the 17th International Conference on Structural Mechanics in Reactor Technology (SMiRT 17), Prague, CzechRepublic, August 17-22, 2003
81. Replacement of Reactor Internals and Full System Decontamination at a Japanese BWR, ISOE INFORMATION SHEET, ISOE Asian Technical Center -NUPEC Information Sheet No. 9, October, 1999
82. Matsumoto Jun, 'Core shroud replacement of Fukushima-Daiichi Unit-3', Tokyo Electric Power Company, April 1999
83. Report of examination of the Sample from Core Shroud (1F4-H4) at Fukushima Dai-ichi Nuclear Power Station Unit-4, JAERI-Tech 2004-004
84. R. M. Horn, G. M. Gordon, F. P. Ford, R. L. Cowan, 'Experience and assessment of stress corrosion cracking in L-grade stainless steel BWR internals' , Nuclear Engineering and Design 174 (1997) 313–325

85. Swati Ghosh, Vishav Preet Singh Rana, Vivekanand Kain, Vivek Mittal, S.K. Baveja, ‘Role of residual stresses induced by industrial fabrication on stress corrosion cracking susceptibility of austenitic stainless steel’, Materials and Design 32 (2011) 3823–3831

86. O. K. Chopra and A. S. Rao, ‘A review of irradiation effects on LWR core internal materials –IASCC susceptibility and crack growth rates of austenitic stainless steels, Journal of Nuclear Materials 409 (2011) 235–256

87. K. Chatani, Y. Kitsunai, M. Kodama, S. Suzuki, Y. Tanaka, S. Ooki, S. Tanaka, and T. Nakamura, ‘Irradiation assisted stress corrosion cracking susceptibility of core component materials, Proceedings of the 12th International Conference on, Environmental Degradation of Materials in Nuclear Power System –Water Reactors – Edited by T.R. Allen, P.J. King, and L. Nelson TMS (The Minerals, Metals & Materials Society), 2005, 349-356

88. H. M. Chung, W. E. Ruther, J. E. Sanecki, A. Hins, N.J. Zaluzec, T.F. Kassner, ‘Irradiation-assisted stress corrosion cracking of austenitic stainless: steels: recent progress and new approaches’, Journal of Nuclear Materials 239 (1996) 61-79

89. T. Onchi, K. Dohi, N. Soneda, Marta Navas, M. L. Castaño, ‘Mechanism of irradiation assisted stress corrosion crack initiation in thermally sensitized 304 stainless steel’ Journal of Nuclear Materials 340 (2005) 219–236

90. Peter L. Andresen, ‘IGSCC of non-sensitized stainless steels in high temperature water’ Journal of Nuclear Materials 383 (2008) 97–111

91. Jinmiao Zhang, Pingsha Dong, Frederick W Brust, William J Shack, Michael E Mayfield, Michael McNeil, ‘Modelling of weld residual stresses in core shroud structures’, Nuclear Engineering and Design 195 (2000) 171–187

92. M. Cvitanovic, E. Oreb, V. Mudronj, V. Zado, H. Bezlaj, M. Petkov, J. Gledatchev, S. Radomirski, T. Ribarska, B. Kroes, ‘Boat Sampling and in-service inspections of the reactor pressure vessel weld No. 4 at Kozoduy NPP, Unit 1’ Nuclear Engineering and Design 191 (1999) 293-312
93. A. Mahi, E.A. Adda Bedia, A. Tounsi, "A new hyperbolic shear deformation theory for bending and free vibration analysis of isotropic, functionally graded, sandwich and laminated composite plates", Applied Mathematical Modelling, 39, (2015) 2489-2508
94. M.S.A. Houari, A. Tounsi, A. Bessaim, S.R. Mahmoud, ‘A new simple three-unknown sinusoidal shear deformation theory for functionally graded plates’, Steel and Composite Structures, 22(2), (2016) 257-276